

September 2019  
Vol. 3 - n. 2 Suppl. 3

2532-3997



# *Substantia*

An International Journal of the  
History of Chemistry

**Water in biology: what's so special about it?**

**Marc Henry, Editor**



**2019  
IYPT**



# *Substantia*

**An International Journal of the History of Chemistry**

**Vol. 3, n. 2 Suppl. 3 - 2019**

**Water in biology: what's so special about it?**

**Marc Henry, Editor**

Firenze University Press

**Substantia. An International Journal of the History of Chemistry**

Published by

**Firenze University Press** – University of Florence, Italy  
Via Cittadella, 7 - 50144 Florence - Italy  
<http://www.fupress.com/substantia>

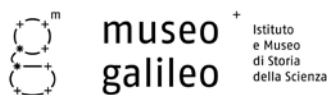
Direttore Responsabile: **Romeo Perrotta**, University of Florence, Italy

Cover image: Differential Interference Contrast micrograph (magnification 40x) from a sodium vanadate crystal, by Keith Yagaloff Ph.D., Hoffmann-La Roche, Nutley, New Jersey, USA. Courtesy of Nikon Small World (8th Place, 1995 Photomicrography Competition, <https://www.nikonsmallworld.com>).

**Copyright** © 2019 **Authors**. The authors retain all rights to the original work without any restriction.

**Open Access**. This issue is distributed under the terms of the [Creative Commons Attribution 4.0 International License \(CC-BY-4.0\)](https://creativecommons.org/licenses/by/4.0/) which permits unrestricted use, distribution, and reproduction in any medium, provided you give appropriate credit to the original author(s) and the source, provide a link to the Creative Commons license, and indicate if changes were made. The Creative Commons Public Domain Dedication (CC0 1.0) waiver applies to the data made available in this issue, unless otherwise stated.

*Substantia* is honoured to declare the patronage of:



Istituto  
e Museo  
di Storia  
della Scienza

Museo Galileo - Institute and Museum of the History of Science  
Piazza dei Giudici, 1 - 50122 Florence, Italy  
<http://www.museogalileo.it>



Fondazione Prof. Enzo Ferroni - Onlus  
Via della Lastruccia, 3  
50019 Sesto Fiorentino, Italy  
<http://www.fondazioneferroni.it>



UNIVERSITÀ  
DEGLI STUDI  
FIRENZE

DIPARTIMENTO  
DI CHIMICA  
"UGO SCHIFF"

With the financial support of:



Fondazione Cassa di Risparmio di Firenze,  
Via M. Bufalini 6 - 50121 Firenze, Italy



# Substantia

An International Journal of the  
History of Chemistry

## No walls. Just bridges

*Substantia* is a peer-reviewed, academic international journal dedicated to traditional perspectives as well as innovative and synergistic implications of history and philosophy of Chemistry.

It is meant to be a crucible for discussions on science, on making science and its outcomes.

*Substantia* hosts discussions on the connections between chemistry and other horizons of human activities, and on the historical aspects of chemistry.

*Substantia* is published *open access* twice a year and offers top quality original full papers, essays, experimental works, reviews, biographies and dissemination manuscripts.

All contributions are in English.

### EDITOR-IN-CHIEF

#### **PIERANDREA LO NOSTRO**

Department of Chemistry "Ugo Schiff"

University of Florence, Italy

phone: (+39) 055 457-3010

email: [substantia@unifi.it](mailto:substantia@unifi.it) - [pierandrea.lonostro@unifi.it](mailto:pierandrea.lonostro@unifi.it)

### ASSOCIATE EDITORS



**Virginia Mazzini**

Australian National University, Australia



**Neil R. Cameron**

Monash University, Australia  
University of Warwick, UK



**Stephen Hyde**

Australian National University, Australia



**Ernst Kenndler**

University of Vienna, Austria

## SCIENTIFIC BOARD

*as of 18 November 2016*

- |   |  |  |
|---|--|--|
| <b>FERDINANDO ABBRI</b><br>University of Siena, Italy               | <b>LUIGI DEI</b><br>University of Florence, Italy                          | <b>PIERLUIGI MINARI</b><br>University of Florence, Italy               |
| <b>TITO FORTUNATO ARECCHI</b><br>University of Florence, Italy      | <b>SARAH EVERTS</b><br>C&ENews, Berlin, Germany                            | <b>JUZO NAKAYAMA</b><br>Saitama University, Japan                      |
| <b>MARCO BERETTA</b><br>University of Bologna, Italy                | <b>JUAN MANUEL GARCÍA-RUIZ</b><br>University of Granada, Spain             | <b>BARRY W. NINHAM</b><br>Australian National University,<br>Australia |
| <b>PAOLO BLASI</b><br>University of Florence, Italy                 | <b>ANDREA GOTI</b><br>University of Florence, Italy                        | <b>MARY VIRGINIA ORNA</b><br>ChemSource. Inc, USA                      |
| <b>ELENA BOUGLEUX</b><br>University of Bergamo, Italy               | <b>ANTONIO GUARNA</b><br>University of Florence, Italy                     | <b>ADRIAN V. PARSEGIAN</b><br>Univ. of Massachusetts Amherst, USA      |
| <b>SALVATORE CALIFANO</b><br>University of Florence, Italy          | <b>MARC HENRY</b><br>University of Strasbourg, France                      | <b>SETH C. RASMUSSEN</b><br>North Dakota State University, USA         |
| <b>LUIGI CAMPANELLA</b><br>University of Rome La Sapienza,<br>Italy | <b>ROALD HOFFMANN</b><br>Cornell University, USA                           | <b>ADRIAN RENNIE</b><br>University of Uppsala, Sweden                  |
| <b>ANDREA CANTINI</b><br>University of Florence, Italy              | <b>ERNST HOMBURG</b><br>University of Maastricht, The Netherlands          | <b>PIERO SARTI FANTONI</b><br>University of Florence, Italy            |
| <b>LOUIS CARUANA</b><br>Gregorian University of Rome, Italy         | <b>STEPHEN HYDE</b><br>Australian National University,<br>Australia        | <b>VINCENZO SCHETTINO</b><br>University of Florence, Italy             |
| <b>ELENA CASTELLANI</b><br>University of Florence, Italy            | <b>JUERGEN HEINRICH MAAR</b><br>Univ. Federal de Santa Catarina,<br>Brasil | <b>SILVIA SELLERI</b><br>University of Florence, Italy                 |
| <b>LUIGI CERRUTI</b><br>University of Turin, Italy                  | <b>ROBERTO LIVI</b><br>University of Florence, Italy                       | <b>BRIGITTE VAN TIGGELEN</b><br>Science History Institute, USA         |
| <b>MARTIN CHAPLIN</b><br>London South Bank University, UK           | <b>STJEPAN MARCELJA</b><br>Australian National University,<br>Australia    | <b>BARBARA VALTANCOLI</b><br>University of Florence, Italy             |
| <b>MARCO CIARDI</b><br>University of Bologna, Italy                 | <b>SIR JOHN MEURIG THOMAS</b><br>University of Cambridge, UK               | <b>RICHARD WEISS</b><br>Georgetown University, USA                     |
|   |  | <b>FRANÇOISE WINNIK</b><br>University of Helsinki, Finland             |

## EDITORIAL BOARD

- MOIRA AMBROSI**, University of Florence, Italy  
**ANTONELLA CAPPERUCCI**, University of Florence, Italy  
**LAURA COLLI**, University of Florence, Italy  
**ANNALISA GUERRI**, University of Florence, Italy

## ASSISTANT EDITOR

- DUCCIO TATINI**, University of Florence, Italy

## MANAGING EDITOR

- ALESSANDRO PIERNO**, Firenze University Press, Italy





*Substantia* proudly contributes to the celebration of 2019 as the International Year of the Periodic Table with the publication of six special issues, edited by eminent experts from our Scientific Committee:

Vincenzo Balzani, Department of Chemistry “G. Ciamician”, University of Bologna  
**An Energy Transition To Save The Planet**

Mary Virginia Orna, ChemSource, Inc., New Rochelle & Marco Fontani, Department of Chemistry “U. Schiff”, University of Florence  
**Development of the periodic system and its consequences**

Seth C. Rasmussen, Department of Chemistry and Biochemistry, North Dakota State University  
**History of Energy Technologies and Lessons for the Future**

Luigi Campanella, Department of Chemistry, “Sapienza” University of Rome  
**Open Science**

Brigitte Van Tiggelen, Science History Institute, Philadelphia; Annette Lykknes, Norwegian University of Science and Technology & Luis Moreno-Martinez, López Piñero Institute for Science Studies, University of Valencia  
**The periodic system, a history of shaping and sharing**

Marc Henry, Chimie Moléculaire du Solide Institut Le Bel, Strasbourg  
**Water in biology: What is so special about it?**



## Preface

It is a great honour for me to write these few lines of preface to the special issues of *Substantia* dedicated to the 150th anniversary of the Periodic Table by Dmitrij Mendeleev. In 2019 there are other important anniversaries besides that of the periodic table. One of these is the centenary of Primo Levi's birth. I believe these two anniversaries are strictly related, in fact *The Periodic Table* by Levi has been considered by the *Royal Institution of Great Britain* as the "best book of science ever written". It would be sufficient to recall an impressive excerpt from "Iron", a tale of the *The Periodic Table*, to acknowledge the uniqueness of this literary work:

*"We began studying physics together, and Sandro was surprised when I tried to explain to him some of the ideas that at that time I was confusedly cultivating. That the nobility of Man, acquired in a hundred centuries of trial and error, lay in making himself the conqueror of matter, and that I had enrolled in chemistry because I wanted to remain faithful to this nobility. That conquering matter is to understand it, and understanding matter is necessary to understand the universe and ourselves: and that therefore Mendeleev's Periodic Table [...] was poetry ..."*

When we designed the project related to these special issues, we had in mind Levi's work and in particular his wonderful tales that belong to *The Periodic Table*. I like to recall this homage to a chemist-writer-witness to introduce the six topics that are associated to the special volumes of *Substantia*.

As President of the University of Florence which is the owner of the publisher *Firenze University Press*, I am truly grateful to the Editors – Marc Henry, Vincenzo Balzani, Seth Rasmussen, Luigi Campanella, Mary Virginia Orna with Marco Fontani, and Brigitte Van Tiggelen with Annette Lykknes and Luis Moreno-Martinez – for accepting the invitation made by the Editor-in-Chief Pierandrea Lo Nostro and for the extraordinary work for the preparation of these special issues. Of course the choice of the six subjects was not accidental: we tried to identify some features of the chemistry realm, related for several reasons to the periodic table. They are strikingly associated to the great challenges for our future: these are water, sustainability, energy, open chemistry, the history and the educational perspectives of the periodic table.

During its long path of progress and civilisation mankind has strongly modified nature to make our planet more comfortable, but at present we must be very careful with some dramatic changes that are occurring in our Earth. Science and technology, and chemistry primarily, can help mankind to solve most of the environmental and energy problems that emerge, to



build a radically different approach from that that has prevailed in the last two centuries. It is a fantastic challenge, since for the first time we can consider nature not as a system to simply exploit, but a perfect ally for improving life conditions in the whole planet. Chemistry has already engaged and won a similar challenge when, understanding the pollution problems generated by a chaotic and rapid development, succeeded in setting up a new branch, green chemistry, that turned upside down several research topics. Now is the time to develop sustainable chemistry: the occurring events demand that chemists propose new routes and innovative approaches. In the last two centuries we have transformed immense amounts of matter from nature into waste without thinking that we were using non renewable energy sources. We have been acting as our natural resources were unlimited, but knowing that they are instead limited. Now we are realizing that it is not possible to continue along this road. Our planet and our atmosphere are made of finite materials and their consumption during the last two centuries has been impressive. Some elements that are crucial for current and future industrial countries are known to be present on Earth crust in very small amounts and their recycling from waste cannot be a choice anymore, but it is rather an obligation.

Climate is another big problem associated to the terrific changes occurring in some equilibria, both as a consequence of the violent industrial development and energy consumption. We need, and we will always need more and more, an immense amount of energy. The only solution to secure wellness to future generations is the conversion to renewable energy sources. In this view, food and water, due to the strong increment in the demographic indices, could become the true emergencies for billions of individuals. Looking at the picture I tried to draw in this short preface it becomes more clear why we selected those topics for our special issues.

I am optimistic, and I have the strong confidence that chemistry, that studies matter and its transformations, will give mankind the picklock to overcome those challenges.

We will definitely need insightful minds, creativity, knowledge and wisdom.

Luigi Dei  
President of the University of Florence



**Citation:** M. Henry (2019) Water and the periodic table. *Substantia* 3(2) Suppl. 3: 9-11. doi: 10.13128/Substantia-701

**Copyright:** © 2019 M. Henry. This is an open access, peer-reviewed article published by Firenze University Press (<http://www.fupress.com/substantia>) and distributed under the terms of the Creative Commons Attribution License, which permits unrestricted use, distribution, and reproduction in any medium, provided the original author and source are credited.

**Data Availability Statement:** All relevant data are within the paper and its Supporting Information files.

**Competing Interests:** The Author(s) declare(s) no conflict of interest.

Editorial

## Water and the periodic table

MARC HENRY

*Université de Strasbourg*  
E-mail: [henry@unistra.fr](mailto:henry@unistra.fr)

Once upon a time, there was a Russian guy named Dmitri Mendeleev (1834-1907), who became Doctor of Science in 1865 at Saint Petersburg State University for his dissertation «*On the Combinations of Water with Alcohol*», a most important mixture in eastern European countries. After becoming a teacher in this university (1867), he planned to prepare a book for his teaching and after a dream, he has envisioned the complete arrangement of the elements as a 2D-table based on the “magic” integer 8. On 6 March 1869, he made a formal presentation to the Russian Chemical Society, describing elements according to both atomic weight and valence. The role of the magic number 8 was elucidated between 1923 and 1930 through the development of quantum mechanics and new magic electron count numbers were discovered: 2 (He), 10 (Ne), 18 (Ar), 36 (Kr), 54 (Xe), 86 (Rn) and 118 (Uuo). In October 1957, a most important paper was published showing that the three most abundant elements in the universe was in that order: H, He and O.<sup>1</sup> As helium is an inert and unreactive gas, it directly follows that the most abundant molecule in the universe should be a combination of hydrogen, a monovalent atom, with oxygen, a divalent atom, i.e. a substance having a H<sub>2</sub>O stoichiometry and with a magic count of 10 electrons.

But, in order to get a better understanding of our universe, ordering chemical elements in a table is just the very first step and the next step is to consider relative chemical abundance, leading to the order: H > He > O > Ne > N > C > Si > Mg > Fe > S > Ar > Al > Ca > Na > Ni > P > Cl > Cr > Mn > K > Ti > Co. Hence, after water, we get the (H, O, N, C) quadruplet for building organic molecules followed by (O, N, C, Si, Mg, Fe) sextuplet for building meteorites. With water, organic matter and meteorites, everything is in place in the universe for the apparition of life. Obviously, as water is by far the most abundant molecule in any living cell (more than 99%), a good understanding of its physical and chemical properties becomes mandatory.

First, by looking at the ratio between Boyle temperature (temperature at which attractive and repulsive forces are in balance in gas) and molecular weight, the most cohesive molecules are found to be H<sub>2</sub>O > HF > NH<sub>3</sub> > H<sub>2</sub>

---

<sup>1</sup> E. M. Burbidge, G. R. Burbidge, W. A. Fowler, F. Hoyle, « Synthesis of the Elements in Stars », *Rev. Mod. Phys.*, **26** (1957) 547.

$> \text{HCl} > \text{H}_3\text{C-NH}_2$ .<sup>2</sup> So, after being the most abundant molecule of the universe, water is also the most cohesive one. Considering the two couples of conjugated thermodynamic variables (volume  $V$ , pressure  $p$ ) and (entropy  $S$ , temperature  $T$ ), liquid water is further characterized by many critical temperatures at a pressure close to 0,1 MPa:

$T = -42^\circ\text{C}$ : lowest limit temperature for super-cooled liquid water.

$T = -13^\circ\text{C}$ : isochoric heat capacity maximum, i.e. minimum  $C_V = \langle(\delta T)^2\rangle$  fluctuations.

$T = 0^\circ\text{C}$ : crystallization of hexagonal ice with a lower density than the liquid.

$T = 4^\circ\text{C}$ : liquid water density maximum, i. e.  $\alpha_p = \langle(\delta S)\cdot(\delta V)\rangle = \langle(\delta p)\cdot(\delta T)\rangle = \gamma_V = 0$ .

$T = 37^\circ\text{C}$ : isobaric heat capacity minimum, i.e. minimum  $C_p = \langle(\delta S)^2\rangle$  fluctuations.

$T = 46^\circ\text{C}$ : Isothermal compressibility minimum, i. e. minimum  $\kappa_T = \langle(\delta V)^2\rangle$  fluctuations.

$T = 64^\circ\text{C}$ : adiabatic compressibility minimum, i. e. maximum  $\kappa_S = \langle(\delta p)^2\rangle$  fluctuations.

$T = 100^\circ\text{C}$ : liquid water vaporization with very high latent heat of vaporization.

$T = 280^\circ\text{C}$ : highest limit temperature for superheated liquid water.

That water should be the cradle of life is thus easily understandable. So, it should be no surprise that water is also the most studied substance in science, literature and arts. Being involved in water science and research since about 40 years, I have asked to 5 scientists having a worldwide reputation to put the focus on domains where water is doomed to play major role for the next century.

I will begin by Dr. José Teixeira, a prominent scientist, expert in water physics. He will give us an overview of a highly debated issue concerning the existence of a second critical point in deeply super-cooled liquid water. Accordingly, if such a critical point really exist in the so-called “No man’s land” ( $160 \text{ K} \leq T \leq 232 \text{ K}$ ) not accessible to experiments owing to hexagonal ice nucleation, a direct consequence would be a theoretical justification for the occurrence of so many temperature minima and maxima for liquid water (see above). As a complementary reading on this crucial subject, see reference 2.

If you have never heard about *aquaphotomics*, you should read carefully the paper by E. B. van de Kraats, J. S. Munćan and R. N. Tsenkova. This novel field shifts the paradigm of seeing water in a system as a passive, inert molecule to one which can build various structures with various functionalities, giving water an active role in biological and aqueous systems. I sincerely think that

it is one of the most promising techniques for characterizing watery systems in the very near future.

As we all know, human beings are currently facing a most prominent danger owing to large climate changes on Earth. After reading the contribution of Ernst Zürcher, you will probably understand why by firing forests for producing more food, we are putting all living beings on Earth, including ourselves, in great danger. You should be aware that the current water cycle on Earth is incomplete and time is ripe for revisiting it at the light of our current knowledge. As a complementary reading to this special issue, I would suggest considering Gerald Pollack’s wonderful book about EZ-water.<sup>3</sup>

Since about 12 000 years, humanity is living near a river or a lake for agricultural as well as industrial reasons. The consequence for our very near future will be that the tiny amount of fresh liquid water on Earth will become more and more polluted. The discovery of the fact that rivers are able to undergo a self-purification process is thus of the utmost importance for future generations. More on this most fascinating subject in the contribution of W. Schwenk and C. Sutter. As a complementary reading concerning the importance of seawater, I would strongly recommend an amazing book devoted to René Quinton’s life and works, the so-called “French Darwin” at the dawn of the XX<sup>th</sup> century.<sup>4</sup>

Finally, our future is also deeply darkened by our inability to heal cancer and neurodegenerative diseases. I think that the main reason for such a failure despite billions and euros and dollars spent, is that we have not yet recognized the role played by water in a cell and that we ignore the basic physical laws responsible for life apparition on Earth. With the contribution of L. Schwartz, one of the best expert in the world in oncology, a new paradigm is proposed based on entropy and water. A possible scenario presenting how water and Earth and Sun have plotted several billions years ago for making life appear on this planet is discussed. Both authors of this contribution are fully convinced that by grounding biology into physics, new ideas for healing people will automatically emerge in the next few years.

Another subject that could have been developed in this special issue and that will take more and more importance over the next years, is related to the interaction of water with very low frequency electromagnetic fields. The scientific demonstration by experiments and theory that molecules are able to leave an electromag-

<sup>3</sup> Pollack, G. H. (2013) : « *The Fourth Phase of Water - Beyond solid, liquid and vapor* », Ebner and Sons, Seattle, USA.

<sup>4</sup> Dray, J.-F., Quattrocchi-Woison, D., Saint-Geours, Y. « *Sur les traces de René Quinton (1866-1925): sa vie, son œuvre, sa postérité en France et en Espagne* », AGAMI-Éditions, Paris (2019).

<sup>2</sup> M. Henry, *Inference : Int Rev. Sci.*, 4, n°3, March 2019; [available online](#).

netic signature in water was a real breakthrough,<sup>5</sup> as well as the confirmation by independent groups of this amazing phenomenon.<sup>6</sup> However, as we have not yet enough hindsight on such a very hot topic, I have made the choice to not include it in this special issue.

Now, going back to Mendeleev and to the celebration of the 150<sup>th</sup> anniversary of the periodic table, I would like stressing that water is probably the only substance on Earth able to carry the whole periodic table from our immediate environment into our body either as ionic species (minerals), nanobubbles (gases) or micelles (organic molecules). Consequently, a third step was needed in order to perpetuate Mendeleev's ideas by considering how water could interact with each element of the periodic table according to its oxidation state and electronegativity. This was the job of my PhD thesis<sup>7</sup> explaining how I was introduced in water chemistry and science some forty years ago. A prolongation of this work was that, in order to understand the crucial role played by water in many fields of science, a good understanding of quantum field theory was mandatory.<sup>8</sup> Accordingly, it is only by moving towards quantum field theory, that one could realize that vacuum is a more important stuff than matter. Accordingly, it is worth recalling that atoms were for Greek philosophers such as Leucippus and Democritus immaterial entities, in perfect harmony with quantum physics that see them either as waves packets (Schrödinger's viewpoint) or transcendental matrices (Heisenberg's viewpoint). Mendeleev was also on the same line of thought as the hydrogen atom hardly exists by itself. The fact that it is nevertheless potentially found in all atoms as the sole building block needed for producing the whole periodic table is then quite remarkable. If a single entity, hydrogen, is able to generate the whole material world, filled with so many different substances with quite different physical or chemical properties, a mandatory conclusion is that a hydrogen atom should be more a fruitful concept, a productive thought, than a material thing. If such is really the case, hydrogen and thus water should

also have something to do with consciousness, a fascinating line of research that have started this year<sup>9</sup> and will be continued in this journal.<sup>10</sup> So stay tuned to the *Substantia* journal, as so many good things are coming very soon.

<sup>5</sup> L. Montagnier & al. (2017), « Water Bridging Dynamics of Polymerase Chain Reaction in the Gauge Theory Paradigm of Quantum Fields », *Water MDPI*, 9, 339. doi:10.3390/w9050339.

<sup>6</sup> B. Ting Qiang & al. (2019), « Rate limiting factors for DNA transduction induced by weak electromagnetic field », *Electromagnetic Biology and Medicine*, 38:1, 55-65, DOI: 10.1080/15368378.2018.1558064.

<sup>7</sup> J.-P. Jolivet, M. Henry, J. Livage (2000), « *Metal oxide chemistry and synthesis : from solution to solid state* », John Wiley & Sons, Chichester, New-York. Based on a French version published in 1994.

<sup>8</sup> M. Henry, « *The topological and quantum structure of zoemorphic water* », in *Aqua Incognita: Why Ice Floats on Water and Galileo 400 Years on*, P. Lo Nostro & B. W. Ninham Eds, Connor Court Pub., Ballarat (2014), chap IX, pp. 197-239. See also my book in French, « *L'Eau et la Physique Quantique* », Dangles, Escalquens (2016).

<sup>9</sup> J.-P. Gerbaulet, M. Henry (2019), «The 'Consciousness- Brain' relationship», *Substantia* 3(1): 113-118. doi: 10.13128/Substantia-161.

<sup>10</sup> M. Henry, J.-P. Gerbaulet (2019) « A scientific rationale for consciousness », *Substantia* 3(2): 37-54. doi: 10.13128/Substantia-508.





**Citation:** E. B. van de Kraats, J. S. Muncan, R. N. Tsenkova (2019) Aquaphotomics - Origin, concept, applications and future perspectives. *Substantia* 3(2) Suppl. 3: 13-28. doi: 10.13128/Substantia-702

**Copyright:** © 2019 E. B. van de Kraats, J. S. Muncan, R. N. Tsenkova. This is an open access, peer-reviewed article published by Firenze University Press (<http://www.fupress.com/substantia>) and distributed under the terms of the Creative Commons Attribution License, which permits unrestricted use, distribution, and reproduction in any medium, provided the original author and source are credited.

**Data Availability Statement:** All relevant data are within the paper and its Supporting Information files.

**Competing Interests:** The Author(s) declare(s) no conflict of interest.

## Aquaphotomics Origin, concept, applications and future perspectives

EVERINE B. VAN DE KRAATS<sup>1</sup>, JELENA S. MUNČAN<sup>2,3</sup>, ROUMIANA N. TSENKOVA<sup>3,\*</sup>

<sup>1</sup> *Water Research Lab, Heidelberg, Germany*

<sup>2</sup> *Biomedical Engineering, Faculty of Mechanical Engineering, University of Belgrade, Serbia*

<sup>3</sup> *Biomeasurement Technology Laboratory, Graduate School of Agriculture Science, Kobe University, Japan*

\*Corresponding author. E-mail: [everine.van.de.kraats@gmail.com](mailto:everine.van.de.kraats@gmail.com), [jmuncan@people.kobe-u.ac.jp](mailto:jmuncan@people.kobe-u.ac.jp), [rtsen@kobe-u.ac.jp](mailto:rtsen@kobe-u.ac.jp)

**Abstract.** Aquaphotomics is a novel scientific discipline which has made rapid progress in just 14 years since its establishment in 2005. The main novelty of this field using spectroscopy is placing the focus on water, as a complex molecular matrix and an integral part of any aqueous system. Water is sensitive to any change the system experiences – external or internal. As such, the molecular structure of water revealed through its interaction with light of all frequencies becomes a source of information about the state of the system, an integrative marker of system dynamics. This novel field shifts the paradigm of seeing water in a system as a passive, inert molecule to one which can build various structures with various functionalities, giving water an active role in biological and aqueous systems. Owing to the high sensitivity of hydrogen bonds, the water molecules are incredibly adaptive to their surroundings, reshaping and adjusting in response to changes of the aqueous or biological systems, and this property in aquaphotomics is utilized as a key principle for various purposes of bio-measurements, bio-diagnostics and biomonitoring. This paper will present the origin and concept of aquaphotomics and will, through a series of examples of applications, illustrate many opportunities and directions opened for novel scientific and technological developments.

**Keywords.** Aquaphotomics, spectroscopy, water, light, bio-measurements.

---

### 1. ORIGIN OF THE NEW SCIENCE

The concept of aquaphotomics grew during years of experience with near-infrared (NIR) spectroscopy and mammary gland disease in cows (mastitis). First realizations about the role of water determining the state of biological systems were made by Roumiana Tsenkova, professor of bio engineering at Kobe University, Japan, during her early works at Hokkaido University while studying biological systems in-vivo with near infrared spectroscopy.

In 1996, when Roumiana Tsenkova moved from Hokkaido University to Kobe University in Japan with a five-year grant in Animal Husbandry,



further investigations started at Kobe University and four other teams in Japan. The findings of this project opened the avenue for investigating water molecular systems in the biological world. She discovered that the water molecular matrix of milk and body fluids changes with inflammation of the mammary gland (mastitis) in dairy cows. In 2001, the seed of aquaphotomics was planted with a paper where R. Tsenkova and colleagues had applied NIR spectroscopy to measure milk proteins of healthy and mastitic cows.<sup>1</sup> They applied chemometrics and found that the two groups had different regression models for protein measurement and somatic cell count and that their average spectra differed in the area of water absorbance bands, which meant that the water structures, shaped by proteins and cells, changed with the disease. This was the first publication showing that water, acting as a biological/chemical matrix, can tell if a system is healthy or diseased. That was the time when the term water matrix started to be in use to denote water as a molecular network consisting of different water molecular structures that cause different behavior inside a system.

During those years, aquaphotomics basic spectroscopic experiments on water were performed as well by adding molecules or changing temperature or humidity or measuring water repeatedly and observing how the water spectrum changed at certain specific wavelength ranges.

One of the most spectacular observations from these early years was that the absorbance spectrum of water changed with consecutive measurements (in aquaphotomics called illumination perturbations). This result was first presented at the International NIRS conference in the year 2000 in Korea. Reactions varied from “I knew somebody would do it” and being interested to explore further, to “If this is true I will quit my job” because in conventional physical chemistry it is expected that good instruments will acquire the same spectra repeatedly. The fact that light changes the water seemed extraordinary and the exploration into the water spectrum as a source of information continued.

Further investigations were performed on cells, plants, and animals. Similar spectroscopic patterns, meaning similar absorbance bands changed when perturbations were introduced on other investigated systems. The realization emerged that the water absorbance bands (WABs) in the found patterns were related to the same wavelength ranges that were influenced in the basic water experiments performed earlier. These wavelength ranges were presented as water matrix coordinates (WAMACs), a new term introduced to denote the ranges in the electromagnetic (EM) spectrum where

measured absorbance of biological and aqueous systems changed due to perturbations, providing information about particular water structures and water functionality.<sup>2</sup> Conventionally, only a few symmetric and asymmetric stretching vibration assignments of water molecules are known in the first overtone of water OH stretching vibrations for pure water systems.<sup>3</sup> However, the experimentally found patterns presented 12 ranges, see Figure 1 for a schematic depiction of those wavelength ranges (WAMACs).

It must be noted that these ranges are not completely fixed and new bands or extensions of the bands have been and will be found in further explorations with other systems and perturbations. It is tempting to try to assign the WAMACs to particular water structures, as has been done in various aquaphotomics publications.<sup>2</sup> In the NIR range, for such endeavors the found bands in wavelengths ( $x$  nm) are multiplied by an integer  $o$ , representing the expected overtone of the fundamental band of water structures (usually  $o$  is two for the first overtone), and converted into wavenumbers ( $y$   $\text{cm}^{-1}$ ) through the following formula:  $y$   $\text{cm}^{-1} = 10,000,000 / (o \cdot x)$  nm (adapted from  $\tilde{\nu} = 1/\lambda$ ) and subsequently searched in literature for known assignments. However, since water vibrational modes and water inter- and intra-molecular bonding is complex and one system of molecules will entertain numerous types of water vibrations and inter and intramolecular bonding, it is usual that overlapping and shifting occurs and more than one band will respond to a change in the water matrix. Consequently,

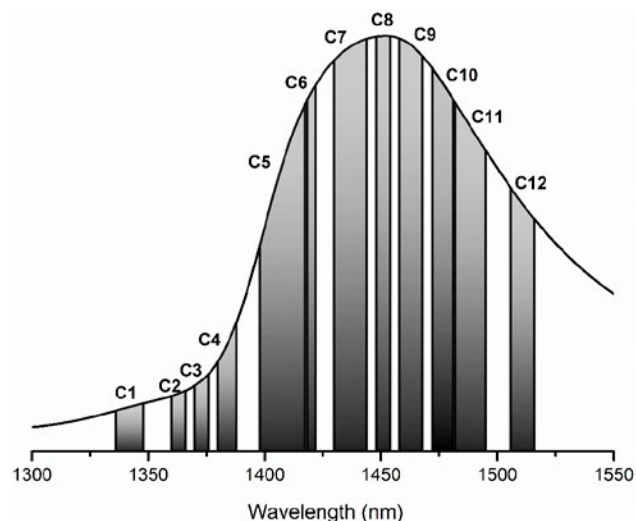


**Figure 1.** Schematic depiction of the water matrix coordinates (WAMACs), which are the wavelength ranges where the spectral absorption changes most in bio-aqueous systems due to perturbations.<sup>4</sup>

it is suggested not only to find assignments based on water molecular structures, but to work with the ‘activated’ water bands as ‘letters’ creating ‘words’ that can be assigned to a functionality per system–perturbation combination.<sup>5</sup>

‘Activated’ water bands are found through aquaphotomics analysis where the steps of the analysis, such as raw data inspection, conventional and chemometric analyses, provide certain quantitative outputs such as derivatives, subtracted spectra, regression vectors or loading vectors, discriminating power and others, which all unravel the water absorbance bands most affected by the perturbation of interest.<sup>6</sup> The spectra of aqueous systems are very complex, and changes caused by any perturbation will usually be subtle, but nonetheless persistent and consistent. Acquiring spectra under a certain perturbation without stabilizing the influence of other factors provides more spectral variations and therefore a robust model for water functionality related to examined perturbation. Averaging towards the main perturbation and subtracting of the average spectra is the first source of information about the specific bands that relate to the highest absorbance variations induced by the perturbation of interest. From all the water absorbance bands discovered during the multiple steps of aquaphotomics analysis, common absorbance bands will emerge to reveal perturbation-induced light absorbance pattern at specific water absorbance bands. In this way, aquaphotomics analysis provides a link between the observed water absorbance bands and the water functionality in the respective system.

Experience and studying the patterns in this ‘vocabulary’ of all observed system-perturbation combinations can result in assignment of certain WAMACs to water structural behavior, see the often seen ‘assignments’ based on R. Tsenkova’s experimental data in Table 1.

Water is such a common element that the same ‘bands’ can be found in spectra of crystals as well as liquids and other (bio) systems. In this way, the building of the aquaphotome, which consists of the water absorbance bands and water spectral patterns (WASPs) related to specific states or dynamics of various systems, started.<sup>2</sup>

Every system–perturbation combination has its unique aquaphotome, i.e. the spectral pattern produced by the respective system under the respective perturbation. Aquaphotomes build up the aquaphotome database that contains all the respective WASPs of various systems under various chemical, physical, mechanical, biological, etc. perturbations.

To illustrate this, two entries in the aquaphotome database, for the wavelength range 1300-1600 nm, representing two system–perturbation combinations, in this

**Table 1.** The 12 WAMACs, their corresponding wavelength ranges, and the general ‘assignments’ often seen in R. Tsenkova’s experimental data. They are in good agreement with the respective published assigned bands in IR range.

| WAMAC | Wavelength range |            | General ‘assignment’  |
|-------|------------------|------------|---|
| C1    | 1336-1348 nm     | vapor like | H <sub>2</sub> O asymmetric stretching vibration<br>Protonated water clusters   |
| C2    | 1360-1366 nm     |            | Hydroxylated water clusters<br>Water solvation shell  |
| C3    | 1370-1379 nm     |            | H <sub>2</sub> O symmetrical stretching vibration and H <sub>2</sub> O asymmetric stretching vibration                              |
| C4    | 1380-1388 nm     |            | Water solvation shell<br>Hydrated superoxide clusters   |
| C5    | 1392-1412 nm     |            | S <sub>0</sub> : Trapped and Free water   |
| C6    | 1421-1430 nm     |            | Water hydration   |
| C7    | 1432-1444 nm     | bulk water | H <sub>3</sub> O (Hydronium)<br>S1: Water molecules with 1 hydrogen bond (dimer)  |
| C8    | 1448-1458 nm     |            | Protein transfer mode in acidic aqueous solutions<br>Water solvation shell  |
| C9    | 1460-1464 nm     |            | S <sub>2</sub> : Water molecules with 2 hydrogen bonds (trimer)   |
| C10   | 1472-1482 nm     |            | S <sub>3</sub> : Water molecules with 3 hydrogen bonds (tetramer)<br>H <sub>3</sub> O <sub>2</sub><br>H <sub>5</sub> O <sub>2</sub> |
| C11   | 1492-1494 nm     | ice like   | S <sub>4</sub> : Water molecules with 4 hydrogen bonds (pentamer)   |
| C12   | 1506-1516 nm     |            | Strongly bound water  |

case cow’s milk – degree of increasing mastitis and water – increasing temperature, are provided in Table 2<sup>2</sup>.

Finally, in 2005, R. Tsenkova proposed the establishment of aquaphotomics<sup>2,9-11</sup> as a new scientific discipline complementary to other “omics” disciplines, with the aim to study water in aqueous and biological systems, using light as a probe and a spectrum, which results from their interaction, as a source of information about the system.

Systematization of knowledge about water from the aquaphotomics research studies and experience in working with various aqueous and biological systems showed that water-light interaction over the entire EM spectrum can significantly contribute to the field of water science and provide better understanding of water molecular systems, and most importantly that it leads to the development of new technologies and applications.<sup>2</sup>

**Table 2.** Example of two entries in the aquaphotome database in the NIR region (1<sup>st</sup> overtone of water OH stretching vibrations, 1300-1600 nm) showing how development of mastitis influences the water matrix of milk and how increasing temperature influences the water matrix of ultrapure water.

| WAMACS |    |    |    |             |    |             |    |    |     |             |     | Perturbation | System                           |                               |
|--------|----|----|----|-------------|----|-------------|----|----|-----|-------------|-----|--------------|----------------------------------|-------------------------------|
| C1     | C2 | C3 | C4 | C5          | C6 | C7          | C8 | C9 | C10 | C11         | C12 |              |                                  |                               |
|        |    |    |    | 1416nm down |    | 1436nm down |    |    |     |             |     |              | Degree of mastitis increasing    | Cow's milk <sup>7</sup>       |
|        |    |    |    | 1410nm up   |    |             |    |    |     | 1492nm down |     |              | Temperature increasing (6-80 °C) | Ultra-pure water <sup>8</sup> |

## 2. SETTING THE STAGE

### 2.1. Aquaphotomics: Water – From passive to active component

The early aquaphotomics works were based on near-infrared spectroscopy. The analysis of water in this field was present since its inception,<sup>12-14</sup> but at that time water was still not considered as a molecular network system or a biologically relevant matrix.

In fact, for years, water has been described as the 'greatest enemy' of infrared (IR) and NIR spectroscopy on account of its dominant absorption. This attitude was a result of, at that time general, dominant opinion in biological sciences that water is an inert, passive medium. Living processes were described in terms of genes, DNA, proteins, metabolites or other single biomolecules acting as entities isolated from water. Research methods were focused on extracting information related to the structure of these biomolecules, and in the near infrared region dominant absorbance of water was seen as an obstacle to observing their absorbance bands. However, the field of water science has seen significant progress in the last decades which has changed the general opinion about water and its role in the living systems.<sup>15-19</sup>

Today, we are witnessing a paradigm shift – water is recognized as an active solvent, adapting its structure to the solutes that it accommodates, and in biological systems, water is seen as a biomolecule in its own right with an active role in the dynamics of biomolecular processes.<sup>2,7,17</sup>

### 2.2. Aquaphotomics: From a segmented to a global water-mirror approach

The main aim of the aquaphotomics field is to understand the role of the water molecular network in biological and aqueous systems by monitoring the interaction with light in the broadest sense, and investigating the whole EM spectrum of those systems under various

perturbations. The name of this discipline is composed of three words: aqua – water, photo – light, and *omics*-all about something.<sup>2</sup>

Aquaphotomics presents the water spectral pattern as a multidimensional, integrative marker related directly to the respective system functionality. The foundation stone of aquaphotomics is a discovery that water in biological and aqueous systems works as a 'mirror' of the components and environment (matter and energy) and therefore its spectral pattern can be used to characterize the system as a whole. This is also called the WAter Mirror Approach (WAMA) (Figure 2).<sup>2</sup>

Water is an invaluable resource for human health, food security, sustainable development, and the environment. Understanding the role of water in aqueous and biological systems is of crucial importance. Historically, water properties have been extensively studied using a variety of methods from X-ray to THz spectroscopy. However, even if these techniques provide valuable information on water molecules, they generally focus on water as an isolated/separate chemical and physical subject only, in contrast to focusing on water as an interdependent connected active and 'functional' system, interrelated to its environment. There are no isolated systems in nature.

Likewise, from biological sciences point of view, up to recently, biologists have been focusing on pinpointing single biomolecules related to natural phenomena, without considering the contribution of all components of the system, and especially without considering water.

However, the function of single biomolecules is highly related to their molecular structure, which in turn is influenced by all components of the system, therefore biomolecules are not to be seen as separate from surrounding components. Moreover, their molecular structure is highly related to the creation of hydrogen bonds with the surrounding water molecules.

Therefore, in aquaphotomics, the water molecular structure of a bio-aqueous system is considered as a global 'mirror' reflecting the state, dynamics, behavior and 'functionality' of the respective system.



**Figure 2.** Water Mirror Approach: Just like the surface of the lake reflects its surroundings, the water on a molecular level is behaving like a mirror – its spectrum reflecting all the molecular components and influences of surrounding energies.

### 2.3. *Aquaphotomics: From single disciplinary to multidisciplinary approach*

Water has been studied by different disciplines in many different ways and all of them use their own particular terminology. It is quite difficult to translate scientific findings from one area into another. Aquaphotomics provides an opportunity to start building up a “water vocabulary”<sup>5</sup> where the water vibrational frequencies, i.e. water absorbance bands (WABs) are the “letters”, and the water absorbance spectral patterns (WASPs) are the “words” identifying different phenomena in order to translate findings of water between different disciplines. These letters and words create fingerprints that are stored in the aquaphotome database, per bio aqueous system and ‘perturbation’, which can be physical (tem-

perature, humidity, pressure, electromagnetic radiation, and so on), biological (disease, certain enzymes, DNA, and so on), or chemical (concentration of salts, and so on) (as presented in Table 2).

### 2.4. *Aquaphotomics: From a reductionist to a global and integrative approach*

Genomics, proteomics, metabolomics, and other “omics” disciplines have revolutionized life science. However, these disciplines study isolated elements, therefore reducing the system to its parts.

Systems biology and other functional “omics” disciplines integrate proteomics, transcriptomics and metabolomics information to provide a better understanding

of cellular biology, thereby taking a more integrative approach, but still integrating isolated elements.

Aquaphotomics is introduced as a global and integrative approach (Figure 3). All elements investigated in other “omics” disciplines can also be investigated through measurements of the water that surrounds them, an ‘indirect’ type of measurements where water serves as a sensor and an amplifier.<sup>20</sup> The status, dynamics, and functionality of an intact system can also be measured directly with aquaphotomics, without reducing the system to its parts, by e.g. measuring the skin, the leaf and so on.

### 2.5. Aquaphotomics: From a static, destructive/invasive to a dynamic, non-destructive/non-invasive approach

In “omics” disciplines such as genomics or proteomics, creating databases and further using them for understanding biological processes, requires isolation of individual elements (genes, proteins) one at a time, making such analyses extremely time-consuming and laborious. It requires the destruction of the analyzed object and thus provides only a single time-point (static) picture of the processes. Considering the speed, plasticity and multifactor-dependence of biological processes it is clear that such static one-at-a-time approach should be complemented with more dynamic and real-time methods.

The aspect of dynamics has been partly addressed by metabolomic profiling, where a snapshot of the physiology of the cell at a specific moment can be acquired.

Even though metabolomics and aquaphotomics are taking completely different approaches, they try to solve the same problem – to provide a systematic view of the processes with time-dependent information of their interconnections. In contrast to metabolomics, aquaphotomics does not destroy the sample with the measurement, therefore it can study the same object **fast, non-destructively, non-invasively and continuously**, thereby it is able to **monitor ongoing processes dynamically**.

Through an understanding of water–light interaction dynamics and its relation to biological functions, aquaphotomics brings together the knowledge acquired by other “omics” disciplines describing single elements of biological systems and upgrades it to a systemic, integrated level as water does in biological and aqueous systems.

### 2.6. Aquaphotomics: Relationship to conventional spectroscopy

The aquaphotomics approach is complimentary to the conventional spectroscopy approaches, too. In most of the VIS-NIR-IR spectroscopy studies, the water absorption bands are considered as masking the real information. For example, in order to measure bio molecules like proteins and glucose, water is evaporated in order to “see” better the absorbance bands of glucose.

In contrast, in aquaphotomics, the **water spectral pattern** is considered as **the main source of information. Water is the matrix, the “envelope”, the “scaffold” of the system.**<sup>21</sup>

## Omics disciplines: Reductionistic approach



monitoring **single parameters**



## Aquaphotomics: Integrative approach



monitoring **water molecular system**

**Figure 3.** Aquaphotomics encompasses all other “omics” disciplines, providing an integrative approach to studying aqueous and biological systems.



In aquaphotomics, the ‘functionality’, the biological state, the biological reaction to a change (dynamics) of the bio-aqueous system is the key, instead of the presence of individual molecules.

In most conventional spectroscopy studies, quantitative models are made for each separate component to be used to diagnose a system, where combining the models multiplies the errors thereby producing inaccurate results. In aquaphotomics, instead of looking for the individual components, the water spectral pattern is used as a global marker, and monitoring this marker can provide information about changes in the system.

In aquaphotomics analysis, specific water molecular structures (presented as water spectral patterns) are related to the status, dynamics and ‘function’ of the bio aqueous systems studied, thereby building an aquaphotome – a database of water spectral patterns correlating water molecular structures to specific ‘perturbations’ (disease state, contamination state, reaction to light, change in temperature, and so on). The process of extracting information from water spectra in aquaphotomics requires a field-specific approach.<sup>6</sup>

### 3. APPLICATIONS

Aquaphotomics is well developed in the visible and near-infrared range of the spectrum. Aquaphotomics is used for fundamental studies as well as many field applications, where various spectroscopic techniques and measurements setups and devices can be applied, such as transmission and transfection spectroscopy, using handheld devices or benchtop systems.

The NIR range is especially suitable, the perfect window for non-invasive measurements of aqueous systems and living biological systems, as NIR light can penetrate deep (1-10 mm)<sup>22</sup> into the aqueous systems, and does not get fully absorbed, making it possible to measure the transfectance spectrum of the light that comes back out of the bio-aqueous system after interacting with the water and other components of the system.

In the next sections, a brief overview of the various areas of aquaphotomics applications will be given.

#### 3.1. Basic studies and solute measurements and analysis

It is well established that different water species, for example, water dimers, trimers, hydration and solvation shells, contribute very specifically to the spectrum.<sup>23–25</sup> The changes in water spectrum accurately and sensitively reflect the changes of water molecular species, hydrogen bonding and charges of the solvated and solvent mol-

ecules or clusters. Big data sets of water spectra acquired under various perturbations reveal immense information about the water molecular system dynamics and the role of water in bio-aqueous systems (‘functionality’).

One of the proof-of-concept studies showing that water behaves as a mirror on a molecular level had an objective of measuring concentrations of different salts ranging from 0.002 to 0.1 mol/L.<sup>26</sup> Salts were used to demonstrate the water mirror approach since they do not have absorption bands in the NIR range, therefore any result would be entirely due to changes of water matrix in response to perturbations of salts at different concentrations. This was also the first work using NIRS to examine the effect of salts in such low concentrations. In a multi-center study, with three different locations and three different spectrometer systems, it was demonstrated that the water mirror approach of aquaphotomics enabled predictions of concentrations with a limit of detection at 1000 ppm level, which indicates that under specified conditions, aquaphotomics approach improved the detection limit for NIRS around five times.<sup>27</sup>

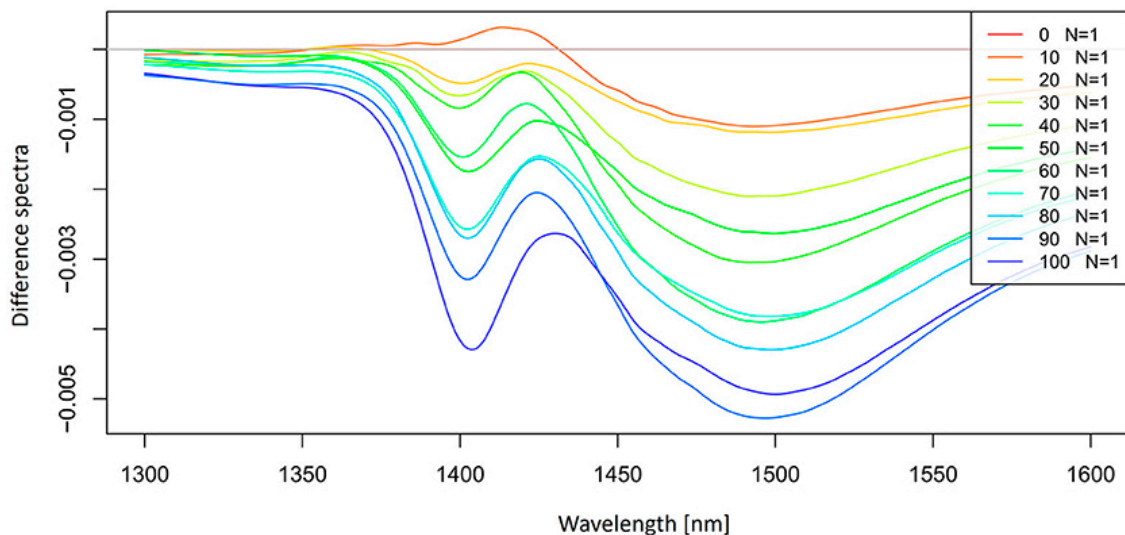
A recent paper on the essentials of aquaphotomics explains the details of the experimental methodology, chemometric tools aquaphotomics uses and how the information on changes of the water matrix in response to perturbation of interest can be extracted from the complex water spectra.<sup>6</sup> This paper shows how simple tools, such as spectra subtraction can reveal that salts (potassium-chloride in the concentration range of 10-100 mM) do change the water molecular system and that change is reflected in the absorbance spectra of salt solutions (Figure 4).<sup>6</sup>

Figure 5 shows the aquagrams corresponding to those solutions. Aquagrams are a visual representation of a WASP – this type of graphs displays the normalized absorbance values at the selected WABs. Aquagrams are very convenient visual tools to explore the differences between different perturbation steps, or different groups of interest.

Using the same concept, other molecules – single or in mixtures, in minute concentrations were measured such as mono- and di-saccharides.<sup>28</sup> This was the first research confirming the applicability of NIR spectroscopy for qualitative and quantitative analysis of mono- and di-saccharides at millimolar concentrations with the detection limit of 0.1-1 mM. Figure 6 shows the aquagrams for lactose in 0.02-100 mM concentration range depicting that higher concentrations of lactose increase strongly hydrogen-bonded water, i.e. act as structure makers, and decrease weakly hydrogen-bonded water.

Similar findings have been reported for proteins in solution,<sup>29</sup> metals in solution,<sup>30</sup> etc.





**Figure 4.** Difference absorbance spectra in the spectral range of 1300–1600 nm (OH first overtone) of pure water and aqueous solutions of potassium-chloride in the concentration range of 10–100 mM. The average spectrum of pure water was subtracted from the spectra of potassium-chloride solutions.<sup>6</sup>

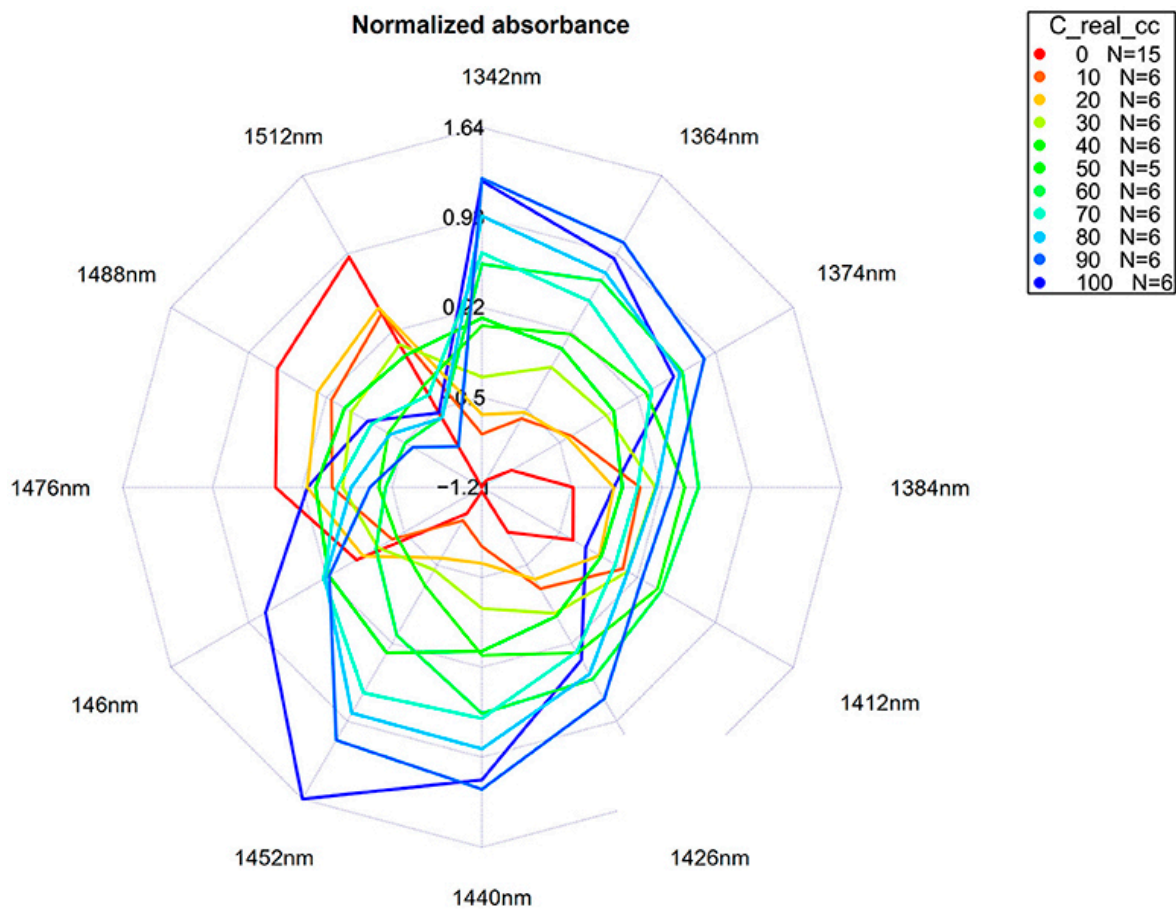


**Figure 5.** Aquagrams of aqueous solutions of potassium-chloride in the concentration range of 10–100 mM in the spectral range of 1300–1600 nm (OH first overtone).<sup>6</sup>

Contrary to the common understanding of overtone spectroscopy (100 to 1000 times lower absorbance than in the mid-IR range), it has been shown that even very small concentrations<sup>31</sup> of the solutes could be measured with NIR. The water-mirror approach provides measurements of solute concentrations previously thought impossible at ppm,<sup>30-32</sup> even ppb levels under certain experimental conditions.<sup>30,33-35</sup>

Apart from the concentration of analytes, this approach also was successfully applied to the measurement of physical parameters of water systems, such as pH and acidity,<sup>36</sup> and the effects of mechanical filtration on water.<sup>37</sup>

Thus, aquaphotomics contributed to basic knowledge about water-light interaction under perturbations and showed potential for fundamental applications.

### 3.2 Protein studies

Through work in the field of protein-water interactions, aquaphotomics provided insight into their dynamics and the significant role water plays in their functionality. One of the first studies analyzed prion protein

isoforms<sup>38</sup> – the proteins which are the cause of neurodegenerative diseases. One of the possible mechanisms of converting the protein into the misfolded form was thought to be binding of Manganese (Mn) instead of Copper (Cu). The aquaphotomics analysis of Mn and Cu prion isoforms in water solutions revealed that while binding of copper resulted in increased protein stability in water, the binding of manganese resulted in protein instability and the subsequent changes led to fibril formation.

Subsequently, another study investigated the formation of amyloid fibrils<sup>39</sup> – another type of protein linked to neurodegenerative diseases. Changes during fibrillation of insulin were monitored in 2050–2350 nm and 1300–1600 nm spectral regions, covering the bands related to protein and related to water absorption. The results showed that all the steps of conformational changes of the protein, confirmed by the results in 2050–2350 nm region were reflected also in the changes of the water molecular network in the 1300-1600 nm region (Figure 7).

These studies unquestionably demonstrated one fundamental fact – proteins and water act together – they

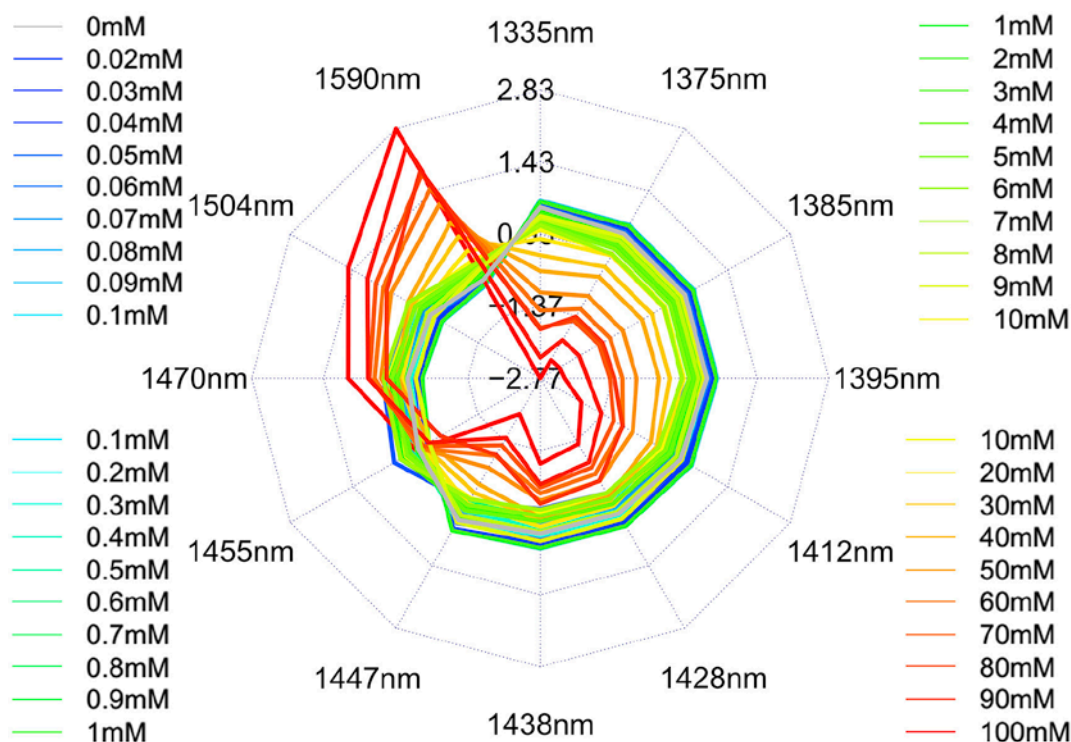


**Figure 6.** Aquagrams of lactose solutions in 0.02–100 mM concentration range. The radial axes are the 12 water matrix coordinates (WAMACs) and the dynamic changes for low to high lactose concentration from structure maker to structure breaker properties – the water spectral pattern (WASP) changes gradually and the dominance of highly hydrogen-bonded water structures increases with increasing lactose concentration. Figure is adapted from original.<sup>28</sup>

are a system. Proteins are not isolated entities in an inert medium, and all the complexity of their function in living systems can only be understood if the water is recognized as an active part of it.

### 3.3. Water quality monitoring

Water monitoring is one of the most natural applications of aquaphotomics. Since measurements of very small concentrations of solutes was proven to be achievable using salts as model systems,<sup>40</sup> the next direction of research was concerned with detection of pesticides (Alachlor and Atrazine, concentration from 1.25 – 100 ppm) which were measured with high accuracy by applying aquaphotomics principles achieving the detection limit of 12.6 ppm for Alachlor and 46.4 ppm for Atrazine.<sup>40</sup>

A great step forward in water quality monitoring was made by moving on from the detection of individual contaminants to monitoring the water by utilizing the water spectral pattern as a holistic, integrative marker.<sup>41</sup> The proposed concept has significant advantages – it allows cost-effective, reagent-free, continuous screening of water quality where even small disturbances are reflected in the water spectral pattern which serve as a signal for possible contamination, reducing the possible need for conventional solute analysis.<sup>41</sup> The concept is radically novel, because it shifts the perspective of water quality defined by a set of physico-chemical and microbiological parameters to the definition of water quality as a water spectrum within some defined limits – i.e. the spectrum integrates the influence of all single markers into one integrative, holistic marker which can be easily monitored in real time. The applicability of the proposed concept was evaluated on different types of water solu-

tions (acid, sugars, and salt served as model contaminants) as well as in real life groundwater system.<sup>41</sup>

In addition, the same principles of using the water spectrum as an integrated marker characteristic for each water was applied for discrimination of commercial mineral waters<sup>42</sup> and for discrimination of water before and after filtering as mentioned earlier.<sup>37</sup>

### 3.4. Food quality monitoring

Most fresh foods contain more than 70% water, while fresh fruits and vegetables can contain up to 95% water.<sup>43</sup> Thus the quality is deeply related to their water status. NIR spectroscopy (780 – 2500 nm wavelength region of the electromagnetic spectrum) has been used as a non-destructive tool for food quality monitoring for a long time.<sup>44</sup> It has been found that in many foods the NIR signal is dominated by the absorbance of water and multivariate analysis of NIR spectra frequently demonstrates that the water absorbance band, located around 1450 nm, is the main contributor to quality prediction.<sup>2</sup> This confirms that water status is a key indicator of food quality.

Aquaphotomics has been applied to understanding the role of water in food quality, for instance in the detection of surface damage in mushrooms,<sup>45,46</sup> quality monitoring of milk,<sup>47,48</sup> detection of honey adulteration,<sup>49</sup> monitoring of the cheese ripening,<sup>50</sup> investigating sugars in dehydration of apples<sup>51</sup> and apple sensory texture,<sup>52</sup> influence of packaging materials on cheese and winter melon<sup>53</sup> and many more.<sup>43</sup>

### 3.5. Materials and nanomaterials studies

Aquaphotomics studies on water-material interaction hold great promise in understanding some of the

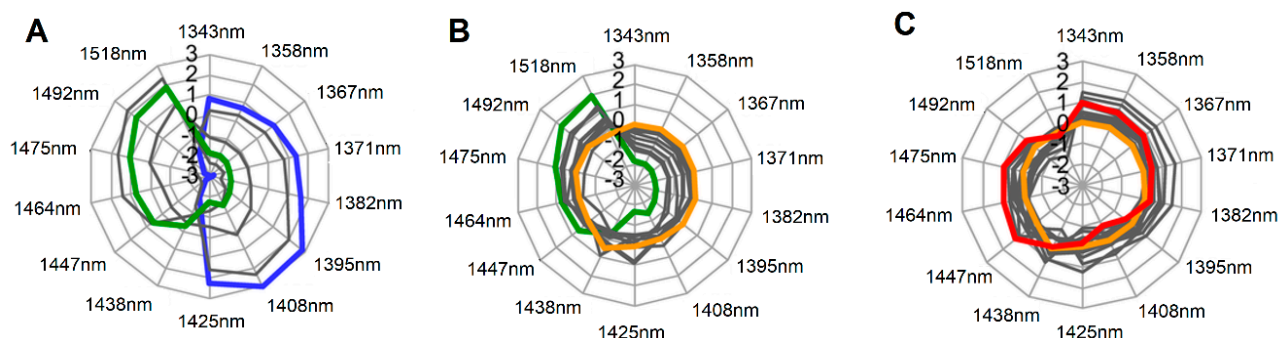


**Figure 7.** Time dependency of water spectral changes along the fibril formation process depicted by aquagrams. (A) 6 to 10 min for nucleation. (B) 10 to 18 min for elongation. (C) 18 to 30 min for the equilibrium phase. The WASP is plotted every 1 min, starting from the 6th minute, and those at 6 min, 10, 18 min and 30 min are colored by blue, green, orange, and red, respectively, the rest are colored grey. Figure adapted from original.<sup>44</sup>

very complex properties that are of interest for many applications such as wettability or biocompatibility.

Recent aquaphotomics studies utilizing time-resolved IR spectroscopy are excellent examples of other regions in EM spectra that contribute to our understanding of water-light interaction and the functionality of different water species in the biocompatibility of polymers.<sup>54–56</sup> Other studies revealed crucial importance of ratios of different water species that contribute to excellent wettability of titanium dioxide surfaces.<sup>57</sup> More recent studies explored the state of water in hydrogel materials of soft contact lenses<sup>58,59</sup> – something that was in the past exclusively done using destructive calorimetric methods, and now for the first time performed on lenses in hydrated conditions similar to physiological conditions – these studies revealed that the water spectral pattern holds information about degree of damage of polymer networks and of protein deposits on the surfaces of worn contact lenses. They show the potential of using aquaphotomics in the exploration of water and hydrophilic materials at the same time in a completely non-destructive manner.

Other aquaphotomics studies showed how nanomaterials shape the water matrix. For example, studies showed that fullerene-based nanomaterials in very low concentrations act as water structuring elements.<sup>60–62</sup> This finding may actually provide the explanation for the peculiar findings of their excellent antioxidant and radioprotective properties which far exceed theoretical calculations based solely on fullerene structure.<sup>63</sup> Similar to the findings on biomolecules and water interaction, nanomaterials, or materials in general should not be viewed as systems functioning in an isolated manner – they form a system when they interact with water, and this results in the functionality and the properties as we know them.

### 3.6. Microbiology studies

Aquaphotomics made a significant contribution to the field of microbiology by not only providing a fast and nondestructive analysis, but by contributing to better understanding of the mechanism of action of some microorganisms.<sup>64–66</sup> An example of such an application was in growth monitoring of probiotic, non-probiotic and moderate bacteria strains.<sup>65</sup> The three groups could be classified according to their probiotic strength with high accuracy – and each bacteria strain influenced the water in a specific way producing unique spectral pattern (Figure 8). The absorbance bands that contributed most to the classification were in the first overtone of water OH stretching vibrations (1300-1600 nm). Aqua-

grams of the three groups are shown in Figure 7, probiotic bacteria strains (in red) were characterized by a higher number of small protonated water clusters, free water molecules and water clusters with weak hydrogen bonds.<sup>65</sup> The discovery that strong probiotic bacteria shape water by producing more free water and less hydrogen-bonded water species, i.e. they break water structures in a way comparable to an increase in temperature, provides novel insight on their mode of action in biological organisms.

Another study showed that even in the first overtone of the combination bands of water OH stretching vibrations (1100-1300 nm) the aquaphotomics approach allows successful, rapid selection of probiotic bacteria strains.<sup>64</sup> It was shown that the differences in the water spectral pattern of different bacteria strains were related to the presence of extracellular metabolites, which have a different influence on water molecular structure.<sup>66</sup>

### 3.7. Plant biology studies

NIR spectroscopy coupled with suitable discrimination analysis provides an opportunity to gain information on the health status of plants in real time and non-destructively, even allowing a biological specimen to remain alive for continuous *in vivo* monitoring during biotic stress such as a viral infection or abiotic stresses such as cold and drought.

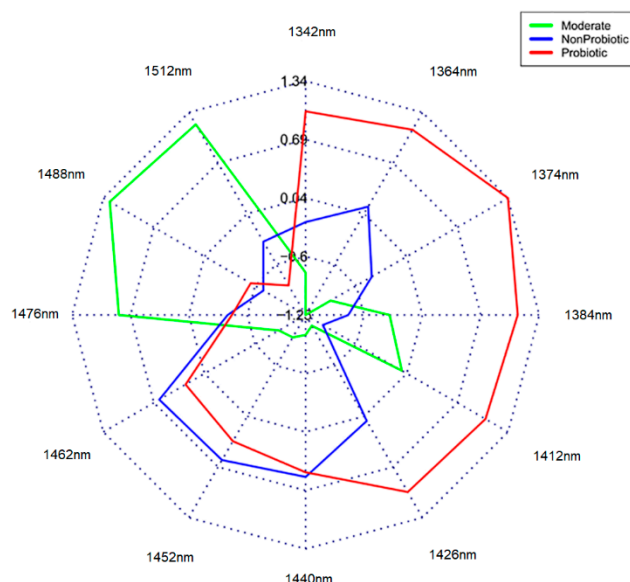


**Figure 8.** Aquagrams of culture media of groups of probiotic, moderate and non-probiotic strains. Average values of normalized absorbance values of the water matrix coordinates for each group are plotted on each wavelength axis. Figure adapted from original.<sup>65</sup>



Aquaphotomics provided a methodology to follow the impact of a virus infection based on tracking changes in water absorbance spectral patterns of leaves in soybean plants during the progression of the disease.<sup>67</sup> Compared to currently used methods such as enzyme-linked immunosorbent assay (ELISA), polymerase chain reaction (PCR), and Western blotting, aquaphotomics was unsurpassable in terms of cost-effectiveness, speed, and accuracy of detection of a viral infection. The diagnosis of soybean plants infected with soybean mosaic virus was done at the latent, symptomless stage of the disease based on the discovery of changes in the water solvation shell and weakly hydrogen-bonded water which resulted from a cumulative effect of virus-induced changes in leaf tissues. Tracking the cumulative effect of various, probably even unknown biomarkers of viral infection in leaves provided grounds for successful, early diagnosis based on aquaphotomics principles.

Similarly, different water spectral patterns were found in leaves of genetically modified soybean with different cold stress abilities.<sup>68</sup> This research on discrimination of soybean cultivars with different cold resistance abilities has proven that resistance to cold can be characterized by different water absorbance patterns of the leaves of genetically modified soybean. Again, different genetic modifications resulted in a multitude of bio-molecular events in response to cold stress, whose cumulative effect was detected as a specific water spectral pattern of leaves – i.e. the higher the cold resistance, the higher was the ability of cultivar to keep the water structure in less-hydrogen bonded state, providing a supply of “working water” in the conditions of decreased temperature.

In another study, aquaphotomics was applied for exploration of the remarkable property of extreme desiccation tolerance i.e. the ability of some plants, called resurrection plants, to survive extremely long periods in the absence of water and then to quickly and fully recover upon rewatering.<sup>69</sup> Application of aquaphotomics to study one such plant *Haberlea rhodopensis* during dehydration and rehydration processes, revealed that in comparison to its biological relative, but a non-resurrection plant species *Deinostigma eberhardtii*, *H. rhodopensis* performs fine restructuring of water in its leaves, preparing itself for the dry period. In the dry state, this plant drastically diminished free water, and accumulated water molecular dimers and water molecules with 4 bonds (Figure 9). The decrease of free water and increase of bonded water, together with regulation during drying which is directed at preservation of constant ratios of water species during rapid loss of water, was thought to be the underlying mechanism that allows preservation

of tissues against the dehydration-induced damages and ultimately the survival in the dry state, as well as resurrection to its fully functional state upon rewatering.

### 3.8. Bio-measurements, bio-diagnostics, and bio-monitoring

As briefly mentioned in the introduction, aquaphotomics was founded as a novel discipline on the applications of NIR spectroscopy for milk quality analysis and cow mastitis (mammary gland infection) diagnosis.<sup>1,33,47,70</sup> These works showed that as the various milk components change during the different stages of infection, they influence the water matrix of milk differently, therefore water spectral patterns found by the aquaphotomics analysis are suitable as a biomarker for diagnosis of mastitis.<sup>71</sup> Furthermore, for blood, and urine, it was shown that water spectral patterns were able to function as a biomarker. The water spectral patterns of blood, milk, and urine of mastitic cows, revealed that the same water absorbance bands are activated in different body fluids in response to the presence of disease.<sup>33</sup>

Not only the presence of disease can be detected using aquaphotomics principles, but also basic physi-

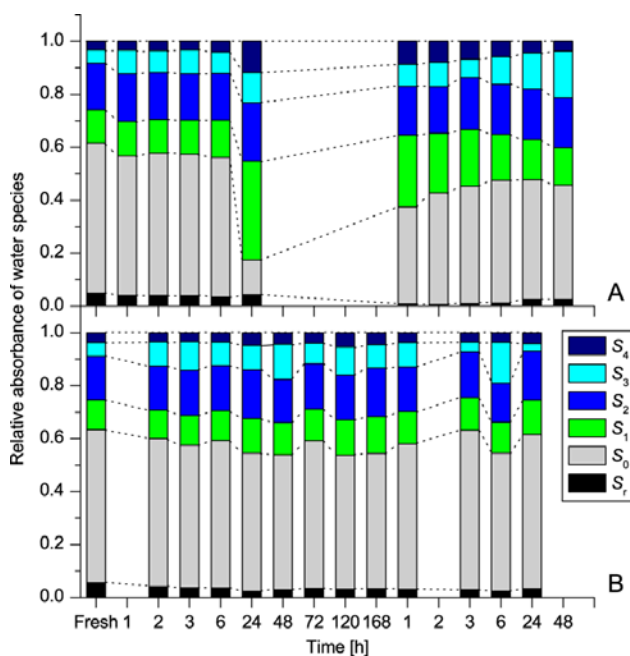


**Figure 9.** Dynamics of different water species ( $S_i$  = water molecules with  $i$  hydrogen bonds,  $S_i$  = protonated water clusters) during dehydration and rehydration of *Haberlea rhodopensis* and *Deinostigma eberhardtii*. Relative absorbance of water species in *Haberlea rhodopensis* (A) and *Deinostigma eberhardtii* (B) during desiccation and subsequent rehydration.<sup>69</sup>

ological changes can be tracked. For example, the water spectral pattern of urine was used to detect the ovulation period in the giant panda,<sup>72,73</sup> as well as in the Bornean orangutan,<sup>74</sup> and the water spectral pattern of milk was used to detect the ovulation period of dairy cows.<sup>75</sup> The method proved to be able to detect hormonal changes in a very low range (0.80 ng/ml to 127.88 n/ml)<sup>73</sup> more rapidly and therefore can be practically done more often than conventional analysis and without using reagents.

Aquaphotomics has also been applied in the human medical field, one of the earliest works utilized NIR spectra (600-1100 nm) for detection of HIV-1 virus in plasma.<sup>76</sup> The results yielded a good correlation with those obtained by the reference ELISA method sug-

gesting that this can be a rapid and accurate screening method for HIV-1 infection, and for other viral diseases too.

Feasibility of discriminating different organ tissues was shown in brain, liver, kidney and testes tissue of mice,<sup>77</sup> and detection of concentrations Cu, Mn, Fe in the same tissues was also reported.<sup>78</sup>

One of the groundbreaking works dealt with the detection of UV induced changes in DNA based on the changes in the water spectral pattern of DNA solutions.<sup>79</sup> Non-invasive identification and measurement of very low concentrations of 3D conformations of DNA were possible, see Figure 9. The formation of UV-induced cyclobutane pyrimidine dimers caused an increase of strongly hydrogen-bonded water, which has been found in previous studies to be typical for oxidative stress. Apart from the effect of UV radiation, even the dose of irradiation could be measured indirectly by the changes induced in the water spectral pattern, i.e. in the strength of water covalent bonds and other changes in the water matrix. Figure 10 shows the Y-fit and regression vector for DNA concentration.

Aquaphotomics was also proposed for *in vivo* monitoring of topical cream effects,<sup>61,62</sup> and in recent international conferences, other applications e.g. in the field of therapy monitoring have been proposed, such as dialysis efficacy, which uses a similar approach to what was used for water quality monitoring. It is expected that new publications about more aquaphotomics applications will follow. The next step with great potential is to bring these aquaphotomics applications to the market.

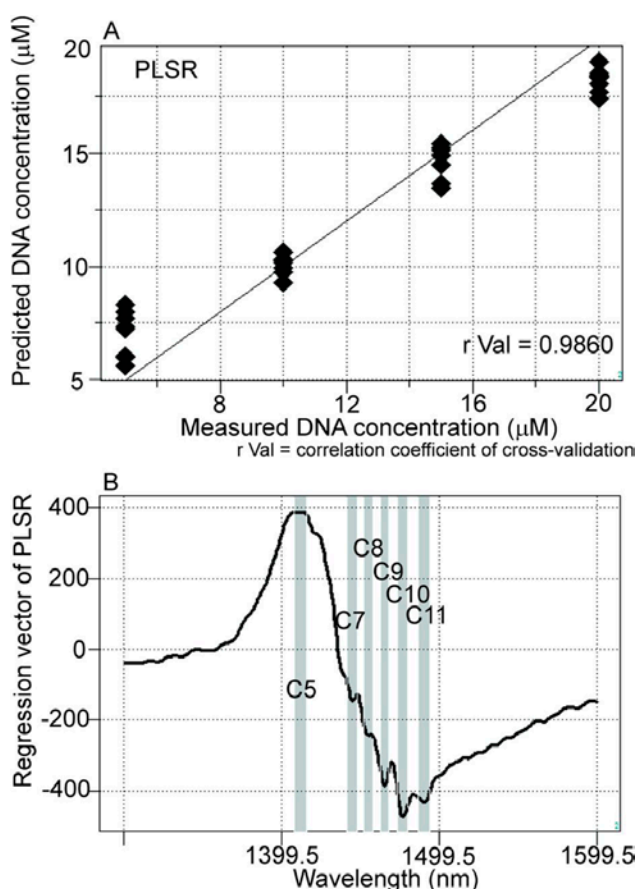


**Figure 10.** NIRs regression model for DNA concentration. (A) Y-fit for DNA concentration of partial least squares regression (PLSR) with pretreatment by mean centering, smoothing (21 points), orthogonal signal correction (OSC) (one component), and active class validation.  $N = 32$ , number of applied latent variables = 2,  $r_{\text{Cal}} = 0.9978$ ,  $\text{SEC} = 0.3882$ ,  $r_{\text{Val}} = 0.9860$ ,  $\text{SECV} = 1.5131$ . (B) Regression vector of the PLSR calibration model for DNA concentration showing characteristic water peaks at the 1400–1500 nm spectral interval.<sup>79</sup>

#### 4. CONSIDERATIONS

As water is highly influenced by its environment, depending on the required limit of detection for the application, environmental changes have to be taken into account. In previous work it has been recommended that parameters of the environment, such as temperature, pressure, humidity, should always be recorded to match every measured spectrum.<sup>6</sup> Sensitive applications for subtler changes in the water matrix may require monitoring of high and low frequency measurements, magnetic fields,  $\text{CO}_2$  levels, background radiation, and other factors such as periodical changes in the year, related to moon phases or sun spot activity, to interpret water spectral changes. All these measurements and controls are needed in order to confirm that the water spectral pattern related to each of these environmental perturbations is different from the water spectral pattern found for the perturbation of interest.



When it comes to unknown possible influences, not only environmental but also related to drift of instrument and more, it has been recommended to scan pure water samples (as environmental control) at regular intervals during the experiments.<sup>6</sup> In subsequent analysis the spectra of these pure water samples are used for correction, either by using EMSC (extended multiplicative scatter correction) using the first loading of PCA (principle component analysis) as an interferent spectrum,<sup>26</sup> or by applying a closest spectrum subtraction technique,<sup>80</sup> in order to remove environmental influences not concerning the perturbation of interest. It is not always possible to 'remove' an influence entirely, but knowing its spectral pattern will help separating it from the spectral pattern of the main perturbation. For that purpose, new data analysis methods have to be explored and developed.

## 5. FUTURE PERSPECTIVES

With the theoretical and technological advancements in spectroscopies in the entire EM range the development of aquaphotomics based applications has become more feasible. Analytical tools and data processing have improved significantly and the miniaturization of sensors on the technological side has opened up the potential for high accuracy field applications being more cost-effective at the same time.<sup>81</sup>

Also, the mentioned advantages of being non-destructive, fast and capable of comprehensive system (real-time) monitoring and diagnosis provide great potential to complement conventional technology used to perform similar tasks. As discussed in this paper, aquaphotomics can be applied in many fields, such as agriculture (plants and animals), biotechnology, life science, medicine, industry, and basic science. Further pilot studies in real-life settings, combined with market research and sensor design specific for each application will pave the way towards implementation of aquaphotomics in daily life.

In our opinion, cross-disciplinary research can also benefit from aquaphotomics by considering water as the matrix of life. Water is the bridge and provides a new common platform for science and technology,<sup>4</sup> a common 'mirror' for all disciplines. For example, the fractality and coherence of liquid water, as predicted by quantum electrodynamics, have been shown through NIR spectral analysis of the isosbestic behavior induced by temperature perturbation.<sup>82</sup> Applying the concept of aquaphotomics in this way opens up the potential for exploring systems on micro and macro level, from cells

to space. In the future, the areas of biotechnology and life science, as well as basic science of water will benefit as aquaphotomics provides a complimentary way of exploring water – through its interaction with matter and energy in real time. These interactions can be observed in various systems, such as liquids, cells, whole organisms, space, using the available technology and its upcoming advancements. A new language around water spectral patterns per system and perturbation, such as being built with the aquaphotome database, will enable new discoveries and understanding of bio aqueous systems and the role that water plays. Next steps, such as the further building of the aquaphotome database, will stimulate cross-disciplinary science and will help understand the role of water as a functional 'biomolecule' in the dynamics of life.

## 6. ACKNOWLEDGEMENTS

Author J.M. gratefully acknowledges the financial support provided by Japanese Society for Promotion of Science (P17406).

## REFERENCES

1. R. Tsenkova, S. Atanassova, S. Kawano, K. Toyoda, J. *Anim. Sci.* **2001**, 79, 2550.
2. R. Tsenkova, *J. Near Infrared Spectrosc.* **2009**, 17, 303.
3. Y. Ozaki, in *Near-infrared spectroscopy: principles, instruments, applications*, ed. by HW Siesler, Y. Ozaki, S. Kawata, HM Heise, Wiley, Chichester, UK, **2002**, Chap. 9, pp. 179–211.
4. J. Munćan, R. Tsenkova, *Molecules* **2019**, 24, 2742.
5. R. Tsenkova, *NIR news* **2009**, 20, 5.
6. R. Tsenkova, J. Munćan, B. Pollner, Z. Kovacs, *Front. Chem.* **2018**, 6, 363.
7. R. Tsenkova, *NIR news* **2008**, 19, 7.
8. V. Segtnan, S. Šašić, T. Isaksson, Y. Ozaki, S. Sasic, T. Isaksson, Y. Ozaki, *Anal. Chem.* **2001**, 73, 3153.
9. R. Tsenkova, *NIR news* **2006**, 17, 12.
10. R. Tsenkova, *NIR news* **2006**, 17, 8.
11. R. Tsenkova, *NIR news* **2006**, 17, 10.
12. T. Hirschfeld, *Appl. Spectrosc.* **1985**, 39, 740.
13. A. Grant, A. M. C. Davies, T. Bilverstone, *Analyst* **1989**, 114, 819.
14. H. Maeda, Y. Ozaki, M. Tanaka, N. Hayashi, T. Kojima, *J. Near Infrared Spectrosc.* 1995, 3, 191.
15. G. H. Pollack, I. L. Cameron, D. N. Wheatley, *Water and the Cell*, Springer, **2006**.

16. E. Del Giudice, P. R. Spinetti, A. Tedeschi, *Water* **2010**, *2*, 566.
17. P. Ball, *Chem Phys Chem* **2008**, *9*, 2677.
18. P. Ball, *Chem. Rev.* **2008**, *108*, 74.
19. M. Chaplin, *Nat. Rev. Mol. Cell Biol.* **2006**, *7*, 861.
20. R. Tsenkova, 12<sup>th</sup> International Conference on Near-infrared Spectroscopy, 514–519.
21. R. Tsenkova, Z. Kovacs, Y. Kubota, in *Membrane Hydration*, ed. by E. A. DiSalvo, Springer, Cham, **2015**, pp. 189–211.
22. J. J. Workman, L. Weyer, *Practical Guide and Spectral Atlas for Interpretive Near-Infrared Spectroscopy*, 2<sup>nd</sup> ed., CRC Press, **2012**.
23. W. H. Robertson, E. G. Diken, E. A. Price, J.-W. Shin, M. A. Johnson, *Science* **2003**, *299*, 1367.
24. Weber, Kelley, Nielsen, Ayotte, Johnson, *Science* **2000**, *287*, 2461.
25. W. A. P. Luck, W. Ditter, *J. Phys. Chem.* **1970**, *74*, 3687.
26. A. A. Gowen, F. Marini, Y. Tsuchisaka, S. De Luca, M. Bevilacqua, C. O'Donnell, G. Downey, R. Tsenkova, *Talanta* **2015**, *131*, 609.
27. C. Pasquini, *Anal. Chim. Acta* **2018**, *1026*, 8.
28. G. Bázár, Z. Kovacs, M. Tanaka, A. Furukawa, A. Nagai, M. Osawa, Y. Itakura, H. Sugiyama, R. Tsenkova, *Anal. Chim. Acta* **2015**, *896*, 52.
29. K. Murayama, K. Yamada, R. Tsenkova, Y. Wang, Y. Ozaki, *Vib. Spectrosc.* **1998**, *18*, 33.
30. A. Sakudo, R. Tsenkova, K. Tei, T. Onozuka, K. Ikuta, E. Yoshimura, T. Onodera, *Biosci. Biotechnol. Biochem.* **2006**, *70*, 1578.
31. A. A. Gowen, J. M. Amigo, R. Tsenkova, *Anal. Chim. Acta* **2013**, *759*, 8.
32. R. Tsenkova, *NIR news* **2007**, *18*, 14.
33. R. Tsenkova, *NIR news* **2008**, *19*, 7.
34. R. Tsenkova, *NIR news* **2008**, *19*, 13.
35. A. Sakudo, R. Tsenkova, T. Onozuka, K. Morita, S. Li, J. Warachit, Y. Iwabu, G. Li, T. Onodera, K. Ikuta, *Microbiol. Immunol.* **2005**, *49*, 695.
36. A. F. Omar, H. Atan, M. Z. MatJafri, *Molecules* **2012**, *17*, 7440.
37. T. M. P. Cattaneo, S. Vero, E. Napoli, V. Elia, *J. Chem. Chem. Eng.* **2011**, *5*, 1046.
38. R. N. Tsenkova, I. K. Iordanova, K. Toyoda, D. R. Brown, *Biochem. Biophys. Res. Commun.* **2004**, *325*, 1005.
39. E. Chatani, Y. Tsuchisaka, Y. Masuda, R. Tsenkova, *PLoS One* **2014**, *9*, e101997.
40. A. A. Gowen, Y. Tsuchisaka, C. O'Donnell, R. Tsenkova, *Am. J. Anal. Chem.* **2011**, *2*, 53.
41. Z. Kovacs, G. Bázár, M. Oshima, S. Shigeoka, M. Tanaka, A. Furukawa, A. Nagai, M. Osawa, Y. Itakura, R. Tsenkova, *Talanta* **2016**, *147*, 598.
42. J. S. Munćan, L. Matija, J. B. Simić-Krstić, S. S. Nijemčević, D. L. Koruga, *Hem. Ind* **2014**, *68*, 257.
43. A. A. Gowen, *Contemp. Mater.* **2012**, *1*, 31.
44. H. Büning-Pfaue, *Food Chem.* **2003**, *82*, 107.
45. A. A. Gowen, C. Esquerre, C. P. O'Donnell, G. Downey, R. Tsenkova, *J. Near Infrared Spectrosc.* **2009**, *17*, 363.
46. C. Esquerre, A. A. Gowen, C. P. O'Donnell, G. Downey, *J. Near Infrared Spectrosc.* **2009**, *17*, 353.
47. R. Tsenkova, S. Atanassova, H. Morita, K. Ikuta, K. Toyoda, I. K. Iordanova, E. Hakogi, *J. Near Infrared Spectrosc.* **2006**, *14*, 363.
48. R. Tsenkova, Near infrared spectroscopy of raw milk for cow's biomonitoring. PhD Thesis, Hokkaido University, Sapporo, Japan, **2004**.
49. G. Bázár, R. Romvári, A. Szabó, T. Somogyi, V. Éles, R. Tsenkova, *Food Chem.* **2016**, *194*, 873.
50. S. Atanassova, *Agric. Sci. Technol.* **2015**, *7*, 269.
51. R. Giangiacomo, P. Pani, S. Barzaghi, *J. Near Infrared Spectrosc.* **2009**, *17*, 329.
52. M. Vanoli, F. Lovati, M. Grassi, M. Buccheri, A. Zanella, T. M. P. Cattaneo, A. Rizzolo, *Adv. Hortic. Sci.* **2018**, *32*, 343.
53. T. M. P. Cattaneo, M. Vanoli, M. Grassi, A. Rizzolo, S. Barzaghi, *J. Near Infrared Spectrosc.* **2016**, *24*, 381.
54. M. Tanaka, T. Hayashi, S. Morita, *Polym. J.* **2013**, *45*, 701.
55. S. Morita, M. Tanaka, Y. Ozaki, *Langmuir* **2007**, *23*, 3750.
56. S. Morita, M. Tanaka, K. Kitagawa, Y. Ozaki, *J. Biomater. Sci. Polym. Ed.* **2010**, *21*, 1925.
57. T. Masato, M. Gianmario, C. Salvatore, A. Masakazu, *J. Phys. Chem. B* **2005**, *109*, 7387.
58. J. Šakota Rosić, J. Munćan, I. Mileusnić, B. Kosić, L. Matija, *Soft Mater.* **2016**, *14*, 264.
59. J. Munćan, I. Mileusnić, J. Šakota Rosić, A. Vasić-Milovanović, L. Matija, *Int. J. Polym. Sci.* **2016**, *2016*, 1.
60. L. R. Matija, R. N. Tsenkova, M. Miyazaki, K. Banba, J. S. Muncan, *FME Trans.* **2012**, *40*.
61. L. Matija, J. Muncan, I. Mileusnic, D. Koruga, in *Nano- and Microscale Drug Delivery Systems: Design and Fabrication*, ed. by Alexandru Mihai Grumezescu, Elsevier, Amsterdam, Netherlands, **2017**, Chap. 4, pp. 49–74.
62. L. Matija, R. Tsenkova, J. Munćan, M. Miyazaki, K. Banba, M. Tomić, B. Jeftić, *Adv. Mater. Res.* **2013**, *633*, 224.
63. G. V. Andrievsky, V. I. Bruskov, A. A. Tykhomirov, S. V. Gudkov, *Free Radic. Biol. Med.* **2009**, *47*, 786.
64. A. Slavchev, Z. Kovacs, H. Koshiha, G. Bazar, B. Pollner, A. Krastanov, R. Tsenkova, *J. Near Infrared Spectrosc.* **2017**, *25*, 423.

65. A. Slavchev, Z. Kovacs, H. Koshiba, A. Nagai, G. Bázár, A. Krastanov, Y. Kubota, R. Tsenkova, *PLoS One* **2015**, *10*, e0130698.
66. Y. Nakakimura, M. Vassileva, T. Stoyanchev, K. Nakai, R. Osawa, J. Kawano, R. Tsenkova, *Anal. Methods* **2012**, *4*, 1389.
67. B. Jinendra, K. Tamaki, S. Kuroki, M. Vassileva, S. Yoshida, R. Tsenkova, *Biochem. Biophys. Res. Commun.* **2010**, *397*, 685.
68. B. Jinendra, Near infrared spectroscopy and aquaphotomics: Novel tool for biotic and abiotic stress diagnosis of soybean. PhD Thesis, Kobe University, Kobe, Japan, **2011**.
69. S. Kuroki, R. Tsenkova, D. P. Moyankova, J. Muncan, H. Morita, S. Atanassova, D. Djilianov, *Sci. Rep.* **2019**, *9*, 3049.
70. R. Tsenkova, S. Atanassova, Y. Ozaki, K. Toyoda, K. Itoh, *Int. Dairy J.* **2001**, *11*, 779.
71. R. Tsenkova, *NIR news* **2006**, *17*, 13.
72. K. Kinoshita, M. Miyazaki, H. Morita, M. Vassileva, C. Tang, D. Li, O. Ishikawa, H. Kusunoki, R. Tsenkova, *Sci. Rep.* **2012**, *2*, 856.
73. K. Kinoshita, H. Morita, M. Miyazaki, N. Hama, H. Kanemitsu, H. Kawakami, P. Wang, O. Ishikawa, H. Kusunoki, R. Tsenkova, *Anal. Methods* **2010**, *2*, 1671.
74. K. Kinoshita, N. Kuze, T. Kobayashi, E. Miyakawa, H. Narita, M. Inoue-Murayama, G. Idani, R. Tsenkova, *Primates* **2016**, *57*, 51.
75. G. Takemura, G. Bázár, K. Ikuta, E. Yamaguchi, S. Ishikawa, A. Furukawa, Y. Kubota, Z. Kovács, R. Tsenkova, *Reprod. Domest. Anim.* **2015**, *50*, 522.
76. A. Sakudo, Y. Sukanuma, R. Sakima, K. Ikuta, *Clin. Chim. Acta* **2012**, *413*, 467.
77. A. Sakudo, R. Tsenkova, K. Tei, H. Morita, K. Ikuta, T. Onodera, *J. Vet. Med. Sci.* **2006**, *68*, 1375.
78. A. Sakudo, E. Yoshimura, R. Tsenkova, K. Ikuta, T. Onodera, *J. Tox. Sci.* **2007**, *32*, 135.
79. N. Goto, G. Bazar, Z. Kovacs, M. Kunisada, H. Morita, S. Kizaki, H. Sugiyama, R. Tsenkova, C. Nishigori, *Sci. Rep.* **2015**, *5*, 11808.
80. D. Kojić, R. Tsenkova, M. Yasui, *Anal. Chim. Acta* **2017**, *955*, 86.
81. C. W. Huck, *NIR news* **2017**, *28*, 17.
82. P. Renati, Z. Kovacs, A. De Ninno, R. Tsenkova, *J. Mol. Liq.* **2019**, *292*, 111449.



**Citation:** M. Henry, L. Schwartz (2019) Entropy export as the driving force of evolution. *Substantia* 3(2) Suppl. 3: 29-56. doi: 10.13128/Substantia-324

**Copyright:** © 2019 M. Henry, L. Schwartz. This is an open access, peer-reviewed article published by Firenze University Press (<http://www.fupress.com/substantia>) and distributed under the terms of the Creative Commons Attribution License, which permits unrestricted use, distribution, and reproduction in any medium, provided the original author and source are credited.

**Data Availability Statement:** All relevant data are within the paper and its Supporting Information files.

**Competing Interests:** The Author(s) declare(s) no conflict of interest.

## Entropy export as the driving force of evolution

MARC HENRY, LAURENT SCHWARTZ\*

*Assistance Publique des Hôpitaux de Paris, Paris, France*

\*Corresponding author: [dr.laurentschwartz@gmail.com](mailto:dr.laurentschwartz@gmail.com)

**Abstract.** The entropy concept was forged by the middle of the nineteenth century to predict how a chemical system may undergo spontaneous evolution over time. At the dawn of the twentieth century, four principles of a new science called “thermodynamics” have been firmly established. Concept of thermal equilibrium (zeroth law), conservation of energy (first law), spontaneous increase in entropy over time (second law) and vanishing entropy at the absolute zero of temperature (third law also called Nernst’s theorem). Among these principles, the most troublesome one was the second law that points to gases as the end final product of any evolution in a closed system. From direct observation, it seems that biological systems undergo spontaneous evolution from gases characterized by a maximum entropy to highly complex structures displaying considerably lower entropies, an apparent violation of the second law. However, it is also perfectly allowed to view the Earth as an open system able to undergo a spontaneous (local) decrease of entropy, provided that the excess entropy could be efficiently exported towards the whole universe through invisible infrared photons. Provided that the entropy exported as invisible infrared radiation is much higher than the entropy decrease observed on Earth, life apparition on this planet becomes fully compliant with thermodynamics laws. The consequences of such an enlarged viewpoint taking into account all kinds of processes (reversible as well as irreversible ones) are studied in depth in this paper. Here we advocate that the first requirement allowing spontaneous life apparition on Earth is the existence of a metabolism, taking the form of thermodynamic cycles able to generate a large output of entropy by degrading low entropy molecular systems (food) into high entropy molecular compounds (waste). Two possible cycles have been identified, relying on the very low entropy of Earth’s metallic core for generating reducing gases (such as H<sub>2</sub>, CO, NH<sub>3</sub>, H<sub>2</sub>S) coupled to the low entropy of sun’s radiation (food) and producing minerals (such as serpentine, metallic sulfide, magnetite, goethite) as well as high entropy gases (water, carbon dioxide) as waste. The large entropy flux generated by such processes can then be used to build low-entropy molecular systems based on reduced carbon species and soluble phosphates that are observed in any living cell. Another consequence of this approach is stressing the ubiquitous role played by water in every feature of life, through the concept of “water activity”.

**Keywords.** Entropy, Life, Water activity, Irreversibility, Thermodynamics, Biology.

---

## INTRODUCTION

The apparition of life is a deep rooted mystery. Life appeared on earth over 3,6 billions years ago. Life is a robust phenomenon with similar concentrations of sodium, potassium and chloride in every living cell. Moreover, similar lipoproteins constitute the membranes and the nucleic acids are always built with the same bases.

Taking the problem from the biological side, focusing on protein-trafficking related to gene activation and transcription, as currently done is a daunting task. Putting numbers on the table, a back of the envelope calculation leads to an average concentration of 3 millions of proteins per  $\mu\text{m}^3$  of cell.<sup>1</sup> This translates into 3 millions of proteins for *E. Coli* ( $V \approx 1 \text{ fL}$ ), 150 millions for budding yeast *S. cerevisiae* ( $V \approx 50 \text{ fL}$ )<sup>2</sup>, and 3 billions for a mammalian cell ( $V \approx 1 \text{ pL}$ ).<sup>3</sup> Concerning the human genome, we are facing about 18,000 genes<sup>4</sup> able producing about 100,000 different types of proteins.<sup>5</sup> Nowadays, only super-computers are able to crawl in huge databases giving rise to new research domains such as genomics, proteomics or metabolomics, epigenomics, lipidomics, glycomics, etc.

An alternative line of research is to admit that such a complexity accessible only through high-speed computers is sustained by laws deep-rooted in physics and chemistry. If this is the case, then identifying some key physicochemical variables should be enough to control cell growth and proliferation.

In deep contrast with biology, physics does not look for detailed mechanisms, facts being the mere consequences of fundamental laws given a certain set of initial conditions. The goal of this paper is to suggest that the universality of only one form of life might be the simple consequence of the second law of thermodynamics.

Such an approach is obviously complementary to the -omics strategy and would allow physicians to act on diseases without the help of computers, would also considerably reduce the number of drugs for healing patient and most importantly would allow using very cheap chemicals instead of drugs characterized by sky-rocketing prices.

The paper is organized as follows. In a first section we will go back to abiotic Hadean times where only physical and chemical events were able to take place. This will allow us to identify key physicochemical parameters that should be still operational in modern cells. The second part of the paper will be the formulation of bioenergetics in terms of irreversible entropy variations instead of energy changes.

In a third part, this new quite general formalism will be applied to prebiotic chemistry of lipids, aminoacids as well as phosphate-based compounds. Finally, a last

part will stress the important role played by the water activity in anabolism and catabolism processes.

## HADEAN TIMES

Life seems to originate with the formation of liquid water on Earth about 4,4 Gyr ago.<sup>6</sup> First forms of life as prokaryotes seem to appear about 3,8 Gyr ago.<sup>7</sup> During this first period covering 600 Myr, we have to make a mapping between what we currently know about the last universal common ancestor of all cells (LUCA) and some basic chemistry. Using phylogenetic trees for 6.1 million protein coding genes from sequenced prokaryotic genomes has allowed reconstructing the microbial ecology of LUCA.<sup>8</sup> With its 355 identified genes, LUCA could be viewed as anaerobic,  $\text{CO}_2$ -fixing,  $\text{H}_2$ -dependent (elimination of acetate via the reduction of acetyl-CoA),  $\text{N}_2$ -fixing and thermophilic. LUCA's biochemistry was replete with FeS clusters and radical reaction mechanisms. Its cofactors reveal dependence upon transition metals, flavins, S-adenosyl methionine, coenzyme A, ferredoxin, molybdopterin, corrins and selenium. Its genetic code required nucleoside modifications and S-adenosyl methionine-dependent methylations.

Our reasoning is based on the hypothesis that entropy-driven networks of small molecules ruled by thermodynamics afford better odds as the initiators of life than a set of highly complex molecules such as RNA and proteins. Among all the scenarios proposed for life apparition on earth, it appears, as explained thereafter, that the geochemical rocky route is the only one compatible with LUCA's portrait emerging from phylogenetic trees analysis. Starting from geochemistry occurring at hot, reduced, alkaline hydrothermal vents, the route leads to a prebiotic era, followed by the successive development of RNAs, RNPs, DNAs molecules as water becomes cooler, more oxidized and more acidic. This means that we may set aside the genetic definition of life to focus on a more water-based picture. The necessity of putting water at the front stage is well illustrated by figure 1 that describes the composition of the Gram-negative prokaryote *Escherichia coli* (*E. coli*).

The key point here is to focus on the molar fraction scale for quantifying the amount of matter. On such a scale, it should be obvious that life is a water-based phenomenon (99.3 mol%) with inorganic ionic species playing the major role (0.5 mol%) over organic matter (0.2 mol%). Basically, every event in a living cell appears to be orchestrated by water and ions, organic matter behavior being under the full control of these two kinds of chemical species.

Shapiro stated five requirements for the emergence of life:<sup>10</sup>

1. Existence of a membrane allowing defining compartments able to sustain ionic concentration gradients.
2. Existence of an external energy source to drive the increase in complexity and biodiversity.
3. Existence of a growing and splitting mechanism for the network allowing information duplication.
4. Existence of a chemical network able to sustain circular transformations (cycles) permitting adaptation and evolution.
5. Existence of coupling mechanisms linking the release of energy with entropy exports.

In fact some of these points have already been answered. Point #1 is by no means mandatory, as it has been demonstrated that water adjacent to hydrophilic surfaces and submitted to radiant energy from the sun or from a geothermal vent, is perfectly able to produce coalescence, order, and even function at multiple levels of organization without any enclosing membrane.<sup>11</sup> Point #2 is thus automatically solved.

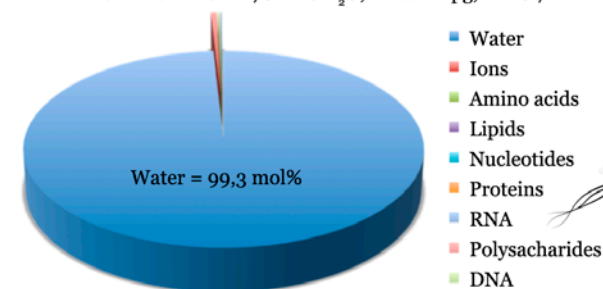
Point #3 is based on the trivial fact that a physical collection of small items holds the same information as a list that describes the items formally with a code. In other words there is no difference in terms of informa-

tion between holding ten real metallic gold coins in your pocket and holding them virtually in a bank account. In both cases, you will be able to take the same decisions on how to spend such an amount of money despite the fact that one set is purely material and the other one is completely dematerialized. There is thus no need to store information in a single molecule such as DNA (playing in the cell the role of the bank account) that have to be duplicated and passed to the descendants as observed in a modern cell. Self-replicating reverse micelles<sup>12</sup> or mere aggregates of iron sulfide bubbles<sup>13</sup> are perfectly able to do such a job (equivalent of gold coins).

Concerning point #4, it should be clear that one cannot rely on the citric acid cycle or on its reverse version owing to the difficulty of achieving all of the required reactions using only mineral catalysts.<sup>14</sup> Accordingly, there is so many side reactions in the citric acid cycle that a large number of different mineral surfaces would be needed to close the cycle. A much simpler version with fewer steps is then required. Fortunately, the existence of a proto-metabolic analog of the TCA involving two linked cycles, which convert glyoxylate into CO<sub>2</sub> has been recently evidenced.<sup>15</sup> To initiate the two cycles, only glyoxylate H-CO-COO- and pyruvate CH<sub>3</sub>-CO-COO- are needed with the help of hydrogen peroxide H<sub>2</sub>O<sub>2</sub> all reactions proceeding under

| Matter          | Number         | Molar fraction mol% |
|-----------------|----------------|---------------------|
| Water           | 23 400 000 000 | 99.3                |
| Ions            | 120 000 000    | 0.51                |
| Lipids          | 25 800 000     | 0.11                |
| Amino acids     | 6 000 000      | 0.03                |
| Proteins        | 3 600 000      | 0.02                |
| Nucleotides     | 3 530 000      | 0.02                |
| RNA             | 220 000        | 0.01                |
| Polysaccharides | 39 000         | 0.00                |
| DNA             | 1              | 0.00                |
| Total           | 23 559 000 000 | 100.00              |

*Escherichia coli* ≈ 70 wt% H<sub>2</sub>O, mass = 1 pg, V = 0.7 fL



Ions = 0,5 mol% & Org. Matt. = 0,2 mol%

Data source: <http://ccdb.wishartlab.com/index.html>

| Ion   | Concentration / mM | Number      | Mol%   |
|---|--------------------|-------------|--------|
| K <sup>+</sup>  | 225                | 94 846 500  | 74.97  |
| Fe <sup>2+</sup>  | 18                 | 7 587 720   | 6.00   |
| Mg <sup>2+</sup>  | 10                 | 4 215 400   | 3.33   |
| Cl <sup>-</sup> , Ca <sup>2+</sup>  | 6                  | 2 529 240   | 2.00   |
| Na <sup>+</sup> , H <sub>2</sub> PO <sub>4</sub> <sup>-</sup>             | 5                  | 2 107 700   | 1.67   |
| ATP <sup>4-</sup>   | 4.2                | 1 770 470   | 1.40   |
| Mn <sup>2+</sup> , Zn <sup>2+</sup> , Mo <sup>4+</sup> , Cu <sup>2+</sup> | 4                  | 1 686 160   | 1.33   |
| PEP <sup>3-</sup>   | 2.8                | 1 180 310   | 0.93   |
| Pyruvate <sup>-</sup>   | 0.9                | 379 390     | 0.30   |
| NADP <sup>3-</sup> , ADP <sup>3-</sup>                                    | 0.63               | 265 570     | 0.21   |
| NADPH <sup>4-</sup>   | 0.56               | 236 060     | 0.19   |
| G6P <sup>2-</sup>   | 0.05               | 21 080      | 0.01   |
| Proton (H <sup>+</sup> )  | 10 <sup>-4.2</sup> | 30          | 0.00   |
| Total   | 300                | 126 521 050 | 100.00 |

Concentration aa / mM, P<sub>osm</sub> = 517 kPa

Thr = 3.49  
Ala = Gly = 0.8  
Val = 0.6  
Glu = Ile = Asn = Pro = Gln = 0.5  
Lys = 0.46  
Cys = Trp = His = 0.2  
Asp = 1.34  
Ser = Tyr = Leu = 0.7  
Arg = Phe = 0.40  
Met = 0.1

297 essentials genes, 1 division after 30 min, 1 cell = 55×10<sup>9</sup> ATP

7941 proteins (translated + mature)

Glycolysis = 6-8 ATP; pyruvate oxidation = 6 ATP; Krebs cycle = 24 ATP  
1 lipid = 7 ATP; 1 protein = 360 aa = 1 500 ATP; 1 RNA = 1 000 nts = 2 000 ATP  
1 polysaccharide = 20 000 ATP; 1 DNA = 72 289 000 ATP

**Figure 1.** Molecular composition and basic energetic needs for the Gram-negative prokaryote *Escherichia coli* according to the CyberCell Database (CCDB).<sup>9</sup>



neutral aqueous conditions and at mild temperatures (figure 2). Here, the molecule oxaloacetate or 2-oxo-succinate (2-OS) is acting as a central hub allowing continuous production of either malonate (upper part) or 4-hydroxy-oxo-glutarate (lower part). So one, could speak of an 2OS-cycle fed by a GPH-flux. It was also shown that aspartic acid, a crucial aminoacid, might be produced by reacting malonate with  $\alpha$ -hydroxy-glycine ( $\alpha$ -HG). Moreover, the conversion of malate to oxaloacetate is an elementary step of the citric acid cycle. The problem now boils down to the emergence of only three chemicals: glyoxylate, pyruvate and hydrogen peroxide from inorganic species. As explained below, hydrogen peroxide is continuously produced using solar radiations, while glyoxylate and pyruvate precursors are continuously produced at the mouth of hydrothermal vents. Hydrogen peroxide plays here the role of the very first electron acceptor and glyoxylate and pyruvate, the very first electron donors. Please notice that there is no need here to invoke negative loops and regulation signals that occur in modern biological systems. Our point is that for the most primitive living cell, a few cycles and the laws of kinetics are all is needed for starting chemical oscillations, as shown by the work of Ilya Prigogine.<sup>16</sup> We should thus at this point speak a little bit of bioenergetics in order to write a plausible scenario in order to discuss point #5 more deeply. Here is a summary of the proposed reformulation of Shapiro's conditions:

1. Lipid membranes replaced by polarized multilayers of water (EZ-water) as proposed by Gilbert Ling in 1962 and Gerald H. Pollack in 2013.
2. External energy source may be of two kinds, sun or earth, as only IR radiations matter for EZ-water creation.
3. No mechanism for information duplication as only brute copying of a full set of molecules is needed.
4. Identification of a 2OS-cycle based on glyoxylate, pyruvate and hydrogen peroxide precursors (GPH-flux) for the first chemical oscillations.
5. Coupling mechanisms concerns only entropy exports as only one kind of energy (IR radiations) is used by the cell for building water layers.

#### BIOENERGETICS: THE KEY ROLE OF ENTROPY

Bioenergetics is a domain based on thermodynamics, a science that is often misinterpreted. The name "bioenergetics" is by itself quite misleading as it could make believe that evolution is ruled by energy exchanges with states of high energy evolving spontaneously into states of low energy. In fact, this cannot be, as energy

being a conserved quantity has nothing to say about spontaneous evolution. The entity giving a preferential direction to energy fluxes is in fact entropy, a state variable characterizing how energy may spread among all the available degrees of freedom. Accordingly, the second law states that entropy should always increase or remain constant in any spontaneous chemical reaction. So, faced with any chemical reaction, we should always refer to entropy variations. But referring to entropy and not to energy is not the attitude adopted by most scientists. In order to speak only in terms of energy and never refer explicitly to entropy, scientists have masqueraded the entropy concept under various expressions such as "internal energy" for adiabatic and isochoric processes, "enthalpy" for adiabatic and isobaric changes, "Helmholtz's free energy" for isothermal and isochoric changes and "Gibbs's free energy" for isothermal and isobaric processes. For open systems able to exchange both heat and matter, it is necessary to introduce chemical potentials, yet another masqueraded form of entropy. If electrons are exchanged during a transformation, entropy is again masqueraded as a redox potential.

As stated by the second law of thermodynamics, any spontaneous irreversible evolution corresponds always to an *increase* in entropy inside the system. However, the price to be paid for any internal increase in entropy is always a loss of *structure*. The reason behind such a loss of structure is merely that energy may be spread either on positions of matter particles (potential energy) or on the velocities of these matter particles (kinetic energy). In such a context, increasing its entropy means that the system spread its energy more on velocities (more kinetic energy) than on positions (less potential energy). When kinetic energies becomes larger than potential energies, chemical bonds responsible for the existence of solid as well as liquid structures break down, the volume occupied by the system becoming delimited by the container and no more by the chemical bonds.

Here, another pitfall should be avoided by speaking of loss of structure upon any entropy increase and not of a loss of *order*. A liquid has always a much smaller entropy than a gas despite the fact that both systems are completely disordered. The lower entropy of the liquid comes from the fact, positions above the liquid/gas interface are accessible only to a very small number of the constituting matter particles (vapor pressure). Similarly, a solid will always have an entropy smaller than a liquid, as constituting matter particles are doomed to remain at fixed points in space, thus being unable to occupy all the available positions in the proper volume. In a liquid, any constituting particles may be found *everywhere* in the proper volume, meaning a much greater entropy. Conse-

quently, there is absolutely no need to invoke order/disorder arguments for discussing entropy changes.

Recognizing that thermodynamic potentials are in fact masqueraded irreversible entropies of variation and definitively not energies, leads to a considerable simplification of thermodynamics. Accordingly, instead of dealing with a multitude of different kind of energies (mechanical, thermal, chemical, electrical, magnetic...), it remains only two basic types of *real* energies. First, the energy stored in electromagnetic waves or in massless photons (radiant energy). Second, the energy associated to particles having a non-zero rest mass (gravitational, kinetic and nuclear energies). All the other forms of “energies” are in fact irreversible entropy variations  $\Delta S_i$  that can be translated into energetic equivalents after multiplication by the temperature at which the transformation occurs. One may thus formally write,  $\Delta G = -T\Delta S_i$ , with a criterion of spontaneous evolution  $\Delta G \leq 0$  owing to the fact that according to the second law one should always have  $\Delta S_i \geq 0$ . As explained above, one is thus obliged to add the term “free” to the term “energy” to remember that we are dealing here with an irreversible entropy change and not with an energy change.

We thus propose here to adopt such a very convenient convention sticking closely to what is in fact really occurring during a spontaneous evolution within a system. The only fundamental law is thus that everything proceeds from a state of low entropy towards a state of high entropy. If the system is not able to export this excess of entropy towards its surroundings the entropy irreversibly grows inside the structure and at some point, the structure breaks down. Such a behavior is typical of transformations occurring in a beaker or in the universe where inert structures are doomed to disappear irreversibly after breaking down into smaller and smaller units of matter. At the end, solids and liquids evaporates leaving only a gas, which is always the state having the largest entropy for a given composition.

The situation is different, if it exists inside the system a mechanism able to export entropy from its interior towards its exterior: this means that the various components of the system should now cooperate in order to absorb compounds having the lowest possible entropies and reject in its environment compounds having the highest possible entropies. As shown by the laws of irreversible phenomena, any system being crossed by

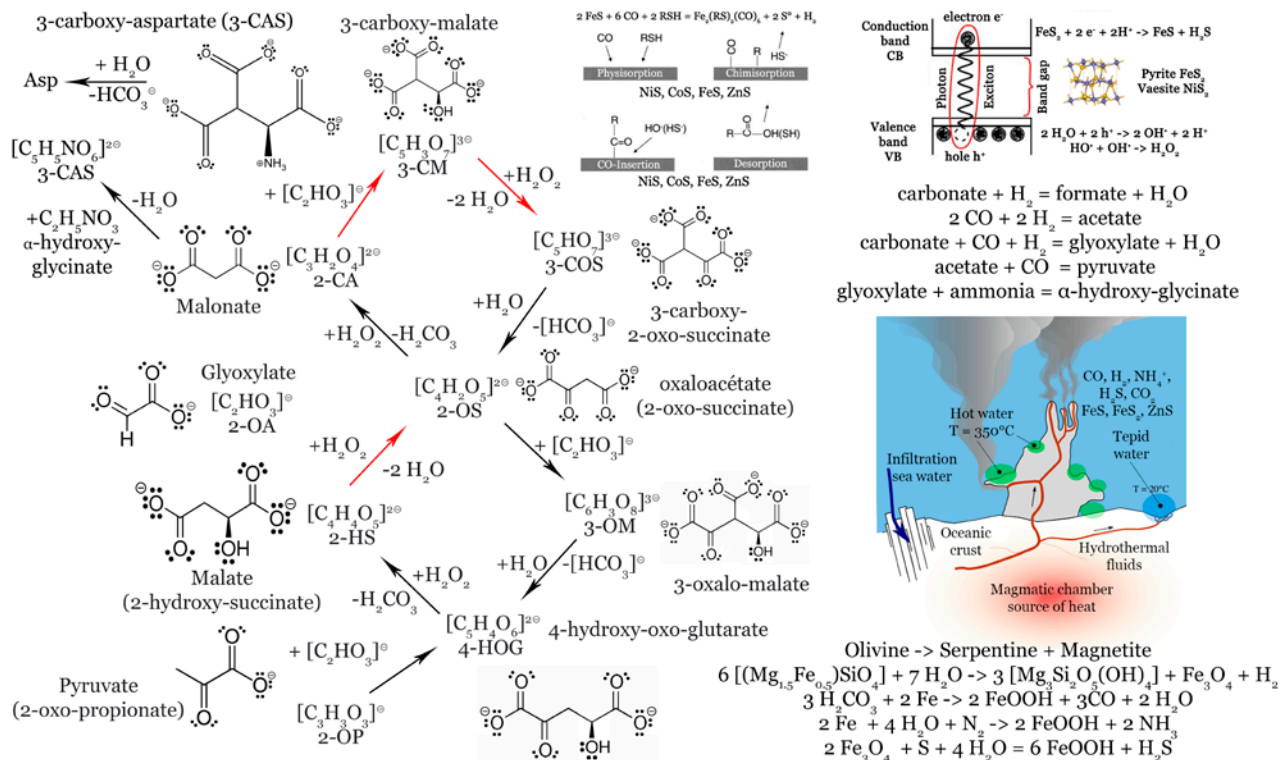


**Figure 2.** Two abiotic cycles each oxidizing glyoxylate into carbon dioxide  $\text{CO}_2$  with the regeneration of oxaloacetate, a key intermediate of the modern tricarboxylic acid cycle. Such reactions progress significantly in hours at pH values 7–8.5 at  $50^\circ\text{C}$  (red arrows) or  $23^\circ\text{C}$  without the help of enzymes.<sup>15</sup>

an irreversible flow of entropy, becomes automatically self-organized.<sup>16</sup> The higher the entropy flux, the higher the number of functional links between different parts of the system. The key point here is the unavoidable existence of fluctuations that could be organized into spatial and temporal coherent behavior (dissipative structures) when the system is brought far enough from equilibrium. Mathematically speaking, one may write the following fundamental equation for entropy variations,  $dS = d_iS + d_eS$ , where  $d_eS$  is the variation of entropy due to exchanges with the surroundings and  $d_iS$  the entropy increase due to irreversible processes occurring inside the system, such as diffusion, chemical reactions, heat conduction and so on.

Basically, one has  $d_eS = 0$  for an isolated system, meaning that  $dS = d_iS \geq 0$ , according to the second law. This means that if a system in evolution is not able to export any irreversible internal increase in entropy towards its surroundings, it is doomed to land in a state of maximum entropy, where all available energy is spread among all the possible degrees of freedom (positions and velocities). In other words, any kind of structural arrangement observed at a given time is doomed to become a gas at an infinite time. This is what is expected for any kind of inert matter.

The situation is completely different as soon as a mechanism is available for exporting the newly generated entropy in order to avoid entropy accumulation. The most interesting case occurs for open systems that are allowed to exchange both heat and matter towards their surroundings. Here, during evolution, ejection of wastes of sufficiently high entropies or release of a sufficient amount of heat, allow reaching a state where entropy is smaller than at the beginning, meaning that  $d_eS \leq 0$ . Such a state which is highly improbable from a statistical viewpoint and doomed to disappear in a closed or isolated system, could in this case survive indefinitely in a steady state (dissipative structure) provided that  $dS = 0$  or  $d_eS = -d_iS \leq 0$ . This basically means that highly improbable states need just highly efficient mechanisms of entropy export, and that there is no upper limit in complexity. The price to pay for being quite complex is that the higher the entropy export, the higher the destruction of the surroundings that have to sustain such a huge flow of entropy coming from the complex system.

It is worth noticing that here we are considering the whole earth as a living system exporting entropy towards the whole universe through infrared radiations centered on a wavelength of about 10  $\mu\text{m}$ . The fact is that the universe has very few structures by itself and is in continuous expansion, meaning that it is able to absorb an almost infinite amount of entropy from the earth.

And if we have so many structures on earth, it is precisely because the universe is almost totally devoid of structures. This obviously does not apply to the earth that is not in expansion. Being on earth, living systems should export their entropy first to the earth putting the burden on the earth for exporting entropy towards the universe, the ultimate garbage. However, the rate of export towards the universe is finite:  $\Delta S \approx 1 \text{ W}\cdot\text{m}^{-2}\cdot\text{K}^{-1}$ . If living systems release entropy in their immediate surroundings at a rate higher than this critical value, the earth will begin to accumulate entropy with the immediate consequence of breaking down structures. Natural means for such breakdowns are tornadoes, hurricanes, floods, fires, volcanoes and earthquakes.

Consequently, when the surroundings becomes saturated with wastes, entropy export is doomed to be reduced, leading to the disappearance of the dissipative structure with a breaking down into smaller components as explained above. Here is the thermodynamic basis for aging and death of any kind of living system. Obviously one of the most efficient ways of exporting entropy is to release gases, explaining why most complex living systems always hold an internal machinery for manipulating gases. Another very efficient way of exporting entropy, is by releasing heat (i.e. infrared radiation), explaining why complex living systems are systematically warmer than their surroundings.

A basic equation for life should then be: foods (in) = biomass (in) + heat (out) + wastes (out), where "in" and "out" refer to a system surrounded by a containment able to exchange heat and matter between the inside and the outside. Now in the following, we will assume that each substance carries within its structure a certain amount of a so-called irreversibility potential noted  $\Pi_i$  hereafter. Such a new term is here introduced for stressing the fundamental role played by irreversible processes and also stressing the fact that it is a thermodynamic entity ruling a possible evolution that may occur or not depending on kinetic factors. Its main role is to put on a quantitative basis the ability of substance of being a food (low irreversibility or entropy-poor substance) or a waste (high irreversibility potential or entropy-rich substance). As shown below, for systems evolving at constant temperature and pressure, the irreversibility potential is measured by the ratio of the opposite chemical potential  $-\mu$  divided by the constant temperature  $T$ , that is to say  $\Pi_i = -\mu/T$ . The irreversibility potential has thus the dimension of an entropy. The reason for changing the name is that such a correspondence between irreversibility potential and chemical potential exists only if pressure and temperature remain constant during the evolution. For other experimental conditions, the numerical values

are changed, but the rule remains the same. For instance for an isolated system unable to exchange heat and matter with its surroundings  $\Pi_i$  may now be identified directly with entropy and no more with the chemical potential.

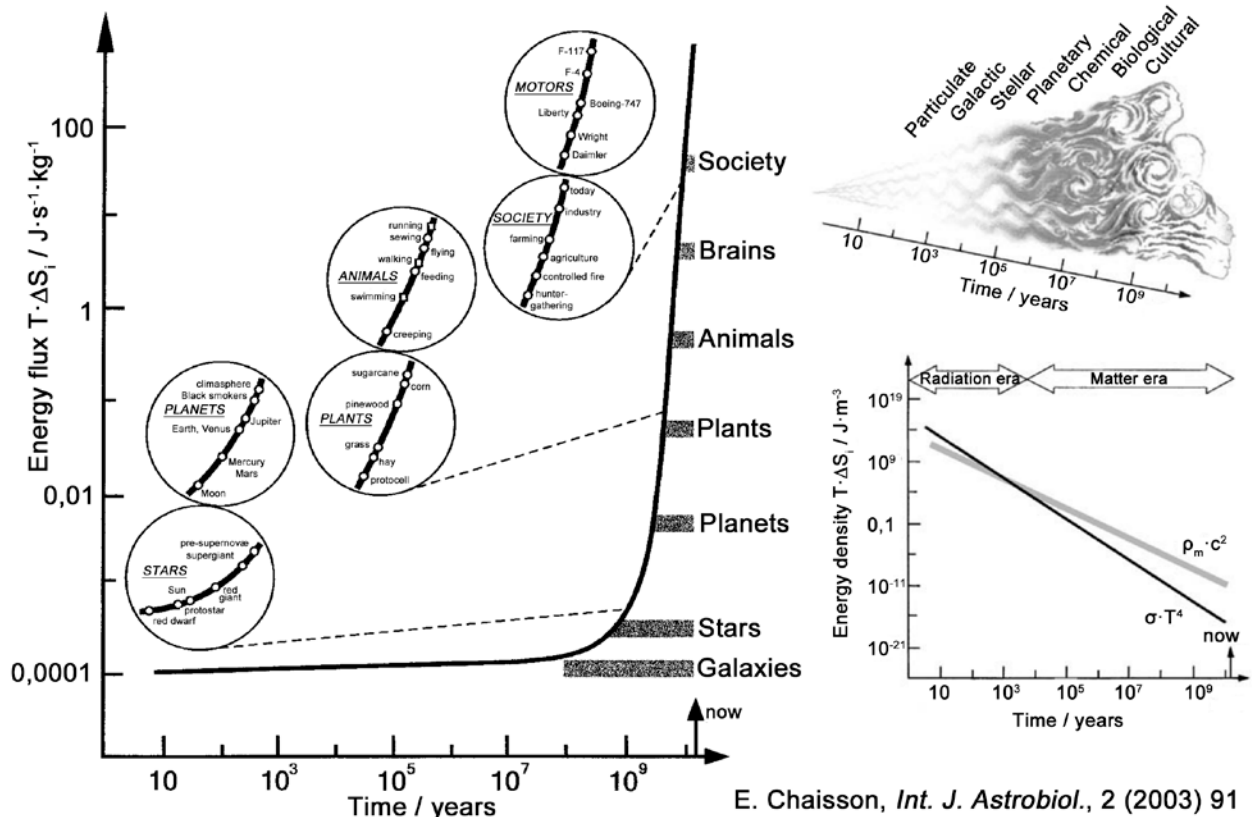
Consequently, for a system absorbing one type of food F having an irreversibility potential  $\Pi_i^F$ , used to create one type of molecule M having an irreversibility potential  $\Pi_i^M$  and generating an amount of heat Q with ejection of one type of waste W having an irreversibility potential  $\Pi_e^W$ , a fundamental law of existence should be:

$$\frac{dS}{dt} = \frac{d_i S}{dt} + \frac{d_e S}{dt} = -\Pi_i^F \cdot \frac{dn_F}{dt} + S \Pi_i^M \cdot \frac{dn_M}{dt} + \frac{1}{T} \frac{dQ}{dt} + \Pi_e^W \cdot \frac{dn_W}{dt} \geq 0 \quad (1)$$

If several types of foods are needed or several types of wastes produced, one should subtract a term

$\Pi_i(k) \cdot dn_k/dt$  or add a term  $\Pi_e(j) \cdot dn_j/dt$  for each type of food (k) or waste (j), n being the number of entities absorbed (food), created (biomass) or ejected (wastes) by the system. Systems with a low  $dS/dt$  are simple, complexity increasing rapidly with any increase in  $dS/dt$ .

Figure 3 gives an illustration of such a relationship.<sup>17</sup> According to such a law, in order to have the largest  $dS/dt$ , one should have on input foods of very low irreversibility potentials ( $\Pi_i^F \approx 0$ ) that should be metabolized at the smallest possible rate ( $dn_F/dt \approx 0$ ) in order to create large entities ( $\Pi_i^M \gg 0$ ) at the highest possible rate ( $dn_M/dt \gg 0$ ). On output, one should evacuate the largest amount of heat at the lowest temperature and/or eject wastes having the highest irreversibility potentials ( $\Pi_e^W \gg 0$ ) at the highest admissible rate ( $dn_W/dt \gg 0$ ). Any increase in  $dn_F/dt$  (overfeeding), decrease in  $dn_M/dt$  (starvation), increase in temperature surroundings (heating) or decrease in  $dn_W/dt$  (clogging) would, below a critical threshold, lower  $dS/dt$  and brings the system closer to its death.



E. Chaisson, *Int. J. Astrobiol.*, 2 (2003) 91

**Figure 3.** The exponential rise in complexity as a function of irreversible energy flux (left). Top-right: arrow of time and major evolutionary phases that have produced the visible universe. Bottom-right: the crossover between evolution in time of radiation energy density (Stefan-Boltzmann  $\sigma \cdot T^4$  law) and matter energy density ( $\rho_m \cdot c^2$ ) leading to neutral atoms formation some  $\approx 10^5$  years after the big-bang. Adapted from Eric J. Chaisson's work.<sup>17</sup>

It is worth noting that these are very general rules that apply to any kind of living system whatever its internal machinery and complexity. More particularly, the higher is  $dS/dt$ , the higher the complexity and the higher the dependence on the surroundings for survival. We will now apply such a universal recipe to prebiotic life as represented in figure 2. To do this, we have to know reasonable values measuring irreversibility potentials. In fact, as explained above, for systems evolving at constant temperature and pressure, we should have  $-T \cdot \Pi_i = \mu$ , where  $\mu$  is Gibbs' chemical potential, or partial molar Gibbs free energy. So, all the data we need are contained in tables of Gibbs' free energies. As such tables give data for a particular reference state (usually  $T^\circ = 298.15$  K and  $p^\circ = 100$  kPa), it is worth knowing how the chemical potential varies with temperature, pressure and composition. We will use the following expression easily derivable from the definition of a chemical potential:<sup>18</sup>

$$\Pi_i(M, T, p, n) = \Pi_i^\circ(M) + \quad (2)$$

$$S_m^\circ(M) \cdot \left[ \frac{T}{T^\circ} - 1 \right] - V_m^\circ(M) \cdot \left[ \frac{p}{T^\circ} - \frac{p^\circ}{T^\circ} \right] - R \cdot \ln a(M)$$

Here,  $S_m^\circ(M)$  and  $V_m^\circ(M)$  are the molar absolute entropy and molar volume of substance M respectively while  $a(M)$  is the activity of the substance when not in pure state, that is to say mixed with other substances. For a pure substance  $a(M) = 1$  by definition, meaning that  $S_i^\circ(M)$  is the standard irreversibility potential at  $T = T^\circ$ ,  $p = p^\circ$  of the pure substance,  $a(M) = 1$ . Choosing the elements in their standard state as setting the level zero of irreversibility potential leads to  $\Pi_i^\circ(M) = -\Delta_f G^\circ(M)/T$ .

Table 1 gives some selected values that we should use to follow the irreversible flux of entropies associated to a possible abiotic metabolism represented formally in figure 2. Concerning units, the usual choice for energy is to use kilojoule per mole ( $\text{kJ} \cdot \text{mol}^{-1}$ ) in chemistry and electron-volt (eV) in physics. In fact, these two units have been arbitrarily chosen as respectively convenient for calorimetry where heat fluxes are expressed in joules and for electrochemistry or nuclear physics where charges are measured in coulombs and potentials in volts. In order to switch from the macroscopic world (joules, volts) to a microscopic world, one uses respectively the Avogadro constant  $N_A = 6.02214129 \times 10^{23} \text{ mol}^{-1}$  and the elementary charge  $e = 1.602176565 \times 10^{-19} \text{ C}$ . The drawback of such units is that they are not related to biological conditions that are centered on a

characteristic temperature  $T \approx 300$  K. A much better unit of energy for biology should thus be  $E = k_B \cdot T \approx 4$  zJ, where  $k_B = 0.013806488 \text{ zJ} \cdot \text{K}^{-1}$ , is Boltzmann's constant and 1 zepto-joule (zJ) =  $10^{-21}$  J. This explains why table 1 uses the zepto-joule as a fundamental unit of energy, with  $1 \text{ kJ} \cdot \text{mol}^{-1} = 1.66 \text{ zJ}$  and  $1 \text{ eV} = 160.2 \text{ zJ}$  as conversion factors between the new unit (zJ) and the old ones. Similarly, the standard volumes are directly expressed in  $\text{nm}^3$  ( $1 \text{ nm}^3 = 10^{-21} \text{ cm}^3$ ) in order to compare the standard entropy  $S^\circ$  with a state where all atoms are just mixed together without making any chemical bonds. For such an "ideal" state where the only source of entropy increase is diffusion through translation in space, one may use the Sackur-Tetrode equation allowing establishing a direct link between  $S^{\text{id}}$  and elementary quantum processes:<sup>19</sup>

$$\frac{S^{\text{id}}}{k_B} = 0.83 + 1.5 \cdot \ln\{(M/Da) \cdot (T/K)\} + \ln(V/\text{nm}^3) \quad (3)$$

## PREBIOTIC CHEMISTRY

Let's now show how such a table should be used for understanding what is happening during any irreversible evolution. First, the table has been organized by ascending order of standard irreversibility potential  $\Pi_i^\circ$  in order to see at once what substance could be a food (top of the table) and what substance would be a waste (bottom of the table). One thus immediately sees that metals and gases are the most interesting foods, while liquids and solids are better qualified as wastes. This explains the basic scheme of most complex living systems: breathing gases (air) and rejecting liquids (urine) and solids (feces).

A fundamental point of living systems is that even a waste can be used as a food by rejecting another waste, provided that such a waste has a higher irreversibility potential than the waste used as a food. A good example is provided by the bacteria *Shewanella oneidensis*, that is able to "respire" from goethite  $\alpha\text{-FeOOH}$ , the iron ore responsible for the brown color of the soil, and reject black magnetite  $\text{Fe}_3\text{O}_4$  as a waste.<sup>20</sup> As can be seen in table 1, this is possible because the irreversibility potential of magnetite is higher than the one of goethite. This shows that when speaking of living system, solids minerals should not be discarded as possible source for food. This explains, why after its apparition, life may be found in different ecological niches.

On such a ground, metallic iron or nickel owing to their very small irreversibility potentials should be

**Table 1.** Irreversible standard potentials  $\Pi_i^\circ$  ( $T = 298.15$  K,  $p = 100$  kPa), standard absolute entropies  $S^\circ$  and standard molecular volume  $V^\circ$  for some selected compounds involved in the prebiotic metabolic cycle shown in figure 2. Values being given per molecule or motif, the unit of energy corresponds to the zepto-joule (zJ), with  $1 \text{ zJ} = 10^{-21}$  joules and  $1 \text{ kJ}\cdot\text{mol}^{-1} = 1,66 \text{ zJ}$ . See annex for the derivation of this table from literature data. (s) = solid, (liq) = liquid, (g) = gas and (aq) = aqueous solution.

| Substance (state)      | Formule  | $\Pi_i^\circ / \text{zJ}\cdot\text{K}^{-1}$ | $S^\circ / \text{zJ}\cdot\text{K}^{-1}$ | $V^\circ / \text{nm}^3$ |
|------------------------|--|---|---|-------------------------|
| Nickel (g)             | Ni   | -2.14146                                    | 0.30255                                 | 41.164                  |
| Iron (g)               | Fe   | -2.06460                                    | 0.29973                                 | 41.164                  |
| Iron (liq)             | Fe   | -0.55808                                    | 0.16550                                 | 0.01321                 |
| Iron (s)               | $\epsilon$ -Fe (hcp)   | -0.02507                                    | 0.05525                                 | 0.01132                 |
| Iron (s)               | $\gamma$ -Fe (fcc)   | -0.02490                                    | 0.05694                                 | 0.01151                 |
| Iron (s)               | $\alpha$ -Fe (bcc)   | 0   | 0.04533                                 | 0.01178                 |
| Nickel (s)             | Ni   | 0   | 0.04965                                 | 0.01094                 |
| Sulfur (s)             | S  | 0   | 0.05322                                 | 0.02576                 |
| Dihydrogen (g)         | H <sub>2</sub>   | 0   | 0.21700                                 | 41.164                  |
| Dinitrogen (g)         | N <sub>2</sub>   | 0   | 0.31816                                 | 41.164                  |
| Di-oxygen (g)          | O <sub>2</sub>   | 0   | 0.34066                                 | 41.164                  |
| Ammonia (g)            | NH <sub>3</sub>  | 0.09134                                     | 0.32010                                 | 41.164                  |
| Hydrogen sulfide (g)   | H <sub>2</sub> S   | 0.18602                                     | 0.34174                                 | 41.164                  |
| Troilite (s)           | FeS  | 0.56419                                     | 0.10013                                 | 0.03022                 |
| Hydrogen peroxide (aq) | H <sub>2</sub> O <sub>2</sub>                                    | 0.74648                                     | 0.23895                                 | -                       |
| Carbon monoxide (g)    | CO   | 0.76358                                     | 0.32762                                 | 41.164                  |
| Pyrite (s)             | FeS <sub>2</sub>   | 0.89167                                     | 0.08784                                 | 0.03975                 |
| Water (g)              | H <sub>2</sub> O   | 1.27386                                     | 0.31351                                 | 41.164                  |
| Ice I <sub>h</sub> (s) | H <sub>2</sub> O   | 1.31769                                     | 0.07434                                 | 0.03193                 |
| Water (liq)            | H <sub>2</sub> O   | 1.32097                                     | 0.11624                                 | 0.03000                 |
| Carbon dioxide (g)     | CO <sub>2</sub>  | 2.19660                                     | 0.35502                                 | 41.164                  |
| Goethite (s)           | $\alpha$ -FeOOH  | 2.73907                                     | 0.10030                                 | 0.03457                 |
| Carbonic acid (aq)     | H <sub>2</sub> CO <sub>3</sub>                                   | 3.47090                                     | 0.30670                                 | -                       |
| Hematite (s)           | $\alpha$ -Fe <sub>2</sub> O <sub>3</sub>                         | 4.14592                                     | 0.14513                                 | 0.05027                 |
| Magnetite (s)          | Fe <sub>3</sub> O <sub>4</sub>                                   | 5.64021                                     | 0.24267                                 | 0.07393                 |
| Fayalite (s)           | Fe <sub>2</sub> SiO <sub>4</sub>                                 | 7.68086                                     | 0.25074                                 | 0.07690                 |
| Forsterite (s)         | Mg <sub>2</sub> SiO <sub>4</sub>                                 | 11.43747                                    | 0.15626                                 | 0.07248                 |
| Serpentine (s)         | Mg <sub>3</sub> Si <sub>2</sub> O <sub>5</sub> (OH) <sub>4</sub> | 22.45835                                    | 0.36748                                 | 0.17851                 |
| Apatite (s)            | Ca <sub>5</sub> (PO <sub>4</sub> ) <sub>3</sub> OH               | 35.29432                                    | 0.64827                                 | 0.26502                 |

considered as the ultimate source of all foods on Earth. This stems from the fact that these two elements are formed from the four most tightly bound nuclides in the universe, with an average binding energy decreasing in the order  $^{62}\text{Ni} > ^{58}\text{Fe} > ^{56}\text{Fe} > ^{60}\text{Ni}$ .<sup>21</sup> Both species form the core of any telluric planet such as the earth. Consequently, any substance on Earth is to doomed to encounter sooner or later metallic nickel or iron during its recycling by the plate tectonics. The importance of nickel and iron for early forms of life is represented nowadays by two crucial metallo-enzymes.<sup>22</sup> First, carbon monoxide dehydrogenase (CODH) using NiFe<sub>3</sub>S<sub>4</sub> and Fe<sub>4</sub>S<sub>4</sub> clusters for transforming carbon dioxide CO<sub>2</sub> into carbon monoxide CO. Second, acetyl-CoA synthase (ACS) combining the CO generated by CODH with a methyl group to form the key metabolite intermediate

acetyl-CoA using a Ni<sub>2</sub>-Fe<sub>4</sub>S<sub>4</sub> cluster. Table 2 shows other important (Ni,Fe)-based metallo-enzymes demonstrating the crucial role played by these two metals in biology,<sup>23</sup> in geochemistry and in astronomy.

Accordingly, Ni-Glx(I) protects the bacteria *E. Coli* against the damages made by methylglyoxal, a reduced form of pyruvic acid, to the arginine-bearing proteins and to nucleic acids. ARD is an enzyme involved in the ubiquitous methionine salvage pathway. Urease protects bacteria, archaea, plants, algae and fungi against harmful acidification of the living medium. Ni-SOD is an enzyme that protects cells from an excess of the superoxide ion, a free radical byproduct of aerobic metabolism. (Ni-Fe)-hydrogenase manage the reversible interconversion of hydrogen gas with protons and electrons in archaea, bacteria and selected eukaryotes. MCR play

**Table 2.** The “two” most tightly bound nuclides in the universe, nickel (Ni) and iron (Fe), are at the heart of many crucial biological processes involving at least nine different Ni-based enzymes used by 80% of the archaea and 60% of the eubacteria. Glx = Glyoxalase, ARD = Acidreductase dioxygenase, SOD = Superoxide dismutase, Hyd = Hydrogenase, CODH = CO dehydrogenase, ACS = Acetyl-CoA synthase, MCR = Methyl-coenzymeM reductase, Lar = Lactate racemase, DHK-MTPene = 1,2-dihydroxy-3-keto-5-methylthiopen- tene, KMTB = 2-keto-4- methylthiobutyrate, FeSP = corrinoid/Fe-S protein.

| Enzyme      | Metals  | Reaction  |
|-------------|---|---|
| Ni-GlxI     | 2 Ni <sup>2+</sup>                              | Me-CO-CHO + ½ O <sub>2</sub> =<br>Me-CHOH-COO <sup>-</sup> + H <sup>+</sup>   |
| ARD         | Fe <sup>2+</sup> or Ni <sup>2+</sup>            | DHK-MTPene + O <sub>2</sub> =<br>KMTB + HCOO <sup>-</sup> + 2H <sup>+</sup>   |
| Urease      | 2 Ni <sup>2+</sup>                              | CO(NH <sub>2</sub> ) <sub>2</sub> + 2 H <sub>2</sub> O = 2 NH <sub>4</sub> <sup>+</sup> + CO <sub>3</sub> <sup>2-</sup> |
| Ni-SOD      | Ni <sup>3+</sup>                                | 2 O <sub>2</sub> <sup>•-</sup> + 2 H <sup>+</sup> = O <sub>2</sub> + H <sub>2</sub> O <sub>2</sub>                      |
| [Ni-Fe]-Hyd | NiFe <sub>2</sub> S <sub>2</sub>                | H <sub>2</sub> = 2 H <sup>+</sup> + 2 e <sup>-</sup>  |
| CODH        | NiFe <sub>3</sub> S <sub>4</sub>                | CO <sub>2</sub> + 2 H <sup>+</sup> + 2 e <sup>-</sup> = CO + H <sub>2</sub> O   |
| ACS         | Ni <sub>2</sub> -Fe <sub>4</sub> S <sub>4</sub> | Me-Co(III)-FeSP + CO + CoASH =<br>MeCO-SCoA + Co(I)-FeSP  |
| MCR         | Ni(I)   | Me-SCoM + CoB-SH =<br>CH <sub>4</sub> + CoM-S-S-CoB   |
| Lar         | Ni <sup>2+</sup>                                | (D)-Me-CHOH-COO <sup>-</sup> =<br>(L)-Me-CHOH-COO <sup>-</sup>  |

a major role in the global carbon cycle by controlling the biological emission of methane. Finally lactic acid (L- and D-isomers) is an important and versatile compound produced by microbial fermentation being involved in the energy metabolism of many prokaryotic species, as a product of sugar fermentation or as a carbon and electron source to sustain growth.<sup>24</sup>

In other words, if something is complex relative to its inner constituents, this means that it is the result of a huge flow of outgoing entropy. Wastes are to be found in its immediate surroundings. If not, the waste may have been exported far away, for example in the form of far-infrared photons that may have escaped towards the intergalactic space. This distant export of entropy may give the false impression, at first glance, that such a complex thing having an incredible low probability of formation from simpler elements apparently violates the second law. In fact, there is no violation at all, the point being that wastes are just invisible photons, i.e. heat for instance.

Another possibility is that wastes generated by a given species have been used as foods for another one, the observable result being a large increase in chemical as well as biological diversity. This is exactly what happens when plants generate O<sub>2</sub>, a waste then breathed by animals. Owing to recycling, the amount of waste may

appear, at first glance, to be lower than what it really is. Figure 2 shows that the two purely abiotic spontaneous cycles can synthesize complex molecules such as glyoxylate, pyruvate and hydrogen peroxide. In accordance with the second law, a spontaneous process is such that the total irreversibility potential after reaction (B) should have increased relative to its initial value (A), or  $\Delta\Pi_i^\circ = \Sigma n_i \cdot \Pi_i^\circ(B) - \Sigma n_i \cdot \Pi_i^\circ(A) > 0$ .

#### SPONTANEOUS FORMATION OF REDUCED CARBON, NITROGEN AND SULFUR SPECIES

It is highly probable that life begins with water encountering a hot magma made of olivine somewhere on the oceanic floor.<sup>25</sup> Upon mixing, olivine will reduce water into hydrogen H<sub>2</sub> leaving as wastes serpentine. Assuming that olivine is made as 75% of forsterite Mg<sub>2</sub>SiO<sub>4</sub> and 25% of fayalite Fe<sub>2</sub>SiO<sub>4</sub> we will assume from table 1 that  $\Pi_i^\circ(\text{olivine}) = 0.75 \times 11.43747 + 0.25 \times 7.68086 = 10.49832 \text{ zJ}\cdot\text{K}^{-1}$ . Before transformation, the total irreversibility potential is thus  $\Pi_i^\circ(A) = 6 \times 10.49832 + 7 \times 1.32097 = 72.23671 \text{ zJ}\cdot\text{K}^{-1}$ , while after transformation we get  $\Pi_i^\circ(B) = 3 \times 22.45835 + 5.64021 = 73.01526 \text{ zJ}\cdot\text{K}^{-1}$ . The difference  $\Delta\Pi_i^\circ = \Pi_i^\circ(B) - \Pi_i^\circ(A) = +0.77855 \text{ zJ}\cdot\text{K}^{-1}$  being positive, this explains the great amount of hydrogen gas escaping from the hydrothermal vent on the oceanic floor where the waste, magnetite, accumulates with time, the other waste, serpentine, remaining within the oceanic crust. In fact, the vent should be viewed as a very powerful entity able transforming a waste H<sub>2</sub>O (low position in table 1) into a valuable food (high position in table 1). Such a reduction that corresponds to a strong decrease in entropy from water's viewpoint is nevertheless possible because wastes high in entropy (serpentine and magnetite) have been produced simultaneously, pushing the overall entropy balance in the good direction.

However, in order to make organic matter, one should also dispose of a valuable source of carbon able to act as a food. Carbon dioxide, which was an abundant molecule in early Earth's atmosphere being a waste rather than a food, one should again make use of the powerful regenerating power of Earth's core containing metallic iron in order to transform it into carbon monoxide. After hydration by a water molecule to form carbonic acid H<sub>2</sub>CO<sub>3</sub>, we have  $\Pi_i^\circ(A) = 3 \times 3.47090 + 0 = 10.4127 \text{ zJ}\cdot\text{K}^{-1}$ . After transformation into carbon monoxide producing goethite and water as wastes, we get  $\Pi_i^\circ(B) = 2 \times 2.73907 + 3 \times 0.76358 + 2 \times 1.32097 = 10.4108 \text{ zJ}\cdot\text{K}^{-1}$ . With a difference  $\Delta\Pi_i^\circ = -0.0019 \text{ zJ}\cdot\text{K}^{-1}$ , we have an almost equal repartition of carbon between carbon-



ic acid and carbon monoxide in such a transformation. However, carbon monoxide being a gas is able to escape from the location of the transformation provoking by its departure more transformation of carbonic acid into carbon monoxide in order to restore the equilibrium fixed by the relative irreversibility potentials in presence.

Concerning nitrogen, a mandatory element for synthesizing aminoacids, table 1 shows that it may already be classified as a food, being in higher position than carbon monoxide and at equal level with hydrogen. However, dinitrogen is a completely apolar molecule with nitrogen atoms engaged into very a stable triple bond that is very difficult to break spontaneously. But table 1 shows that another nitrogen-based molecule, ammonia  $\text{NH}_3$ , is almost at the same level of irreversibility potential without the problem of the triple bond. Here one may use again Earth's core to perform the transformation of  $\text{N}_2$  into ammonia  $\text{NH}_3$  with as always the help of the ubiquitous water molecule. Before transformation we have  $\Pi_1^\circ(\text{A}) = 4 \times 1.32097 + 0 + 0 = 5.28388 \text{ zJ}\cdot\text{K}^{-1}$ , while after transformation into ammonia producing goethite as a waste, we get  $\Pi_1^\circ(\text{B}) = 2 \times 2.73907 + 2 \times 0.09134 = 5.66082 \text{ zJ}\cdot\text{K}^{-1}$ . With a difference  $\Delta\Pi_1^\circ = +0.37694 \text{ zJ}\cdot\text{K}^{-1}$ , the reaction thus proceeds quite easily. Accordingly, in the laboratory it was possible to convert 17 mol% of nitrogen gas into ammonia by reaction with iron and water at a temperature of  $700^\circ\text{C}$  and a pressure of 0.1 GPa according to:

$3(1-x) \text{ Fe} + \text{N}_2 + 3 \text{ H}_2\text{O} = 3 \text{ Fe}_{(1-x)}\text{O} + 2 \text{ NH}_3$ ,<sup>26</sup> Ammonia was also obtained by with a mixture of nitrogen and formic acid at the surface of magnetite.

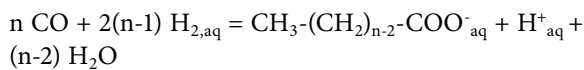
What have been said for  $\text{N}_2$ , applies also to sulfur that exists as a solid and not as a gas under standard conditions. Here also, transformation of sulfur into hydrogen sulfide having a position rather close to sulfur in table 1 could be envisaged with the help of water as before and of a previous waste, magnetite, acting now as a food. This would allow disposing of the last important organic element necessary for building living matter as a gas and not as a solid. Accordingly, before transformation we have  $\Pi_1^\circ(\text{A}) = 2 \times 5.64021 + 0 + 4 \times 1.32097 = 16.5643 \text{ zJ}\cdot\text{K}^{-1}$ , while after transformation into  $\text{H}_2\text{S}$  producing goethite as a waste, we get  $\Pi_1^\circ(\text{B}) = 6 \times 2.73907 + 0.18602 = 16.62044 \text{ zJ}\cdot\text{K}^{-1}$ . With a difference  $\Delta\Pi_1^\circ = +0.05614 \text{ zJ}\cdot\text{K}^{-1}$ , the reaction is thus in favor of  $\text{H}_2\text{S}$  over a mixture of water and sulfur.

According to the previous considerations we understand that a hydrothermal vent could be viewed as a powerful source of foods in the form of  $\text{H}_2$ ,  $\text{CO}$ ,  $\text{NH}_3$  and  $\text{H}_2\text{S}$  gases. However, these gases are released in water, a protic solvent, they may exist under several forms depending on the pH of water. For instance, at  $\text{pH} = 7$ , hydrogen sulfide exists as a 50-50 mixture of  $\text{H}_2\text{S}$  and  $\text{HS}^-$  species. For ammonia, it is the ammonium form  $\text{NH}_4^+$  that is the predominant species at  $\text{pH} \approx 7$ . It follows that a given irreversible process may be represented by several chemical reactions involving species differing by their number of H-atoms and that can bear a non-zero electrical charge. In order to deal with such situations, one should use an apparent irreversible potential  $\Pi_1^\circ(\text{pH}, \text{I})$  that reflects all the possible protonated forms of a chemical species in water existing at a given pH at a specified ionic strength I. Specific procedures have been designed to retrieve such apparent potentials from thermodynamic data of each chemical species at  $\text{pH} = 0$  and  $\text{I} = 0 \text{ M}$ .<sup>27</sup> When the necessary thermodynamic data is not available, one may decompose a given chemical species into various characteristic functional groups and add all the contribution to retrieve the corresponding apparent potential.<sup>28</sup> Table 3 gives such group contributions for  $\text{pH} = 7$  and three ionic strength,  $\text{I} = 0 \text{ M}$ , 100 mM and 250 mM adapted to our entropy units ( $\text{zJ}\cdot\text{K}^{-1}$ ). As with table 1, we have listed irreversibility potentials in ascending order in order distinguishing between potential foods (top of the table) and potential wastes (bottom of the table).

In order to convince of the usefulness of such a table, we will try to see if fatty acids may synthesized inside the mouth of a hydrothermal vent:

**Table 3.** Group contributions to aqueous irreversibility potentials  $\Pi_1^\circ$  at a pressure of 100 kPa,  $\text{pH} = 7$  and three different ionic strengths I. This table is based on the convention that  $\Pi_1^\circ = 0$  for species  $\text{H}^+$ , adenosine,  $\text{NAD}^-$  and  $\text{NADP}^{3-}$  at zero ionic strength.

| Group                              | I = 0 M  | I = 0.1 M | I = 0.25 M |
|------------------------------------|----------|-----------|------------|
| Adenosine                          | -2.89295 | -2.93729  | -2.95160   |
| C- $\text{CH}_2$ - $\text{NH}_3^+$ | -0.94837 | -0.96876  | -0.97538   |
| $\text{C}_2$ -CH- $\text{NH}_3^+$  | -0.88070 | -0.89780  | -0.90326   |
| Methyl: C- $\text{CH}_3$           | -0.56235 | -0.57254  | -0.57588   |
| Methylene: C- $\text{CH}_2$ -C     | -0.47396 | -0.47736  | -0.47842   |
| Ammonium: C- $\text{NH}_3^+$       | -0.38602 | -0.39621  | -0.39950   |
| - $\text{CH}_2$ -OH                | 0.23876  | 0.22852   | 0.22517    |
| $\text{C}_2$ -CH-OH                | 0.37594  | 0.36909   | 0.36692    |
| Aldehyde: C-CHO                    | 0.44634  | 0.44294   | 0.44183    |
| $\text{C}_3$ -C-OH                 | 0.45915  | 0.46706   | 0.47006    |
| Amide                              | 0.59248  | 0.57889   | 0.57438    |
| Keto: -CO-                         | 0.67892  | 0.67324   | 0.67886    |
| Ol: C-OH                           | 0.80111  | 0.80106   | 0.80106    |
| Carboxyl: C-COO $^-$               | 1.95160  | 1.95500   | 1.95606    |
| C-O-P-O-P-O- $\text{PO}_3^-$       | 4.81002  | 4.82640   | 4.83302    |
| C-O-P-O- $\text{PO}_3^-$           | 4.82796  | 4.83976   | 4.84450    |
| C-O- $\text{PO}_3^-$               | 4.93973  | 4.95338   | 4.95823    |



The resulting fatty acid being composed of 1 methyl, 1 carboxyl groups and (n-2) methylene groups, one should expect from table 3 for an ionic strength  $I = 0.25 \text{ M}$  the following irreversibility potential:

$$\Pi'_i(C_n\text{H}_{2n+2}) = 1.95606 - 0.57588 - (n-2) \times 0.47842 = (2.33702 - 0.47842 \times n) \text{ zJ}\cdot\text{K}^{-1}$$

The prime symbol is a remainder that such a value is an apparent irreversibility potential valid for  $\text{pH} = 7$  and  $I = 0.25 \text{ M}$ . Its negative value above  $n \approx 5$  means that formation of fatty acids with long hydrocarbon tails involves a large decrease in entropy relative to its constituting elements (carbon C and hydrogen gas H<sub>2</sub>). Consequently, the higher n, the less the probability of seeing such a species forms spontaneously. However, we are not interested here by the formation from the constituting elements, but rather by the formation from carbon monoxide (food) reacting with hydrogen to produce the fatty acid with elimination of water as a waste. For the small molecules, we will use  $\Pi'_i(\text{CO}) = 0.66778 \text{ zJ}\cdot\text{K}^{-1}$ ,  $\Pi'_i(\text{H}_2) = -0.55210 \text{ zJ}\cdot\text{K}^{-1}$  and  $\Pi'_i(\text{H}_2\text{O}) = 0.86695 \text{ zJ}\cdot\text{K}^{-1}$  valid for  $\text{pH} = 7$  and  $I = 0.25 \text{ M}$ ,<sup>28</sup> leading to:

$$\Delta\Pi'_i = (n-2) \times 0.86695 + (2.33702 - 0.47842 \times n) - 0.66778 \times n + 0.55210 \times (2n-2) = (0.82495 \times n - 0.50108) \text{ zJ}\cdot\text{K}^{-1}$$

This now shows that fatty acid formation is always a spontaneous process ( $\Delta\Pi'_i > 0$ ) for all values of n larger than  $n = 1$ .

#### SELF-ASSEMBLY OF LIPIDS INTO MICELLES

This is an important result, as every living cell has a membrane made of long-chain fatty acids. A crucial point, here, is that as soon as the number of carbon atoms becomes large enough, such fatty acids are able to self-assemble spontaneously into micelles, vesicles and membranes. Accordingly, a long-chain fatty acid is basically a small rigid pinhead welded on a flexible whip strap. In water, these long chain fatty acid assembles to form cavities not accessible to water molecules. This translates into a prohibitive entropy cost explaining the very low solubility of such species.

However, provided that the hydrocarbon tail is long enough, it becomes possible to have a large gain in entropy by creating in water large cavities hold-

ing several tails instead of a single one.<sup>29</sup> For instance, for a spherical cavity of radius R able holding N tails of volume V of a fatty acid, one should have  $N \cdot V = 4\pi R^3/3$ . But the fatty acid has also a head-group sweeping an area A, so that one has simultaneously  $N \cdot A = 4\pi R^2$ , leading to  $R \cdot A = 3 \cdot V$ . Now, R cannot be greater than the maximal length L of the fully stretched hydrocarbon chain. With  $R = 3V/A \leq L$ , it comes that a criterion for making a spherical micelle is to have a packing parameter  $PP = V/(L \cdot A) \leq 1/3$ . Fatty acids having a packing parameter such that  $PP > 1/3$  should then look for another less curved topology. Let us then consider a cylinder of arbitrary length D and radius R. Here, one should have  $N \cdot V = \pi R^2 \times D$  and  $N \cdot A = 2\pi R \times D$ , leading to  $R \cdot A = 2 \cdot V$  or  $R = 2V/A \leq L$  as before. It follows that a criterion for making a cylindrical micelle is to have a packing parameter  $PP = V/(L \cdot A) \leq 1/2$ . If  $PP > 1/2$ , the fatty acid is not able to aggregate as a cylinder and should look again for another topology. A possibility is to make closed spherical bilayers having a radius equal to twice the hydrocarbon chain length R. For such a vesicle one may write that  $N \cdot V = 4\pi (2R)^3/3$  to be compared to  $N \cdot A = 4\pi (2R)^2$ , leading to  $R = 3V/2A \leq L$  that is to say  $PP = V/(L \cdot A) \leq 2/3$ . Finally, if  $PP > 2/3$ , the solution is to make a planar double layer having a thickness equal to 2R. For a square having an arbitrary area equal to  $D^2$ , one may write that  $N \cdot V = 2R \times D^2$  and  $N \cdot A = 2D^2$ , leading to  $R = V/A \leq L$  that is to say  $PP = V/(L \cdot A) \leq 1$ . Finally, if  $PP > 1$ , the area of the head-group is too small to pack into bilayers and inverse micellar structures are formed (figure 4).

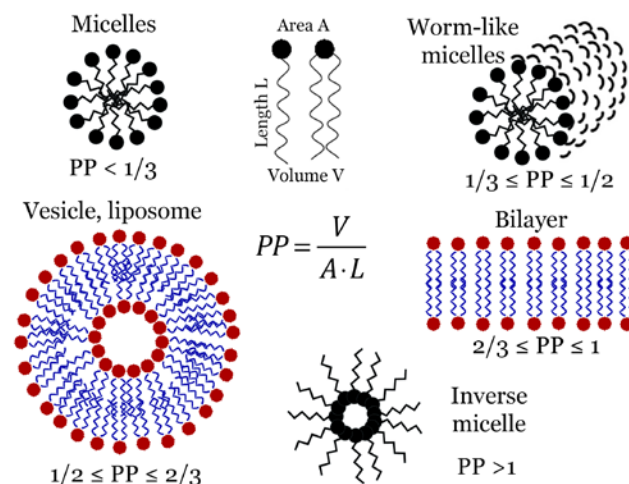


**Figure 4.** Spontaneous self-assembly in water of fatty acids characterized by the volume V of the hydrocarbon tail, the area A of the head-group, the maximum chain length L and observed topologies as a function of the packing parameter PP.

The final topology of the self-assembly process is thus controlled by a simple geometric criterion  $PP = V/(A \cdot L)$ . Now, for saturated hydrocarbon chains  $C_nH_{2n+1}$ , one has  $V \approx (0.0274 + 0.0269 \times n) \text{ nm}^3$  and  $L = (0.150 + 0.1265 \times n) \text{ nm}$ , leaving only the area of the head-group  $A$  as a variable. Depending on the number of water molecules associated with the head-group, a given fatty acid may adopt any of the topologies represented in figure 3. The head-group area in the bilayer phase may be measured from force-area isotherms of squeezed monolayers giving an average value  $A_0 = 0.247 \text{ nm}^2$  for fatty acids ( $n = 16-22$ ).<sup>30</sup> Now, the average volume  $V_w$  occupied by a single water molecule may be computed from the observed density of liquid water  $\rho \approx 1 \text{ g} \cdot \text{cm}^{-3}$ , water's molecular weight  $M_w = 18.0015 \text{ Da}$  and Avogadro's constant  $N_A = 0.602214129 \times 10^{24} \text{ mol}^{-1}$  leading to  $V_w = M_w \times 10^{-3} / (N_A \times \rho) \approx 0.03 \text{ nm}^3$ . It follows that hydrating the carboxyl head-group with  $N$  water molecules would lead to an effective area  $A = (A_0^{3/2} + k \times N \times V_w)^{2/3}$ , with  $k$  a shape factor equal to  $6 \times \pi^{1/2} \approx 10.635$  for spherical head-groups. For instance, for stearic acid ( $n = 18$ ), we get  $V = 0.5116 \text{ nm}^3$  and  $L = 2.427 \text{ nm}$ . With two water molecules per head-group ( $N = 2$ ), we get an effective area  $A = 0.833 \text{ nm}^2$ , leading to  $PP = 0.25 < 1/3$ , pointing to spherical micelles formation when ordinary soap is dissolved in water. For  $N = 1$ , the area is reduced to  $A = 0.580 \text{ nm}^2$ , leading to  $PP = 0.36 > 1/3$ , that is to say formation of worm-like micelles responsible for the high viscosity of concentrated soap solutions. Finally, for a fully dehydrated head-group  $A = A_0 = 0.247 \text{ nm}^2$ , leading to  $PP = 0.85 > 2/3$ , that is to say formation of stacked planar bilayers typical of solid soap.

This shows that the same fatty acids are able to form spherical, worm-like or planar bilayers depending on the fatty acid molar fraction relative to water. In other words, the shape of a cell is dictated by the amount of water molecules available in the medium. Obviously, the trouble with fatty acids is that they form bilayers only when the polar carboxylate head-group is not solvated by water molecules. In order to get stable bilayers in a large amount of water, it is mandatory to select a polar head-group not heavily solvated by water molecules and find a trick to increase the hydrocarbon volume  $V$  without increasing too much the chain length  $L$ . For the polar head-group a smart solution was to use a quaternary ammonium moiety, such as  $-NMe_3^+$ , as methyl groups are not able to be hydrogen-bonded with water molecules, explaining the ubiquitous choline head-group  $HO-CH_2-CH_2-NMe_3^+$ , in modern living membranes.

As shown in table 4 giving irreversibility potentials at  $\text{pH} = 7$  as a function of ionic strength for prebiotic species, choline is a most valuable low entropy food with

a quite negative irreversibility potential. Reaction (a) and (b) in table 5 shows that its abiotic synthesis within a hydrothermal vent may occur spontaneously by reducing carbon monoxide or dioxide with hydrogen gas in the presence of ammonia and with an appropriate mineral surface for catalyzing the reaction.

Concerning the chain length, the trick was to use 2 fatty-acids chains instead of one, allowing doubling the volume without changing the length of the hydrocarbon tail. In order to get a molecule with 2 tails and one head-group welded together to form a single entity, an obvious choice was to select glycerol molecules  $HO-CH_2-CHOH-CH_2-OH$  having three OH groups available for esterification. As ether-links  $-C-O-C-$  are much more difficult to synthesize than ester links  $-C(O)-O-C-$ , it was necessary for welding choline to glycerol to recruit a divalent weak inorganic acid for bridging two alcohol moieties together. Sulfuric acid  $H_2SO_4$  being a strong acid and carbonic acid  $H_2CO_3$  being too instable, a good candidate was phosphoric acid  $H_3PO_4$  existing in aqueous solution around  $\text{pH} \approx 7$  under a di-hydroxy form  $H_2PO_4^-$ .

A convenient source of phosphate on earth is hydroxyapatite  $Ca_5(PO_4)_3(OH)$ , but this mineral appears to be definitively a waste and not a food as it is found at the very bottom of table 4. To realize the difficulty of extracting phosphate groups from apatite by water, we see that reaction (c) in table 5 leads to a negative irreversibility potential variation  $\Delta\Pi_i^\circ$ , meaning that such a transformation cannot occur spontaneously. It should thus be coupled with another transformation releasing enough entropy to compensate for such a large decrease. As explained below, this is precisely the role of a metabolism to furnish such entropic compensation.

#### ABIOTIC ORGANIC CHEMISTRY

Concerning the formation of glycerol, another mandatory ingredient for having a double chain phospholipid, reactions (d) and (e) in table 5 shows that such a molecule may be formed spontaneously by reducing carbon monoxide or dioxide by hydrogen gas, as was the case for fatty acids or choline. Taking into account the fact that phosphate groups were not available for welding using a choline head-group, a possibility could be to use glycerate,  $HO-CH_2-CHOH-COO^-$ , obtained according to reactions (f) or (g) in table 5. This shows that abiotic glycerate synthesis is less favorable than that of glycerol but nevertheless still possible.

The apparition of double chain amphiphiles was an important step for evolution because it has made pos-

**Table 4.** Aqueous irreversibility potentials  $\Pi_i^\circ$  (zJ·K<sup>-1</sup>) at a pressure of 100 kPa, pH = 7 and three different ionic strengths I. This table is based on the convention that  $\Pi_i^\circ = 0$  for species H<sup>+</sup>, adenosine, NAD<sup>-</sup> and NADP<sup>3-</sup> at zero ionic strength.

| Compound  | I = 0 M  | I = 0.1 M | I = 0.25 M | Compound  | I = 0 M | I = 0.1 M | I = 0.25 M |
|---|----------|-----------|------------|---|---------|-----------|------------|
| NADH  | -6.13461 | -6.21303  | -6.23831   | Formate   | 1.73233 | 1.73233   | 1.73233    |
| NAD <sup>+</sup>  | -5.78590 | -5.87117  | -5.89867   | α-HG  | 1.80434 | 1.78730   | 1.78173    |
| Choline (C <sub>5</sub> H <sub>14</sub> NO <sup>+</sup> ) | -3.39955 | -3.44411  | -3.45820   | Ribose (C <sub>5</sub> H <sub>10</sub> O <sub>5</sub> ) | 1.88933 | 1.85525   | 1.84422    |
| Adenine (C <sub>5</sub> H <sub>5</sub> N <sub>5</sub> )   | -2.84297 | -2.85942  | -2.86550   | Pyruvate (2-OP)   | 1.96268 | 1.95589   | 1.95366    |
| Cyanide   | -0.88917 | -0.89251  | -0.89357   | Glutamate   | 2.10426 | 2.08042   | 2.07268    |
| Adenosine   | -1.80969 | -1.85402  | -1.86834   | Glyoxylate (2-OA)                                       | 2.38730 | 2.38730   | 2.38730    |
| Methane-thiol   | -0.84734 | -0.86099  | -0.86539   | Aspartate (Asp)   | 2.54052 | 2.52347   | 2.51796    |
| Dihydrogen  | -0.54308 | -0.54993  | -0.55210   | Glycerate   | 2.56630 | 2.55260   | 2.54815    |
| Ammonia   | -0.44845 | -0.45865  | -0.46193   | Carbonate   | 3.04817 | 3.04734   | 3.04706    |
| Valine  | -0.45040 | -0.48789  | -0.50003   | AMP   | 3.13027 | 3.09958   | 3.09011    |
| Proline   | -0.28861 | -0.31930  | -0.32921   | Malonate (2-CA)   | 3.38556 | 3.43263   | 3.43369    |
| Sulfide   | -0.28037 | -0.28338  | -0.28416   | Malate (2-HS)   | 3.80301 | 3.80301   | 3.80301    |
| Dinitrogen  | -0.10128 | -0.10128  | -0.10128   | 2-OS  | 3.97310 | 3.97995   | 3.98212    |
| Dioxygen  | -0.09134 | -0.09134  | -0.09134   | 4-HOG   | 4.48410 | 4.47463   | 4.47947    |
| Thioacetate   | 0.08442  | 0.07742   | 0.07519    | Portlandite Ca(OH) <sub>2</sub>                         | 4.55633 | 5.54948   | 4.54731    |
| Hydrogen peroxide   | 0.30142  | 0.29418   | 0.29240    | 3-CAS   | 4.58852 | 4.58502   | 4.58396    |
| Formaldehyde  | 0.34470  | 0.33784   | 0.33567    | 3-CM  | 5.84516 | 5.85190   | 5.85413    |
| Alanylglycine   | 0.49758  | 0.46349   | 0.45246    | Phosphate P <sub>i</sub>                                | 5.89562 | 5.89902   | 5.90080    |
| Alanine   | 0.50855  | 0.48467   | 0.47697    | 3-COS   | 6.14363 | 6.15605   | 6.16608    |
| Carbon monoxide   | 0.66778  | 0.66778   | 0.66778    | 3-OM  | 6.52408 | 6.52514   | 6.52787    |
| Glyceraldehyde  | 0.68510  | 0.67146   | 0.66700    | Ribose-5-phosphate                                      | 6.81676 | 6.79654   | 6.79025    |
| Methane   | 0.69897  | 0.71256   | 0.71696    | ADP   | 7.95839 | 7.93957   | 7.93483    |
| Water   | 0.87597  | 0.86912   | 0.86695    | Pyrophosphate PP <sub>i</sub>                           | 10.7767 | 10.7999   | 10.8085    |
| Glycylglycine   | 0.94848  | 0.92125   | 0.91239    | ATP   | 12.7686 | 12.7661   | 12.7680    |
| Glycerol  | 0.99042  | 0.96313   | 0.95433    | Triphosphate PPP <sub>i</sub>                           | 15.6178 | 15.6665   | 15.6838    |
| Acetate   | 1.38925  | 1.38246   | 1.38023    | Hydroxyapatite  | 34.9609 | 34.9575   | 34.9564    |

sible the appearance of endocytosis and exocytosis. We will take the example of egg lecithin, that have the following geometrical parameters:  $V = 1.063 \text{ nm}^3$ ,  $A = 0.717 \text{ nm}^2$ ,  $L = 1.75 \text{ nm}$ ,<sup>31</sup> leading to  $PP = 0.84$  favoring planar bilayers. However, by mixing such lecithin molecules with a fat such as stearic acid we get for a 50:50 mixture an average PP-value of  $(0.30 + 0.84)/2 = 0.57$ , i.e. formation of a closed spherical double layer. For a lecithin/fat ratio of 75:25, it comes  $\langle PP \rangle = (0.30 + 3 \times 0.84)/4 = 0.705$  and now we are back again with a planar bilayer. We have thus here a very basic mechanism of exocytosis ( $PP < 2/3$ ) or endocytosis ( $PP > 2/3$ ) allowing such micelles to absorb foods and reject wastes. Another quite important molecule for membranes was cholesterol that have the following geometrical parameters:  $V = 0.630 \text{ nm}^3$ ,<sup>31</sup>  $A = 0.41 \text{ nm}^2$ ,<sup>32</sup>  $L = 1.03 \text{ nm}$ ,<sup>33</sup> leading to  $PP = 1.49$  favoring inverse closed spherical double layer, allowing transport of water in oil and not oil in water as with direct micelles. Owing to such a property cholesterol may be used to favor very stable planar bilayers for molecules having a packing parameter not close to 1, the

optimal value for such a topology. For instance by mixing egg-lecithin with cholesterol in a 75:25 ratio, one get  $\langle PP \rangle = (1.49 + 3 \times 0.84)/4 = 1.00$ .

Now, we should understand that extracting phosphate group from apatite was a crucial problem that has to be solved before the spreading of life on Earth. When a transformation is not thermodynamically allowed owing to a decrease of the total entropy ( $\Delta \Pi_i^\circ < 0$ ), a good solution is usually to make a coupling with radiant energy coming from the sun as visible light or from the Earth as infrared radiation. Characterizing radiations by their wavelengths  $\lambda$ , such a coupling may be expressed by the following relationship:

$$-\lambda \cdot T \cdot \Delta \Pi_i^\circ = h \cdot c = 198.645 \text{ zJ} \cdot \mu\text{m} \quad (4)$$

Thus, for reaction (c) in table 5 characterized by  $\Delta \Pi_i^\circ = -2.32000 \text{ zJ} \cdot \text{K}^{-1}$ , one should use at  $T = 298.15 \text{ K}$  a photon having a wavelength less than  $\lambda = 287 \text{ nm}$ . The problem is that apatite is a solid that could be used for storing radioactive nuclides generated by nuclear power

**Table 5.** Thermodynamic analysis of some abiotic reactions generating important compounds for the emergence of life on Earth. (a,b) Choline; (c) Phosphate; (d,e) Glycerol; (f,g) Glycerate; (h) Hydrogen peroxide; (i,j) Formate; (k,l) Acetate; (m,n) Methanethiol; (o,p) Thioacetic acid; (q,r,s) Glyoxylate; (t,u,v) Pyruvate. All values are given at pH = 7 and I = 0.25 M and reported in  $\text{zJ}\cdot\text{K}^{-1}$ .

| Reaction  | $\Sigma \Pi_i^\circ$ (left) | $\Sigma \Pi_i^\circ$ (right) | $\Delta \Pi_i^\circ$ |
|---|-----------------------------|------------------------------|----------------------|
| (a) $5 \text{ CO} + \text{NH}_4^+ + 9 \text{ H}_2 = \text{C}_5\text{H}_{14}\text{NO}^+ + 4 \text{ H}_2\text{O}$               | -2.09193                    | 0.0096                       | +2.10153             |
| (b) $5 \text{ H}_2\text{CO}_3 + \text{NH}_4^+ + 14 \text{ H}_2 = \text{C}_5\text{H}_{14}\text{NO}^+ + 14 \text{ H}_2\text{O}$ | 7.04397                     | 8.6791                       | +1.63513             |
| (c) $\text{Ca}_5(\text{PO}_4)_3\text{OH} + 9 \text{ H}_2\text{O} = 5 \text{ Ca}(\text{OH})_2 + 3 \text{ P}_i$                 | 42.75895                    | 40.43895                     | -2.32000             |
| (d) $3 \text{ CO} + 4 \text{ H}_2 = \text{C}_3\text{H}_8\text{O}_3$   | -0.20506                    | 0.95433                      | +1.15939             |
| (e) $3 \text{ H}_2\text{CO}_3 + 7 \text{ H}_2 = \text{C}_3\text{H}_8\text{O}_3 + 6 \text{ H}_2\text{O}$                       | 5.27648                     | 6.15603                      | +0.87955             |
| (f) $3 \text{ CO} + 2 \text{ H}_2 + \text{H}_2\text{O} = \text{C}_3\text{H}_5\text{O}_4^-$                                    | 1.76615                     | 2.54815                      | +0.78200             |
| (g) $\text{HCO}_3^- + 2 \text{ H}_2\text{CO}_3 + 5 \text{ H}_2 = \text{C}_3\text{H}_5\text{O}_4^- + 5 \text{ H}_2\text{O}$    | 6.38068                     | 6.88290                      | +0.50222             |
| (h) $2 \text{ H}_2\text{O} + \text{FeS}_2 = \text{H}_2\text{O}_2 + \text{H}_2\text{S} + \text{FeS}$                           | 2.62557                     | 0.57243                      | -2.05314             |
| (i) $\text{CO} + \text{H}_2\text{O} = \text{HCOO}^- + \text{H}^+$   | 1.53473                     | 1.73233                      | +0.19760             |
| (j) $\text{HCO}_3^- + \text{H}_2 = \text{HCOO}^- + \text{H}_2\text{O}$  | -2.49496                    | 2.59928                      | +0.10432             |
| (k) $2 \text{ CO} + 2 \text{ H}_2 = \text{CH}_3\text{COO}^- + \text{H}^+$   | 0.23136                     | 1.38023                      | +1.14887             |
| (l) $\text{HCO}_3^- + \text{H}_2\text{CO}_3 + 4 \text{ H}_2 = \text{CH}_3\text{COO}^- + 4 \text{ H}_2\text{O}$                | 3.88572                     | 4.84803                      | +0.96231             |
| (m) $\text{CO} + 2 \text{ H}_2 + \text{H}_2\text{S} = \text{CH}_3\text{-SH} + \text{H}_2\text{O}$                             | -0.72058                    | 0.00156                      | +0.72214             |
| (n) $\text{H}_2\text{CO}_3 + 3 \text{ H}_2 + \text{H}_2\text{S} = \text{CH}_3\text{-SH} + 3 \text{ H}_2\text{O}$              | 1.10660                     | 1.73546                      | +0.62886             |
| (o) $\text{CO} + \text{CH}_3\text{-SH} = \text{CH}_3\text{COS}^- + \text{H}^+$  | -0.19761                    | 0.07519                      | +0.27280             |
| (p) $\text{HCO}_3^- + \text{H}_2 + \text{CH}_3\text{-SH} = \text{CH}_3\text{COS}^- + 2 \text{ H}_2\text{O}$                   | 1.62957                     | 1.80909                      | +0.17952             |
| (q) $\text{HCOO}^- + \text{CO} = \text{C}_2\text{HO}_3^-$   | 2.40001                     | 2.38730                      | -0.01281             |
| (r) $\text{HCO}_3^- + \text{H}_2\text{CO}_3 + 2 \text{ H}_2 = \text{C}_2\text{HO}_3^- + 3 \text{ H}_2\text{O}$                | 4.98992                     | 4.98815                      | -0.00177             |
| (s) $\text{HCO}_3^- + \text{CO} + \text{H}_2 = \text{C}_2\text{HO}_3^- + \text{H}_2\text{O}$                                  | 3.16274                     | 3.25425                      | +0.09151             |
| (t) $\text{CH}_3\text{COO}^- + \text{CO} = \text{C}_3\text{H}_3\text{O}_3^-$  | 2.04801                     | 1.95366                      | -0.09435             |
| (u) $\text{HCO}_3^- + 2 \text{ H}_2\text{CO}_3 + 5 \text{ H}_2 = \text{C}_3\text{H}_3\text{O}_3^- + 6 \text{ H}_2\text{O}$    | 6.38068                     | 7.15536                      | +0.77468             |
| (v) $3 \text{ CO} + 2 \text{ H}_2 = \text{C}_3\text{H}_3\text{O}_3^- + \text{H}^+$  | 0.89914                     | 1.95366                      | +1.05452             |

plants during a geological period of time.<sup>34</sup> Consequently, if apatite remains stable upon heavy irradiation with gamma photons, there is no chance that a UV-C photon will be able to extract phosphate from apatite. It is at this point that a metabolic cycle being a perpetual source of entropy alimanted by Earth plate tectonics and emerging at the mouth of hydrothermal vents could be very useful. From, figure 2 we know that to start the cycle, three ingredients should be able to meet upon a mineral surface: glyoxylate, pyruvate and hydrogen peroxide. A look at table 4 immediately shows that the most critical food will be hydrogen peroxide  $\text{H}_2\text{O}_2$ , as it is the compound that displays the smallest irreversibility potential. The problem is then how to reduce water  $\text{H}_2\text{O}$  into hydrogen peroxide  $\text{H}_2\text{O}_2$ . A possible solution is to consider that there was on the primitive Earth probably a lot of pyrite  $\text{FeS}_2$  that could react according to the scheme (h) in table 5 and illustrated in figure 2. Such a reaction is characterized by a large decrease in total entropy, but could be compensated according to (6), by a UV-A photon having a wavelength less than  $\lambda = 325$  nm, using pyrite's surface as a photo-electrode (figure 2). Here, the solid reacts only by its surface and does

not need to be solubilized as in the case of apatite. The fact that all form of life uses extensively ferredoxins containing iron-sulfur clusters as source of electrons is thus probably a vestige of these Hadean times where pyrite and sun was the sole source of hydrogen peroxide. Such a reaction has been tested in the laboratory and it was shown that upon UV-irradiation water could be decomposed into hydrogen peroxide with steady-state concentration of  $34 \mu\text{M}$ .<sup>35</sup> It was also shown that pyrite was not the most efficient photo-catalytic surface as a concentration of  $400 \mu\text{M}$  was obtained in the presence of vaesite  $\text{NiS}_2$ , pointing to the crucial role played by nickel and iron for the apparition of life on a primitive Earth. On the other hand, it was also found that  $\text{FeS}$  and  $\text{ZnS}$  surfaces were not able to catalyze such a reaction.

With the help of the sun and pyrite, hydrogen peroxide could be absorbed by the primitive oceans and reach the mouth of hydrothermal vents located upon the oceanic floor. Now, the problem is to explain how  $\alpha$ -keto-acids such as glyoxylate and pyruvate could also be present here in order to react with hydrogen peroxide. In fact, laboratory experiments has shown that metal sulfides could acts as catalysts for hydrocarboxy-

**Table 6.** Thermodynamic analysis of the 4-hydroxy-2-oxo-glutarate cycle represented at the bottom of figure 2. Such a cycle consume one glyoxylate molecule that is oxidized into carbon dioxide and water with an overall largely positive increase in entropy. All values are given at pH = 7 and I = 0.25 M and reported in zJ·K<sup>-1</sup>.

| Reaction  | $\Sigma \Pi_i^\circ$ (left) | $\Sigma \Pi_i^\circ$ (right) | $\Delta \Pi_i^\circ$ |
|---|-----------------------------|------------------------------|----------------------|
| 2-OP + 2-OA = 4-HOG   | 4.34096                     | 4.47947                      | +0.13851             |
| 4-HOG + H <sub>2</sub> O <sub>2</sub> = 2-HS + carbonate  | 4.77187                     | 6.85007                      | +2.07820             |
| 2-HS + H <sub>2</sub> O <sub>2</sub> = 2-OS + 2 H <sub>2</sub> O  | 4.09541                     | 5.71602                      | +1.62061             |
| 2-OS + 2-OA = 3-OM  | 6.36942                     | 6.52514                      | +0.15572             |
| 3-OM + H <sub>2</sub> O = 4-HOG + carbonate   | 7.39482                     | 7.52653                      | +0.13171             |
| C <sub>2</sub> HO <sub>3</sub> <sup>-</sup> + 2 H <sub>2</sub> O <sub>2</sub> = H <sub>2</sub> CO <sub>3</sub> + HCO <sub>3</sub> <sup>-</sup> + H <sub>2</sub> O | 26.97248                    | 31.09723                     | +4.12475             |

lation (Koch's reaction) where a  $\alpha$ -keto-acid is obtained via carbonyl insertion at a metal-sulfide-bound alkyl group in the absence of peptide-based enzymes.<sup>36</sup> It was found that the sulfides of nickel, cobalt, iron and zinc were able to catalyze such an insertion but not copper sulfides. Glyoxylate would thus be the result of inserting carbon monoxide into formate, while pyruvate would be the result of inserting carbon monoxide into acetate. As shown in table 5, formate could be formed according to scheme (i) or (j) and acetate according to scheme (j) and (k) with a moderate increase in entropy in the case of formate and a substantial one in the case of acetate.

Table 5 also shows that formation of methane-thiol through reactions (l) or (m) and thioacetate through reactions (n) or (o) proceeds with a neat increase of entropy, larger for the thiol derivative than the thiolate one. This basically means that alkyl sulfides were available around hydrothermal vents. However, scheme (p) in table 5 shows that direct insertion of carbon monoxide into formate yielding glyoxylate, proceeds with a slight decrease in total entropy. The direct reduction of a mixture of carbon monoxide and dioxide by hydrogen gas according to scheme (q) is a better solution. However, the best way to form glyoxylate leading to an increase in total entropy is scheme (r) proceeding by insertion of carbon monoxide into bicarbonate followed by reduction with hydrogen gas. The abiotic synthesis of pyruvate by insertion of carbon monoxide into acetate according to scheme (t) in table 5 appears to be not favorable. Direct reduction of bicarbonate by hydrogen gas according to scheme (u) is a much better solution, the best one being direct reduction of carbon monoxide following scheme v). Having checked the availability of glyoxylate, pyruvate and hydrogen peroxide, we should now focus

**Table 7.** Thermodynamic analysis of the malonate cycle represented at the top of figure 2. Such a cycle consume one glyoxylate molecule that is oxidized into carbon dioxide and water with an overall largely positive increase in entropy. All values are given at pH = 7 and I = 0.25 M and reported in zJ·K<sup>-1</sup>.

| Reaction  | $\Sigma \Pi_i^\circ$ (left) | $\Sigma \Pi_i^\circ$ (right) | $\Delta \Pi_i^\circ$ |
|---|-----------------------------|------------------------------|----------------------|
| 2-OS + H <sub>2</sub> O <sub>2</sub> = 2-CA + H <sub>2</sub> CO <sub>3</sub>  | 4.27452                     | 6.48075                      | +2.20623             |
| 2-CA + 2-OA = 3-CM  | 5.82099                     | 5.85413                      | +0.03314             |
| 3-CM + H <sub>2</sub> O <sub>2</sub> = 3-COS + 2 H <sub>2</sub> O   | 6.14563                     | 7.89998                      | +1.75435             |
| 3-COS + H <sub>2</sub> O = 2-OS + HCO <sub>3</sub> <sup>-</sup>   | 7.03303                     | 7.02918                      | -0.00385             |
| C <sub>2</sub> HO <sub>3</sub> <sup>-</sup> + 2 H <sub>2</sub> O <sub>2</sub> = H <sub>2</sub> CO <sub>3</sub> + HCO <sub>3</sub> <sup>-</sup> + H <sub>2</sub> O | 23.27417                    | 27.26404                     | +3.98987             |

on the 4-hydroxy-oxo-glutarate cycle shown at the bottom of figure 2 and analyzed for its feasibility in table 6. The result is impressive and shows that such a cycle is a totally abiotic "respiration" relying on carbon monoxide and hydrogen gas that are precursors of glyoxylate and pyruvate generated by the Earth that are burned by hydrogen peroxide generated by the sun, rejecting as waste carbon dioxide and water. On such a ground, there is no major difference between such a purely abiotic respiration supported transition metal sulfides and a plant capturing the energy from the sun to make organic matter that would be burned away releasing entropy at night. Moreover, by coupling the 4-hydroxy-2-oxo-glutarate cycle generating a large amount of entropy with the solubilization of apatite reaction (c) in table 5, it becomes possible extracting inorganic phosphate and release simultaneously 537 zJ of heat. These inorganic phosphate would be used to create phospholipids during the Hadean period, then coenzyme-A and its derivatives (NADH, NADPH, FAD, FMN, etc...) and most importantly nucleotides.

We could also have a look at the upper malonic cycle (table 7), that starts from 2-oxo-succinate (also called oxalo-acetate), an intermediate molecule synthesized during the revolving of the 4-HOG cycle. This cycle is not so efficient as the first one, but it also leads to the burning of glyoxylate by hydrogen peroxide with a large entropy increase available for coupling with a process associated to a decrease in entropy together with the eventual release of any excess entropy as heat. One may notice that a critical step in this cycle is the decarboxylation of 3-carboxy-2-oxo-succinate, which is the only step with a negative entropic contribution. However, as most of the irreversibility potentials for such intermediates has been estimated using Alberty's group contribution

**Table 8.** Thermodynamic analysis of the abiotic synthesis of the aspartate aminoacid from malonate  $-\text{OOC}-\text{CH}_2-\text{COO}-$ , carbon monoxide, ammonia and hydrogen gas. All values are given at pH = 7 and I = 0.25 M and reported in  $\text{zJ}\cdot\text{K}^{-1}$ .

| Reaction   | $\Sigma \Pi_1^\circ$<br>(before) | $\Sigma \Pi_1^\circ$<br>(after) | $\Delta \Pi_1^\circ$ |
|--|----------------------------------|---------------------------------|----------------------|
| $\text{HCO}_3^- + \text{CO} + \text{H}_2 + \text{NH}_4^+$<br>$= \alpha\text{-HG} + \text{H}_2\text{O}$   | 2.70081                          | 2.64868                         | -0.05213             |
| $\alpha\text{-HG} + 2\text{-CA} = 3\text{-CAS} + \text{H}_2\text{O}$   | 5.21542                          | 5.45091                         | +0.23549             |
| $3\text{-CAS} + \text{H}_2\text{O} = \text{C}_4\text{H}_6\text{O}_4\text{N} + \text{HCO}_3^-$  | 5.45091                          | 5.56502                         | +0.11411             |
| $\text{C}_3\text{H}_2\text{O}_4^- + \text{CO} + \text{H}_2 + \text{NH}_4^+$<br>$= \text{C}_4\text{H}_6\text{O}_4\text{N} + \text{H}_2\text{O}$ | 13.36714                         | 13.66461                        | +0.29247             |

method,<sup>28</sup> such a very small value is within the errors of the algorithm. But again, this does not really matter as there is enough entropy release in the other steps for keeping the cycle into a permanent running state.

As shown in figure 2, the malonate cycle is of crucial importance because as it allows formation of the important aminoacid aspartate by reacting malonate with alpha-hydroxy-glycine (see table 8).<sup>15</sup>

## ABIOTIC AMINOACID SYNTHESIS

As shown in figure 5, five other aminoacids may be derived from aspartate: lysine, asparagine, threonine, isoleucine and methionine. Another important precursor of aminoacids, sugars, cofactors and lipids is pyruvate, that is an important hub metabolite that have been obtained from FeS surfaces.<sup>37</sup> Another study has shown that pyruvate could be transformed readily in the presence of transition metal sulfide minerals under simulated hydrothermal fluids at temperature  $T = 25\text{-}110^\circ\text{C}$ .<sup>38</sup> Depending on the relative concentration of  $\text{H}_2\text{S}$  (3-110 mM),  $\text{H}_2$  (0.1-50 mM), alanine could be obtained among nine other species with yields ranging from 0.1% to 60%. With 100 mM  $\text{H}_2$ , 100 mM  $\text{CO}_2$  and 20 mM  $\text{H}_2\text{S}$  at  $T = 25^\circ\text{C}$  on FeS pyrrhotite, it was also possible to perform aldol condensation of pyruvate to 2-hydroxy-2-methyl-4-oxo-pentane-dioate with a yield of 13%. On such surfaces, it was also possible to form various thio-derivatives.

Now experimental studies have shown that the full sequence complexity of naturally occurring proteins is not required to generate rapidly folding and functional proteins, i.e. proteins can be designed with fewer than 20 letters.<sup>39</sup> Using combinatorial mutagenesis in an

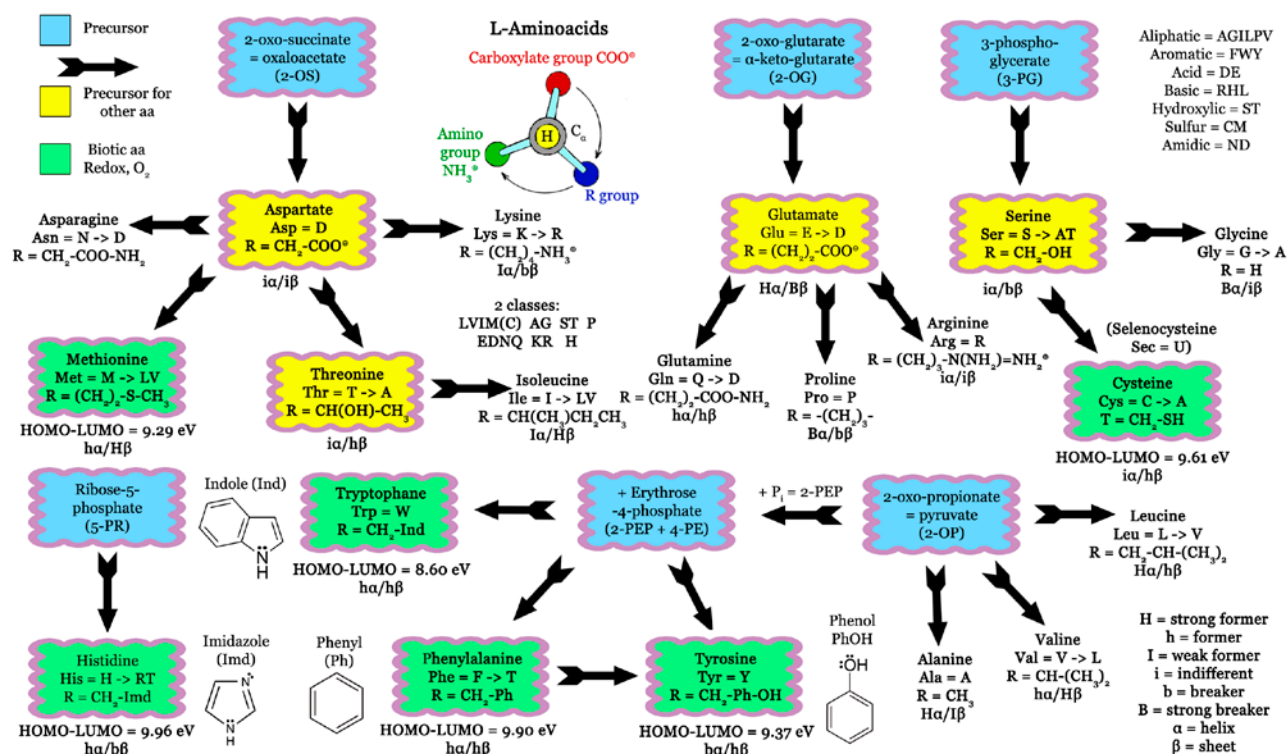


**Figure 5.** Relationships between the twenty aminoacid within their 3-letters and 1-letter codes, possible substitutions in proteins and secondary structure (helix or sheet) preference. Primary organic precursors are highlighted in blue, secondary aminoacid precursors of other aminoacids are highlighted in yellow. Aminoacids added lately to the universal genetic code under oxic conditions are highlighted in green.



enzyme of the bacterium *E. coli*, it has thus been shown that it was possible grouping the 20 aminoacids to a reduced set of 7 groups: Asp (Asn, Glu, Gln); Ala (Gly, Ser, Thr, Cys); Val (Met, Leu, Ile); Arg (Lys, His); Tyr (Phe), Trp and Pro.<sup>40</sup> Among these groups the four aromatic aminoacids (His, Tyr, Phe, Trp) and Met are characterized by an HOMO-LUMO gap smaller than 10 eV.<sup>41</sup> This indicates that in demanding building blocks with more versatile redox chemistry, biospheric molecular oxygen triggered the selective fixation of these last amino acids in the genetic code. Similarly, arginine may be discarded on the ground that it is essential only for catalytic activity and not for conformational stability.<sup>42</sup> Consequently, one may retain only four critical aminoacids for building prebiotic peptides precursors of proteins: Asp, Ala, Val, and Pro. In such a minimal set, we find a strong former of  $\alpha$ -helix (Ala) and a strong former of  $\beta$ -sheet (Val). We have also a breaker of helices and sheets (Pro) and an indifferent aminoacid (Asp) bringing acidic properties. The next aminoacid that will be logically recruited upon evolution is also an indifferent aminoacid (Arg) bringing basic properties.

Table 9 shows that alanine, valine and proline may be formed from pyruvate with an increase in entropy in all cases. We have also considered the formation of glutamate, which is expected to be an important intermediate for the synthesis of arginine. Accordingly, glutamate has also been obtained under hydrothermal conditions at a concentration of about 4  $\mu$ M.<sup>43</sup> Table 8 also shows that condensation of two amino acids to form a dipeptide is a non-spontaneous process that requires coupling with another process releasing at least +0.2 zJ·K<sup>-1</sup> of entropy. As there is plenty of entropy release in the two abiotic cycles represented in figure 2, oligomerization of amino acids into polypeptides just needs an adequate mineral surface. Accordingly, it is a well-established fact that amino acids concentrate and polymerize on clay minerals or apatite to form small, protein-like molecules containing up to 12 amino-acids.<sup>44</sup> For instance, the sanidine feldspar not only favors the peptide bond formation from both a thermodynamic and kinetic viewpoint but also prevents their hydrolysis.<sup>45</sup> Moreover, some mineral surfaces are known to be chiral, an important requirement for explaining the chirality of biomolecules. It has also been demonstrated that formation of a dipeptide from two amino acids is about eight times more difficult than subsequent condensations of an amino acid to a dipeptide or longer chain.<sup>46</sup> The same study has shown that adding an amino acid to a peptide of any size is five times more difficult than joining small peptides together. This demonstrates that the rather small entropy decrease associated to formation of a peptide bond is not a real prob-

**Table 9.** Thermodynamic analysis of the abiotic synthesis of the some aminoacid from pyruvate and their condensation into di-peptides. Alanine = C<sub>3</sub>H<sub>7</sub>NO<sub>2</sub>; Valine = C<sub>5</sub>H<sub>11</sub>NO<sub>2</sub>; Proline = C<sub>5</sub>H<sub>9</sub>NO<sub>2</sub>; Glutamate = C<sub>5</sub>H<sub>9</sub>NO<sub>4</sub>; Glycine = C<sub>2</sub>H<sub>5</sub>NO<sub>2</sub>; Glycylglycine = C<sub>4</sub>H<sub>8</sub>N<sub>2</sub>O<sub>3</sub>; Alanylglycine = C<sub>5</sub>H<sub>10</sub>N<sub>2</sub>O<sub>3</sub>. Also shown the analysis for the formation of inorganic as well as organic polyphosphates and polymers of formaldehyde (sugars) or cyanhydric acid (purine base). Ribose = C<sub>5</sub>H<sub>10</sub>O<sub>5</sub>; Glyceraldehyde = C<sub>2</sub>H<sub>4</sub>O<sub>2</sub>; Adenine = C<sub>5</sub>H<sub>10</sub>O<sub>5</sub>. All values are given at pH = 7, I = 0.25 M and reported in zJ·K<sup>-1</sup>.

| Reaction   | $\Sigma \Pi_i^\circ$ (left) | $\Sigma \Pi_i^\circ$ (right) | $\Delta \Pi_i^\circ$ |
|--|-----------------------------|------------------------------|----------------------|
| C <sub>3</sub> H <sub>3</sub> O <sub>3</sub> <sup>-</sup> + H <sub>2</sub> + NH <sub>4</sub> <sup>+</sup> =<br>alanine + H <sub>2</sub> O            | 0.93963                     | 1.34392                      | +0.40429             |
| C <sub>3</sub> H <sub>3</sub> O <sub>3</sub> <sup>-</sup> + 2 CO + 5 H <sub>2</sub> + NH <sub>4</sub> <sup>+</sup> =<br>valine + 3 H <sub>2</sub> O  | 0.06679                     | 2.10082                      | +2.03403             |
| C <sub>3</sub> H <sub>3</sub> O <sub>3</sub> <sup>-</sup> + 2 CO + 4 H <sub>2</sub> + NH <sub>4</sub> <sup>+</sup> =<br>proline + 3 H <sub>2</sub> O | 0.61889                     | 2.27164                      | +1.65275             |
| C <sub>3</sub> H <sub>3</sub> O <sub>3</sub> <sup>-</sup> + 2 CO + 2 H <sub>2</sub> + NH <sub>4</sub> <sup>+</sup> =<br>glutamate + H <sub>2</sub> O | 1.72309                     | 2.93963                      | +1.21654             |
| HCO <sub>3</sub> <sup>-</sup> + H <sub>2</sub> CO <sub>3</sub> + 3 H <sub>2</sub> + NH <sub>4</sub> <sup>+</sup> =<br>glycine + 4 H <sub>2</sub> O   | 3.97589                     | 4.44847                      | +0.47258             |
| Gly + Gly = Gly-Gly + H <sub>2</sub> O   | 1.96134                     | 1.77934                      | -0.18200             |
| Ala + Gly = Ala-Gly + H <sub>2</sub> O   | 1.45764                     | 1.31941                      | -0.13823             |
| 2 P <sub>i</sub> = PP <sub>i</sub> + H <sub>2</sub> O  | 11.8016                     | 11.6755                      | -0.1261              |
| AMP + P <sub>i</sub> = ADP + H <sub>2</sub> O  | 8.99091                     | 8.80178                      | -0.18913             |
| 3 P <sub>i</sub> = PPP <sub>i</sub> + 2 H <sub>2</sub> O   | 17.7024                     | 17.4177                      | -0.2847              |
| P <sub>i</sub> + PP <sub>i</sub> = PPP <sub>i</sub> + H <sub>2</sub> O   | 16.7093                     | 16.5508                      | -0.1585              |
| ADP + P <sub>i</sub> = ATP + H <sub>2</sub> O  | 13.8356                     | 13.6350                      | -0.2006              |
| 2 H <sub>2</sub> CO <sub>3</sub> + 4 H <sub>2</sub> =<br>glyceraldehyde + 4 H <sub>2</sub> O   | 3.88572                     | 4.13480                      | +0.24908             |
| 5 H <sub>2</sub> CO = ribose   | 1.67835                     | 1.84835                      | +0.17000             |
| 5 HCN = adenine  | 4.46785                     | -2.86655                     | +1.60130             |
| Ribose + P <sub>i</sub> =<br>Ribose-5-phosphate + H <sub>2</sub> O   | 7.74502                     | 7.65720                      | -0.08782             |
| Ribose + adenine =<br>Adenosine + H <sub>2</sub> O   | -1.02128                    | -1.00139                     | +0.01989             |

lem and could be easily overcome. According to (4), one could for instance make a coupling with the absorption of an infrared photon having a wavelength  $\lambda = 4.8 \mu$ m. According to Wien's displacement law the light emitted by a black body,  $4.9651 \cdot \lambda_{\max} \cdot (k_B T) = h \cdot c$  i.e.  $\lambda_{\max} \cdot T = 2898 \mu$ m·K, such photons are emitted in great amount by any surface heated to a temperature  $T \approx 600 \text{ K} \approx 330^\circ\text{C}$ . Such a temperature is typical of hydrothermal vents and experiments have confirmed that peptide synthesis was indeed favored in hydrothermal fluids.<sup>47</sup>

#### ABIOTIC PHOSPHATE-BASED COMPOUNDS

Our last concern will be the exact role played by ATP, a molecule intimately associated with any kind of

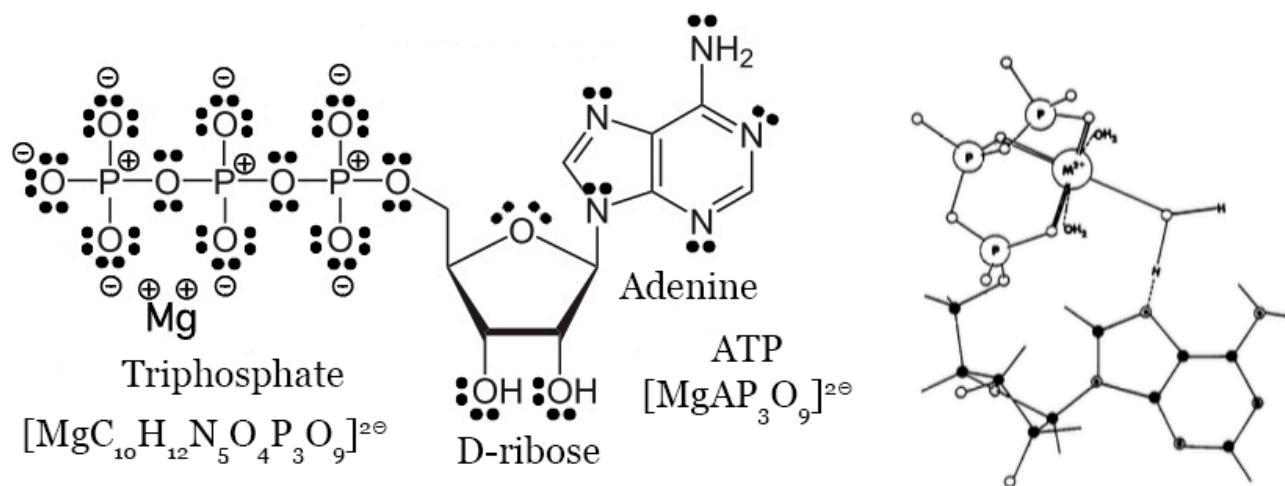


life process. As shown in figure 6, this molecule is made of three main parts: a triphosphate, a C5-sugar and a heterocyclic base named adenine. Table 8 shows that formation of polyphosphates, whether inorganic or organic is always associated to a decrease of the total entropy. Consequently, such reaction should be coupled with an entropy-generating process. Here, coupling with an infrared photon is unlikely as this would require a wavelength  $\lambda \approx 3.3 \mu\text{m}$  generated by surfaces heated at  $T = 870\text{K} \approx 600^\circ\text{C}$ , a temperature much too hot for hydrothermal vents. Here coupling with a metabolic cycle seems thus mandatory for the synthesis of such polyphosphate species. The same conclusion obviously applies to other phosphate-based species such as RNA or DNA.

The abiotic synthesis of the ribose and adenine moieties poses no particular problems, as a sugar is just an addition polymer of formaldehyde ( $\text{H}_2\text{C}=\text{O}$ )<sub>5</sub>, while adenine is an addition polymer of cyanhydric acid ( $\text{HCN}$ )<sub>5</sub>. Table 8 shows that formation of these polymers is associated to a significant increase in total entropy in both cases and may thus proceed without the need for an extra source of entropy. Obviously, such reactions need to be catalyzed by serpentinizing olivine and borate minerals for the formation of ribose from formaldehyde and small quantities of glycolaldehyde.<sup>48</sup> This last compound is necessary for catalyzing the first step of dimerization of formaldehyde that requires a high energy of activation. As shown in table 8, it could be easily formed in hydrothermal vents or derived from surface hydrogenation of CO molecules in interstellar dark cloud regions of the universe.<sup>49</sup> Similarly, the mechanism of formation of adenine, a HCN pentamer, under prebiotic

conditions has been studied, and it seems that catalysis by water and ammonia molecules is needed.<sup>50</sup> From table 8, one may see that the condensation of the ribose moiety with an inorganic phosphate is associated with a small decrease of entropy. For the condensation between adenine and ribose to yield adenosine, we are within the errors ( $\pm 0.02 \text{ zJ}\cdot\text{K}^{-1}$ ) of the method and nothing can be said about such a process.

Figure 5 also shows that the ATP molecule has a particularly good geometry for chelating divalent metallic ions<sup>51</sup> and has in particular a quite high affinity for magnesium ions.<sup>52</sup> Consequently, one should be cautious when computing irreversibility potential differences involving species bearing a strong negative charge such as ATP. But, the most interesting aspect of ATP is its position at the very bottom of table 4 giving irreversibility potentials in ascending order. One can see that the overall effect of phosphorylation is to strongly increase the irreversibility potential. It follows that ATP should be more assimilated to a waste than to a food. Moreover, one can see from table 8 that the energy released upon hydrolysis of ATP, about 60 zJ, is of the order of magnitude of at most two hydrogen bonds (about 40 zJ between two water molecules in liquid water). Speaking of the P-O-P linkage as a “high energy” bond seems thus quite exaggerated. One may also compare such an energy with the energy released by one turn of the two abiotic cycles shown in figure 2 that are 1330 zJ for the 4-hydroxy-2-glutarate cycle and 1190 zJ for the malonate cycle. This means that about 20-22 molecules of ATP would be needed for storing the energy liberated by the combustion of glyoxylate. The question is thus why con-



$$\text{pK}_a = 0.9; 1.5; 2.3; 4.06 (\text{N}); 6.95 \Rightarrow \text{pH} = 7.4 \Rightarrow \text{q}(\text{ATP}) = -3.3 \quad \mu \approx 230 \text{ D}$$

Figure 6. Lewis structure of adenosine triphosphate (ATP) shown here chelating a magnesium ion.

sidering a waste as a ubiquitous agent for storing energy? Table 4, shows that much better agents would be  $\text{NAD}^+$  or  $\text{NADH}$  that are at the very top of the table. Such a position is perfect for “high energy” molecules and accordingly the  $\text{NAD}^+/\text{(NADH,H}^+)$  couple is the universal energy pool in any kind of respiratory chain.

One of the reasons for focusing attention on ATP is merely that without a continuous production of such a compound, a cell is not able to survive. As a consequence, “high-energy” molecules such as  $\text{NADH}$  that are basically foods are systematically degraded to produce ATP, a very valuable waste indeed for the cell. A recent publication on the real role of ATP in the cell gives a clue.<sup>53</sup> It was shown that ATP at physiological concentrations 5-10 mM has properties of a biological hydrotrope, preventing the formation of protein aggregates and dissolving them if they happen to be formed. In other words, without ATP the intracellular medium is doomed to precipitate owing to its very high molecular crowding. Such a property of maintaining solubility is more in line with the position of ATP in table 4 and points to the importance of a systematically neglected factor, water activity  $a_w$ .

#### WATER ACTIVITY $A_w$

To understand this crucial point, we have to go back to equation (2) and see that an irreversibility potential for a given substance depends on temperature  $T$ , pressure  $p$  and on the activity  $a$  of this substance. Let's us recall that  $a = 1$  for a species in a pure state and that  $a < 1$  as soon as the substance is mixed with other substances. For condensed states such as liquids or solids, activity may be written as a product of two terms,  $a = \gamma X$ , where  $X$  is the molar fraction of the substance in the mixture and  $\gamma$  an activity coefficient taking into the deviations from ideal behavior of the mixture. Basically, an ideal mixture is a medium where constituents do not interact with each other. In other words, by considering an ideal mixture we implicitly assume that it exists only a single form of energy: kinetic energy. In such a case, one has  $\gamma = 1$  and the activity is essentially ruled by molar fractions  $X$ , that is to say molecular composition. However, as soon as the constituents interact through potential energy, one has  $\gamma \neq 1$  and activity is no more ruled by molar fractions alone. A situation where the molecular interactions between constituents are repulsive would lead to  $\gamma > 1$ , meaning that activity is increased relative to the ideal non-interacting case. Now, if molecular interactions are attractive then  $\gamma < 1$ , meaning that activity is decreased relative to the ideal non-interact-

ing case. From a practical viewpoint, for species having a sufficiently high vapor pressure, activities may be defined as the ratio  $a = p_{\text{vap}}(T)/p_{\text{vap}}^\circ(T)$ , where  $p_{\text{vap}}(T)$  and  $p_{\text{vap}}^\circ(T)$  are the vapor pressure measured at saturation and temperature  $T$  for the mixture and the species in a pure state respectively.

As a substance ubiquitous in the cell, water has its own activity that depends on the composition and of the interactions between water molecules and all the species in contact with water. A common assumption is that in a cell one should have  $a_w \approx 1$ , on the ground that the molar fraction of water  $X_w$  is very high ( $X_w > 0.99$ ) relative to all other constituents (see figure 1). By doing this, one automatically assume that  $\gamma_w \approx 1$ , meaning that water molecules do not interact at all with the solutes. Such an assumption is obviously utterly wrong, as water is a solvent that always interacts quite strongly with any kind of solute, meaning that one has necessarily  $\gamma_w < 1$ . As soon as this is posed, the immediate question is to quantify the deviation from unity for the activity coefficient of water. Obviously, there will be some substances provoking a large decrease of  $\gamma_w$  even at very low molar fraction and other substances needing high molar fractions to significantly decrease  $\gamma_w$ . A direct proof of the crucial importance of water activity for life is given by the fact that no microbial growth is possible below  $a_w < 0.6$  for the three domains of life (prokaryotes, archaea and eucaryotes).<sup>54</sup> In fact most microbes living at room temperature and ambient pressure are able to grow only if  $a_w > 0.9$ . Such a finding is clear evidence of the importance of water activity for life processes.

Norrish's equation is the best approach to understand how water activity changes upon adding a solute:<sup>55</sup>

$$K = (\text{KBI}_{\text{WW}} + \text{KBI}_{\text{SS}} - 2 \cdot \text{KBI}_{\text{SW}}) / 2V_w = a_w = X_w \cdot \exp(K \cdot X_s)$$

Here  $\text{KBI}_{\text{WW}}$ ,  $\text{KBI}_{\text{SS}}$  and  $\text{KBI}_{\text{SW}}$  are Kirkwood-Buff integrals (KBI) that are function of the radial distribution functions of water-water (WW), solute-solute (SS) and water-solute (SW) interactions. In practice, Norrish's equation applies up to moderate solute concentrations (ca 60 wt%, 5-10 M or 0.1-0.2 mole fraction) and may thus be applied to any kind of living cell.

As Norrish's constant  $K$  is generally negative, it follows that water activity always decreases when molar fraction of solutes increases. However, the variation of water activity with  $X_s$  appears to be modulated by the value of  $K$  that strongly depends on the chemical nature of the solute. In fact, owing to its very small size (ca 0.3 nm in diameter), it follows that the water-water integral  $\text{KBI}_{\text{WW}}$  does not change very much upon adding a sol-

ute. This is not the case of the two other integrals that are generally both negative owing to the existence of large excluded volumes. Generally speaking, the larger the solute species, the larger the exclusion volume and the more negative the Kirkwood-Buff integral. It thus follows that as a glucose molecule is bigger than a glycerol molecule, the decrease in water activity is stronger at the same concentration for glucose than for glycerol. This explains the phenomenon of cryptobiose where a cell produces a large amount of sucrose ( $K = -6.47$ ) in order to protect itself against freezing, dehydration, osmotic stress or low pressure. By strongly lowering its water activity, the cell is no more able to grow but can survive under very harsh conditions waiting eagerly for better conditions. As soon as water activity rises again, the sucrose is exchanged for water and the cell become able to grow again, as soon as  $a_w > 0.9$ .

Now, we are in the position of understanding that ATP owing to its very large negative charge and its big size is in fact an agent able to strongly decrease water activity. Table 10 gives the water activity calculated at  $X_w = 0.91$  for different substances soluble in water.<sup>56</sup> Values for  $Na_3ADP$  and  $Na_2ATP$  were derived from measurements of hydration isotherms of the solids.<sup>57</sup> It should be clear that the water activity coefficient  $\gamma_w$  is never equal to 1 and is strongly dependent on the nature of the solute. The water activity coefficient is in most cases less than one, pointing to attractive solute-water inter-

actions. The smaller the activity coefficient, the stronger is the attraction. The only exception is urea that has an activity coefficient greater than one pointing to repulsive interactions with water molecules. We have also indicated in table 10, the equivalent temperature that should be applied to supercooled water to get the same water activity value.<sup>58</sup> The lower the temperature, the stronger is the interaction. Values in table 9 are sorted in ascending order in order to highlight the fact that  $Na_3ADP$  and  $Na_2ATP$  salts are quite efficient in decreasing significantly water activity for a concentration below 2M. All other compounds require concentrations higher than 2M.

It is worth recalling that as shown in figure 7, no life is possible below  $a_w \approx 0.6$  corresponding to an osmotic pressure  $P \approx 70 \text{ MPa} \approx 0.7 \text{ kbar}$  and to a temperature less than  $-40^\circ\text{C}$ . The fact that  $Na_3ADP$  leads to a larger decrease in water activity than  $Na_2ATP$  at the same molar fraction comes from the fact that  $Na_3ADP$  has one additional negative charge relative  $Na_2ATP$ . One may then expect that the decrease in water activity for the salt  $Na_4ATP$  will be much larger than for  $Na_3ADP$ . Similarly, it may be expected that the complexation of  $ATP^{4-}$  by magnesium ions, yielding  $MgATP^{2-}$  will be associated to large increase in water activity, allowing inducing conformational changes of many proteins. Accordingly, it was shown that the  $F_1$  part of the ATP synthase present in the inner mitochondrial membrane was strongly dependent on water activity, the reaction

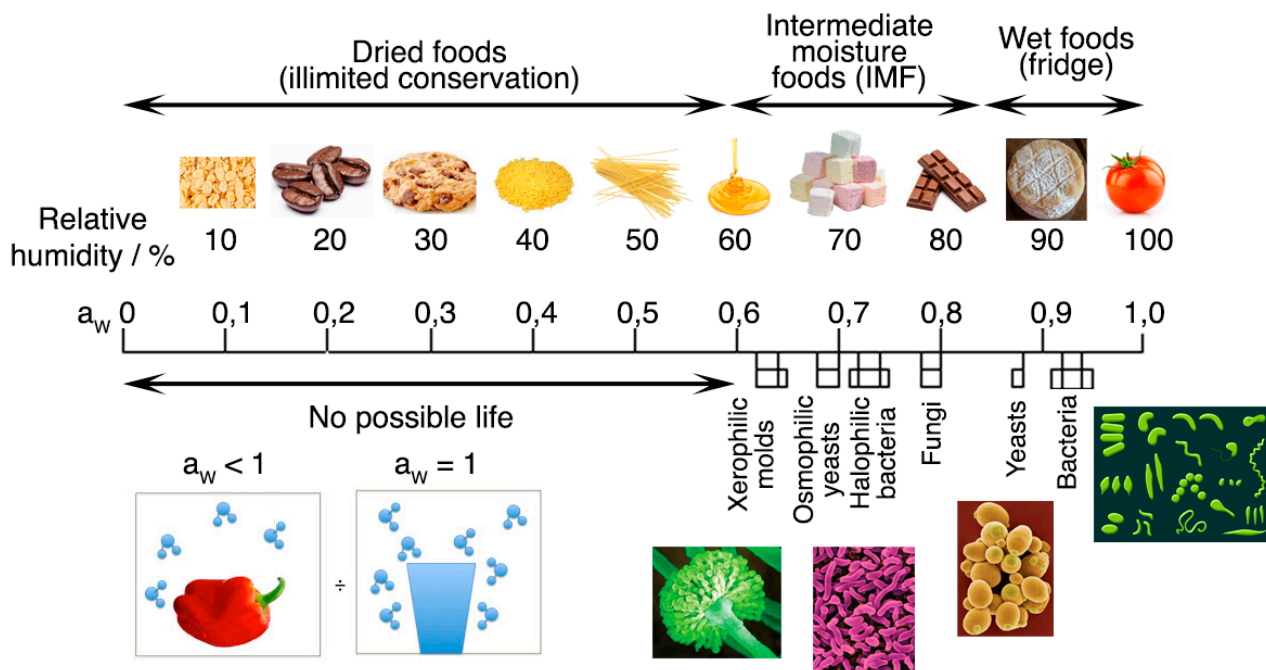


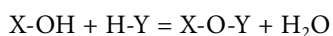
Figure 7. Water activity and growth of several kinds or microorganisms in relation with food preservation.

**Table 10.** Water activity  $a_w$ , water activity coefficient  $\gamma_w$  and equivalent equilibrium temperature T relative to supercooled water for a constant molar fraction  $X_w = 0.91$  of common solutes. One may convert water activities to equivalent osmotic pressures at  $T = 298.15$  K through the relationship  $P(\text{MPa}) = -137.15 \times \ln(a_w)$ .

| Substance S         | M.W. / Da | Concentration / M | $a_w$ | $\gamma_w$ | T / °C |
|---------------------|-----------|-------------------|-------|------------|--------|
| PEG600              | 400.00    | 2.28              | 0.578 | 0.635      | < -40  |
| Na <sub>3</sub> ADP | 493.15    | 1.85              | 0.606 | 0.666      | < -40  |
| NaCl                | 58.44     | 15.57             | 0.790 | 0.868      | -24    |
| KCl                 | 74.55     | 12.21             | 0.834 | 0.917      | -19    |
| Na <sub>2</sub> ATP | 551.14    | 1.65              | 0.838 | 0.921      | -18    |
| Lactose             | 342.30    | 2.66              | 0.838 | 0.921      | -18    |
| Lactulose           | 342.30    | 2.66              | 0.853 | 0.937      | -16    |
| Trehalose           | 342.30    | 2.66              | 0.862 | 0.947      | -15    |
| Sucrose             | 342.30    | 2.66              | 0.864 | 0.950      | -15    |
| Citric acid         | 192.12    | 4.74              | 0.866 | 0.952      | -15    |
| Tartaric acid       | 150.09    | 6.06              | 0.876 | 0.963      | -14    |
| Maltose             | 342.30    | 2.66              | 0.877 | 0.964      | -14    |
| Propylene glycol    | 76.09     | 11.96             | 0.881 | 0.968      | -13    |
| Fructose            | 180.16    | 5.05              | 0.889 | 0.977      | -12    |
| DMSO                | 78.13     | 11.65             | 0.889 | 0.977      | -12    |
| Glucose             | 180.16    | 5.05              | 0.894 | 0.982      | -12    |
| Galactose           | 180.16    | 5.05              | 0.894 | 0.982      | -12    |
| Malic acid          | 134.09    | 6.79              | 0.897 | 0.986      | -11    |
| Xylitol             | 152.15    | 5.98              | 0.898 | 0.987      | -11    |
| Sorbitol            | 182.17    | 5.00              | 0.898 | 0.987      | -11    |
| Lactic acid         | 90.08     | 10.10             | 0.898 | 0.987      | -11    |
| Xylose              | 150.13    | 6.06              | 0.899 | 0.988      | -11    |
| Arabinol            | 152.14    | 5.98              | 0.900 | 0.989      | -10    |
| Erythritol          | 122.12    | 7.45              | 0.900 | 0.989      | -10    |
| Glycerol            | 92.09     | 9.88              | 0.901 | 0.990      | -10    |
| Mannitol            | 182.17    | 5.00              | 0.903 | 0.992      | -10    |
| Urea                | 60.06     | 15.16             | 0.925 | 1.017      | -8     |

$F_1 \cdot \text{ADP} + P_i = F_1 \cdot \text{ATP}$  being shifted to the right by adding DMSO, a molecule able to decrease water activity below  $a_w = 0.80$  at a concentration of 40 vol%.<sup>59</sup> Similarly, it was observed that reduction in water activity upon addition of DMSO greatly retards the phosphoryl transfer from ATP to enzyme protein in the catalytic cycle of sarcoplasmic reticulum  $\text{Ca}^{2+}$ -ATPase.<sup>60</sup> Finally, synthesis of ATP after a single catalytic cycle of the same enzyme was promoted by water activity jumps.<sup>61</sup>

It follows that a cyclic activity of many enzymes could be related to cyclic variations in water activity. This is in fact quite logical when it is realized that most reactions in a living cell corresponds to the following reaction:



Where X and Y may be C, CO or P and Y may be O, S or NH. Proceeding to the right, we have anabolism,

while proceeding to the left we have catabolism. In both cases, the presence of the water molecule means that changing water activity could easily shift such equilibria. As shown in table 9, any variations in salt concentrations or in small organic solutes (sugars, polyols, carboxylic acids or urea) will change more or less water activity and shift the above equilibrium either to the left if  $a_w$  increases or to the right if  $a_w$  decreases. As this concerns water, the most abundant species in a living cell, we have here a quite general binary code. More importantly, any cyclic variation in  $a_w$  could be associated to the existence of a clock, a prerequisite for having coherent movements in a living cell.

## CONCLUSION

The main result of our approach is the crucial role played by the entropy for understanding any kind of

biological transformation. Most previous publications focused on energy not on entropy. Energy applies to the first law of thermodynamics, entropy to the second law. Our analysis is based on the second law and therefore on entropy.

Such a distinction between energy and entropy becomes obvious when one tries to understand the physical origin of the entropy concept. From Boltzmann's formulation of entropy,  $S = -k_B \sum_i p_i \ln p_i$ , we may link this concept to the number of indistinguishable microscopic configurations of a system corresponding to a single macroscopic state. Here, a clear link could then be established with Shannon's information content,  $H = -\sum_i p_i \ln p_i$ , of a message as both expression differs only by a universal scaling constant. In other words, if energy has something to do with mass or frequency (times a universal constant), entropy has something to do with information. As far as evolution is concerned, knowledge of the involved masses and frequencies is useless, relative to the information content. Accordingly, as energy should never increase or decrease during any evolution, the focus should be put on information that can be created at will and once created will never be destroyed. Variations of information contents (entropy) is the real driving force for any kind of evolution, available energy being here to set up the *speed* at which such an evolution may occur. As shown above, it is possible to describe the bioenergetics principles in terms of irreversibility potentials, leaving energy considerations to kinetics. On such a ground, one accounts for a fundamental splitting of the bioenergetics field into two distinct fields: biothermodynamics on one hand ruling evolution and focusing on entropy variations, and biokinetics on the other hand focusing on energy flux. Such a splitting is fully coherent with the fact that thermodynamics considerations are useless for discussing kinetics problems and vice-versa.

The main consequence of such a formulation is the existence of a single criterion of evolution in terms of irreversibility potentials  $\Delta\Pi \geq 0$ , instead of five different ones  $\Delta S \geq 0$  (evolution for an isolated system),  $\Delta U \leq 0$  (evolution at constant entropy and volume),  $\Delta H \leq 0$  (evolution at constant entropy and pressure),  $\Delta F \leq 0$  (evolution at constant temperature and volume) and  $\Delta G \leq 0$  (evolution at constant temperature and pressure) when focusing on the energy/entropy duality. In other words, instead of putting experimental constraints on the thermodynamic potentials, a simpler approach is to have a single thermodynamic potential measuring irreversible power and distinct numerical tables according to the experimental constraints. For instance, the values of the  $\Pi_i^\circ$  potentials used here applies to transformations occurring at constant temperature and pressure and they

should thus not be used for transformations occurring at constant entropy and volume for instance. For such transformations, other tables with different numerical values have to be used. In other words, the revolution for biologists is not the data (they are unchanged), but simply, putting entropy at the center of the equations. Life could be summarizing as able to export a large amount of entropy from the inside to the outside ( $\Delta S \gg 0$ ). It is the progressive decrease in entropy export ability that causes aging ( $\Delta S > 0$ ), death ( $\Delta S = 0$ ) and finally dispersion ( $\Delta S < 0$ ) when entropy becomes imported from the surroundings, instead of being exported towards the surrounding ( $\Delta S > 0$ ).

By putting entropy at the forefront, the quest for survival is deep-rooted in the ability for exporting entropy rather than in the ability of finding energy that is always available. On such a ground, existence of a metabolism based on a food/waste balance appears to be a prerequisite for any form of life, even the most rudimentary ones. Defining life by entropy export establishes a natural link with information quest. A system could then be qualified as 'living' as soon as it is able to export information towards its environment, keeping the useful and pertinent one for maintaining its internal structure. As demonstrated by the DNA molecule, an information content of about 1 Gb is enough to encode in all details a whole human being. Another advantage of the proposed approach is to qualify the whole Earth as a living system through its plate tectonics allowing mixing of the high entropy upper materials in the atmosphere and the crust with the low entropy lower materials in the mantle and the core. Having a self-assembled membrane lipidic bilayer is thus not a mandatory condition for being qualified as a living system. Any rocky system could be a potential living entity as soon as an exporting mechanism of entropy becomes available. Again, the differentiation between a living rocky system and a living biological cell is just a matter of kinetics with a time scale of billions years for the rocks and of a few years for cells.

Finally, such a reformulation of the emergence of life has deep implications in medicine where illness could now be viewed by a decrease of the ability for exporting entropy. Restoring the entropy export ability at its optimum level, or preventing entropy importation could be very valuable tools for healing. The main characteristics of such new healing methods would be treat the body as a whole and to use very simple chemical compounds able to restore compromised entropy outputs (breath, sweat, urine, feces, heat for instance) by changing water activity. Time seems then to be ripe for stopping discussing biological events in terms of energy variations.

Any “energy” variation should be reformulated as an irreversible entropy increase, by changing the sign of the involved energy and dividing the result by the temperature of the medium. This is not at all just a mathematical game, but rather the clear acknowledgment that what drives evolution is entropy and not energy. Without a clear recognition that an expression such as “chemical energy” is meaningless, evolution of biology as a science will be deeply hampered.

#### APPENDIX A

At the root of the development of thermodynamics, two notions are usually introduced: energy that is always conserved (first law) and entropy that should never decrease (second law). Such a dichotomy has led to much confusion, with an opposition between processes occurring in inert matter piloted by an increase in entropy and processes occurring in living matter supposed to proceed with a decrease in entropy. It is thus quite strange that the notion of chemical potential introduced at the beginning of the XX century by John Willard Gibbs is seldom used in chemistry and biology. One of the big advantage of considering chemical potential rather than energy or entropy is that there is a single fundamental law stating that a spontaneous transformation is always associated to a *decrease* of the total chemical potential  $\mu$ . Accordingly moving a weight up, increasing a speed, heating a body, decreasing volume of gases, increasing an area, increasing concentration of a solution, increasing an electrical potential difference are not processes occurring spontaneously. In our universe, weights always fall down, speeds always decrease, hot bodies always cool down, gases always expands, areas always decrease, solutions becomes always diluted, and potential differences always decrease. The fundamental reason behind such phenomena is always the same: a decrease in each case of an entity having the dimension of a mass times an area times the square of a frequency. In the previous examples, such an entity was the product of a force by a height, the product of a linear momentum by a speed, the product of an entropy by a temperature, the product of a volume by a pressure, the product of a number of moles by a chemical potential and the product of an amount of electrical charge by a voltage.

Confusion immediately arises as soon as such an entity is called “energy”. This stems from the fact that in physics energy is defined as mass ( $m$ ) times the square of the velocity of light in vacuum  $c$  (theory of relativity) or as frequency ( $f$ ) times Planck’s constant  $h$  (quantum theory). So, even if the propensity to spontaneous evolution

in thermodynamics and energy in physics are quantified by the same physical unit (joule), they should not be confused. The consecrated name “Gibbs free energy” (symbol  $G$ ) for measuring propensity for spontaneous evolution in thermodynamics is a first step, but has the drawback of still making a link with the energy concept of physics ( $E$ ). We will use the symbol  $U$  and write according to the first law:  $\Delta U = \Delta Q - p \cdot \Delta V$ , where  $\Delta Q$  is the amount of heat,  $p$  the pressure and  $\Delta V$  the variation in volume. For energy we have on the other hand,  $\Delta E = \Delta m \cdot c^2$  from relativity theory or  $\Delta E = h \cdot f$ , from quantum theory. One should easily understand that setting  $\Delta E = \Delta U$  is quite absurd, despite the fact that both quantities share the same physical unit. The absurdity is that mass is assumed to be conserved in  $\Delta U$ , but is allowed to change in  $\Delta E$ . Similarly,  $\Delta U$  refers to systems made of matter whereas  $\Delta E = h \cdot f$  refers to photons that have no mass.

In order to unveil the real significance of  $\Delta U$ , one may consider that pressure  $p$  is a kind “mechanical potential” associated to variations in volume. This fundamentally means that spontaneous changes are expected as soon as it exists pressure differences in a system, mechanical equilibrium being reached when pressure is the same everywhere (no more changes in volume). It was a quite brilliant idea of Rudolf Clausius, to introduce a state function named “entropy”  $S$  ruling reversible infinitesimal heat transfers between a system and its surroundings, associated to a “thermal potential”, measured by the temperature  $T$ ,  $dQ = T \cdot d_e S$ . As with pressure, this fundamentally means that spontaneous changes are expected as soon as it exists temperature differences in a system, thermal equilibrium being reached when temperature is the same everywhere (no more changes in entropy). But, it was also realized by Clausius, that entropy exchanges  $d_i S$  could also occur inside a system with the constraint that  $d_i S \geq 0$ . In other words, if  $d_e S$  is perfectly allowed to increase ( $d_e S > 0$ ) or decrease ( $d_e S < 0$ ),  $d_i S$  has the unique property of being a quantity that should always increase or remain constant.

Taking into account these two laws and writing the total entropy variation as  $dS = d_e S + d_i S$ , leads to  $dU = T \cdot d_e S - p \cdot dV = T \cdot dS - p \cdot dV - T \cdot d_i S$ . It follows that for any evolution occurring at constant entropy and volume ( $dS = dV = 0$ ), one should have  $dU = -T \cdot d_i S \leq 0$  as  $T$  and  $d_i S$  are both positive quantities. The drawback of such a formulation is that most transformations occurs at constant pressure ( $dp = 0$ ) and constant temperature ( $dT = 0$ ). However, one may introduce a new potential  $G = U + p \cdot V - T \cdot S$ , leading to  $dG = dU + V \cdot dp + p \cdot dV - T \cdot dS - S \cdot dT = V \cdot dp - S \cdot dT - T \cdot d_i S$ . Now, for any isobaric ( $dp = 0$ ) and isothermal ( $dT = 0$ ) evolution, we get  $dG = -T \cdot d_i S \leq 0$ . It is an easy matter to check that the same criterion

of evolution could also be written  $dH = -T \cdot d_i S \leq 0$  for isobaric ( $dp = 0$ ) and adiabatic ( $dS = 0$ ) evolution and  $dF = -T \cdot d_i S \leq 0$  for isochoric ( $dV = 0$ ) and isothermal ( $dT = 0$ ) evolution. It thus appears that there is a single universal criterion of evolution,  $d_i S \geq 0$ , whatever the pair of variable chosen for controlling the system. Consequently, any spontaneous evolution always corresponds to an irreversible increase in entropy. For chemistry, one speaks of irreversible transformation while for biology one speaks of irreversible aging. In all cases, the thing that is decreasing has nothing to do with the energy of physicists related to mass content for material systems or to frequency of oscillations for radiations.

The above considerations apply rigorously for a closed system allowed to exchange only heat with its surroundings. If exchange of matter are also allowed, one may introduce a “chemical potential”  $\mu$  in addition to the mechanical potential  $p$  and the thermal potential  $T$  and writes that  $dG = V \cdot dp - S \cdot dT + \mu \cdot dN - T \cdot d_i S$ . Consequently, any substance is characterized by a set of three thermodynamic properties, a molar volume  $V_m = (\partial G / \partial p)_{T, N}$ , a molar entropy  $S_m = -(\partial G / \partial T)_{p, N}$  and a chemical potential  $\mu = (\partial G / \partial N)_{T, p}$ . Choosing a standard reference state  $T^\circ = 298.15$  K,  $p^\circ = 100$  kPa allows writing the chemical potential as  $\mu(p, T) = \mu^\circ - S_m^\circ \cdot (T - T^\circ) + V_m^\circ \cdot (p - p^\circ)$ . A universal rule is then that if a substance is able to exist under different states, the observed state will always be the state having the lowest chemical potential. As  $S_m^\circ(\text{gas}) > S_m^\circ(\text{solid})$  and  $V_m^\circ(\text{gas}) > V_m^\circ(\text{solid})$ , it directly follows that any pure substance should vaporize at a sufficiently high temperature ( $\Delta T > 0$ ) or low pressure ( $\Delta p < 0$ ). Similarly one should expect a solid at a sufficiently high pressure ( $\Delta p > 0$ ) or low temperature ( $\Delta T < 0$ ). If a solid substance exists under several polymorphs, the observed polymorph at high temperature and pressure will be the one displaying respectively the highest entropy and the lowest molar volume.

Chemical potentials may also be defined for mixtures of substances, as  $\mu_i(p, T, N_i) = \mu_i(p, T) + RT \cdot \ln a_i$ , where  $0 < a_i \leq 1$  measures the “activity” of each substance in the mixture. By definition,  $a_i = 1$  for a pure substance. For mixture of liquids containing  $N$  molecules, the activity of each component is given by the product of the molar fraction  $X_i = n_i / N$  by an activity coefficient  $\gamma_i$  characterizing how the various molecules interact together either through attractive ( $\gamma_i < 1$ ) or through repulsive ( $\gamma_i > 1$ ) forces:  $a_i = \gamma_i \cdot X_i$ . For solutions, the activity corresponds to a molarity ratio,  $c_i / c^\circ$ , or molality ratio,  $m_i / m^\circ$ , times an activity coefficient  $\gamma_i$ :  $a_i = \gamma_i \cdot c_i / c^\circ$  or  $a_i = \gamma_i \cdot m_i / m^\circ$ . Here,  $c^\circ$  and  $m^\circ$  refer to a reference state such that  $c^\circ = 1$  M or  $m^\circ = 1$  mol·kg<sup>-1</sup>. For

gases, the activity is function of the partial pressure  $p_i = p \cdot X_i$  relative to a standard pressure  $p^\circ$  times an activity coefficient  $\gamma_i$ :  $a_i = \gamma_i \cdot p_i / p^\circ$ , the reference pressure being  $p^\circ = 100$  kPa. Concerning activity coefficients, a general rule is that for low molar fraction  $X_i \ll 1$ , highly diluted solution  $c_i \ll c^\circ$  and low partial pressure  $p_i \ll p^\circ$  one may safely assume that  $\gamma_i \approx 1$ .

## APPENDIX B

As the existence of irreversibility potentials should be quite new for most of the readers, we will give here some clues for decoding its physical significance. It should first be realized that such potentials results from the competition between two antagonistic kind of energies, the first one being kinetic energy favoring expansion and repulsion, the second one being electrical potential energy of attraction between positively charged nuclei and negatively charged electronic clouds. The stronger this attraction, the lower the irreversibility potential of the substance. But this is not the whole story, as these potentials are also dependent on the ability to liberate a large number of different kinds of chemical species during any transformation. This explains why elements, substances able to generate only a single kind of atom upon reaction and making strong covalent bonds under standard conditions, have the lowest  $\Pi_i^\circ$  values and may thus be considered as primitive foods. This also explain why complex substances made of a large number of different atoms have higher  $\Pi_i^\circ$  values. The larger the number of different constituting atoms, the larger the  $\Pi_i^\circ$  values.

Taking for instance the case of carbon dioxide  $\text{CO}_2$  that appears from table 1 to be rather close to solid wastes, despite the fact that it is a gas. This stems from the fact that electrical interactions between  $\text{CO}_2$  molecules are here very weak (absence of permanent dipole moment owing to a very high symmetry) and that carbon dioxide may be cleaved into 2 different chemical species carbon monoxide CO on the one hand and dioxygen  $\text{O}_2$  on the other hand. Carbon monoxide CO, being more polar than  $\text{CO}_2$  owing to its asymmetric structure and being more reluctant to give off its oxygen owing a triple bond between carbon and oxygen has logically a much lower  $\Pi_i^\circ$ -value. Finally dioxygen  $\text{O}_2$  and dinitrogen  $\text{N}_2$  molecules are still less polar than CO and may give off upon dissociation only a single kind of atom, explaining their position near the top of the table.

Water  $\text{H}_2\text{O}$ , which is able as  $\text{CO}_2$  to be cleaved into two gases (here  $\text{H}_2$  and  $\text{O}_2$ ), but is also a highly polar substance has thus a  $\Pi_i^\circ$ -value intermediate between that



of CO and CO<sub>2</sub>. On the other hand hydrogen sulfide H<sub>2</sub>S which is a gas and which may be also cleaved into two different substance, sulfur S and H<sub>2</sub>, has a much lower  $\Pi_i^\circ$ -value because one of these substance, sulfur, is made of molecules S<sub>8</sub> that display attractive interactions strong enough to form a solid under standard conditions. As irreversibility potentials for compounds are all measured relative to the irreversibility potentials of the constituting elements, these elements all have the same zero  $\Pi_i^\circ$ -value. In order to distinguish between them, one may use their absolute standard entropy  $S^\circ$  or their volume  $V^\circ$  under standard conditions of pressure and temperature. Here, the lower  $S^\circ$ , the tighter the organization of atoms in space. For gases, the Sackur-Tetrode equation (3) shows that the higher the molecular weight, the higher the entropy. Consequently, one gets  $S^\circ(\text{O}_2) > S^\circ(\text{N}_2) > S^\circ(\text{H}_2)$  as  $M(\text{O}_2) = 31.999$  Da,  $M(\text{N}_2) = 28.013$  Da and  $M(\text{H}_2) = 2.016$  Da.

For condensed phases such as solids and liquids, it becomes more difficult to interpret changes in absolute entropy. However, the Sackur-Tetrode equation (3) shows that entropy always increases with temperature, meaning that we should always expect the order:  $S^\circ(\text{g}) > S^\circ(\text{liq}) > S^\circ(\text{s})$ . Now, a general rule is that if a substance is able to exist under different phases the phase observed at given temperature and pressure will always be the one with the largest irreversibility potential. Consequently, from the definition of  $\Pi_i^\circ$ -values given in equation 2, it follows that at sufficiently high temperature every substance should exist as a gas, as entropy is always maximized in the gaseous state. Similarly, if a solid substance may exist under several distinct crystalline polymorphs, the polymorph observed at high temperature below melting temperature would be the one with largest  $S^\circ$ . For iron, for instance, we see from table 1 that Fe(bcc) is expected to transform into Fe(fcc) or Fe(hcp) as temperature is increased.

The Sackur-Tetrode equation predicts that entropy  $S^\circ$  should also increases with volume, meaning that one may expect:  $V^\circ(\text{s}) < V^\circ(\text{liq}) < V^\circ(\text{g})$ . From equation (2) it follows that at sufficiently high pressure any substance should be transformed into a solid, as owing to the negative sign before  $V^\circ$ , it is phases with the smallest volume that would have the largest irreversibility potentials. For iron, this means again that Fe(bcc) is expected to transform into Fe(fcc) or Fe(hcp) as pressure is increased. One should also understand that with  $V^\circ(\text{liq}) < V^\circ(\text{s}) < V^\circ(\text{g})$ , water appears as a quite strange substance, as it displays a lower volume than ice despite having a larger entropy. Basically, this means that upon heating, an increase in kinetic energy leads to a decrease in volume leading to a liquid being more dense than ice, the solid form of

water. Similarly, by applying pressure on ice, one should get a liquid. Such ‘‘anomalies’’ for water has deep consequences for life on Earth. The fact that ice floats upon water, means that it is impossible to transform a large mass of liquid water into a block of ice. This is because below 4°C, the liquid always sink at the bottom of the container, thus escaping from the freezing. The fact that ice melts upon applying a pressure means that large masses of ice cannot remain static but should always flow downwards as observed with glaciers. Being able to break down rocks by its increase in volume upon freezing and to abrade them away by flowing under an icy form, water is thus the main shaper of Earth with time.

It is also worth noting that irreversibility potentials given in table 1 applies to a single particle of each concerned species. Consequently, if one has in one part of the system  $N(\text{A})$  particles characterized by an irreversibility potential  $\Pi_i(\text{A})$  and in another part  $N(\text{B})$  particles having irreversibility potential  $\Pi_i(\text{B})$ , the irreversibility potentials of both parts should be  $P(\text{A}) = N(\text{A}) \cdot \Pi_i(\text{A})$  and  $P(\text{B}) = N(\text{B}) \cdot \Pi_i(\text{B})$  respectively. If both part are allowed to exchange particles and if  $P(\text{A}) = P(\text{B})$ , the system is said to be in equilibrium. In such a case the number  $N(\text{A})$  and  $N(\text{B})$  does not change with time. But if  $P(\text{A}) \neq P(\text{B})$ , the system becomes out of equilibrium and changes in  $N(\text{A})$  and  $N(\text{B})$  will be observed until restoration of the equilibrium  $P(\text{A}) = P(\text{B})$ . A direct consequence is then that if  $N(\text{A}) \cdot \Pi_i(\text{A}) = N(\text{B}) \cdot \Pi_i(\text{B})$ , then  $N(\text{A})/N(\text{B}) = \Pi_i(\text{B})/\Pi_i(\text{A})$ . One may thus compute relative populations from the knowledge of irreversibility potentials.

Applying such considerations to a pure substance ( $a = 1$ ) assumed to exist under two phases A and B means that equilibrium between both phases is expected as soon as  $N(\text{A}) = N(\text{B})$  or  $\Pi_i(\text{A}) = \Pi_i(\text{B})$ . At constant pressure ( $p = p^\circ = 0.1$  MPa), it comes from (2) that:  $\Pi_i^\circ(\text{A}) + S^\circ(\text{A}) \cdot (T - T^\circ) = \Pi_i^\circ(\text{B}) + S^\circ(\text{B}) \cdot (T - T^\circ)$ , leading to:

$$T = T^\circ \cdot \left[ 1 + \frac{\Pi_i^\circ(\text{A}) - \Pi_i^\circ(\text{B})}{S^\circ(\text{B}) - S^\circ(\text{A})} \right] \quad (B1)$$

Using equation (2) and table 1, it is thus possible to approximate melting ( $T_m$ ) and vaporization ( $T_{\text{vap}}$ ) temperatures of pure substances. For instance one may understand the very high cohesive energy of metallic iron as with A = solid phase (bcc) and B = liquid, (4) predicts that  $T_m = 1682$  K versus  $T_m(\text{exp}) = 1811$  K, while with A = liquid and B = gas, it comes that  $T_{\text{vap}} = 3644$  K versus  $T_{\text{vap}}(\text{exp}) = 3343$  K. The differences with experimental values may be accounted for by the fact that in (4) we have used  $S^\circ$ -values at  $T = 298.15$  K and neglected the variation of these standard entropies with tempera-

ture. Nevertheless, this clearly shows that iron atoms are in strong attractive interactions in the solid or in the liquid. One may also use table 1 to predict that upon heating  $\alpha$ -Fe(bcc) should be transformed into  $\gamma$ -Fe(fcc) and not into  $\epsilon$ -Fe(hcp). Now, applying (4) to water with A = ice and B = liquid leads to  $T_m = 275 \text{ K} = 2^\circ\text{C}$ , while with A = liquid and B = gas, it comes  $T_{\text{vap}} = 369 \text{ K} = 96^\circ\text{C}$ . Again, this shows the ability of irreversibility potentials to account approximately for observed melting and ebullition temperatures.

One may also consider what happens at constant temperature ( $T = T^\circ = 298.15 \text{ K}$ ) with (2) giving a new equilibrium condition as function of applied pressure  $\Pi_i^\circ(A) - V^\circ(A) \cdot (p - p^\circ)/T^\circ = \Pi_i^\circ(B) - V^\circ(B) \cdot (p - p^\circ)/T^\circ$  and leading to:

$$p(\text{MPa}) = p^\circ + \frac{\Pi_i^\circ(B) - \Pi_i^\circ(A)}{V^\circ(B) - V^\circ(A)} \cdot T^\circ \quad (\text{B2})$$

Consequently, one predicts that the transformation of A =  $\alpha$ -Fe(bcc) into B =  $\epsilon$ -Fe(hcp) should be observed at about  $p = 16.3 \text{ GPa}$ , in good agreement with experiments revealing a transition pressure above  $11 \text{ GPa}$  (see L. Miyagi et al., *J. Appl. Phys.*, **2008**, *104*, 103510). These considerations shows the usefulness of such irreversibility potentials for a good understanding of the behavior of a pure substance as a function of temperature and pressure.

#### REFERENCES

1. R. Milo, *Bioassays*, **2013**, *35*, 1050.
2. P. Jorgensen, J. L. Nishikawa, B. J. Breitzkreutz, M. Tyers, *Science*, **2002**, *297*, 395.
3. P. Echave, I. A. Conlon, A. C. Llyod, *Cell Cycle*, **2007**, *6*, 218.
4. F. Abascal, D. Juan, I. Jungreis, L. Martinez, M. Rigau, J. M. Rodriguez, J. Vazquez, M. L. Tress, *Nucleic Acids Research*, **2018**, *46*, 7070.
5. N. Savage, *Nature*, **2015**, *527*, 86.
6. D. L. Pinti, *Lectures in Astrobiology*, M. Gargaud & al. (Eds), Springer-Verlag, Berlin, **2005**, Vol. I, p. 83.
7. S. J. Mojzsis, G. Arrhenius, K. D. McKeegan, T. M. Harrison, A. P. Nutman, C. R. L. Friend, *Nature*, **1996**, *384*, 55.
8. M. C. Weiss, F. L. Sousa, N. Mrnjavac, S. Neukirchen, M. Roettger, S. Nelson-Sathi, W. F. Martin, *Nature Microbiology*, **2016**, *1*, 16116.
9. S. Sundararaj, A. Guo, B. Habibi-Nazhad, M. Rouani, P. Stothard, M. Ellison, D. S. Wishart, *Nucleic Acids Res.*, **2004**, *32* (Database issue): D293.D295.
10. R. Shapiro, *Scientific American*, **2007**, 12 Feb.
11. G. H. Pollack, X. Figueroa, Q. Zhao, *Int. J. Mol. Sci.*, **2009**, *10*, 1419.
12. P. A. Bachman, P. Walde, P. L. Muisi, J. Lang, *J. Am. Chem. Soc.*, **1990**, *112*, 8200.
13. W. Martin, M. J. Russell, *Phil. Trans. R. Soc. Lond. B*, **2003**, *358*, 59.
14. L. E. Orgel, *PLoS Biology*, **2008**, *6*, e18.
15. G. Springsteen, J. R. Yerabolu, J. Nelson, C. J. Rhea, R. Krishnamurthy, *Nature Commun.*, **2018**, *9*, 91.
16. I. Prigogine, G. Nicolis, A. Babloyantz, *Phys. Today*, **1972**, *11*, 23.
17. E. Chaisson, *The Scientific World Journal*, **2014**, 384912.
18. G. Job, F. Herrmann, *Eur. J. Phys.*, **2006**, *27*, 353.
19. W. Grimus, *Ann. Phys. (Berlin)*, **2013**, *525*, A32.
20. J. E. Koska, D. D. Dalton, H. Skelton, S. Dollhopf, J. W. Stucki, *Appl. Environ. Microbiol.*, **2002**, *68*, 6256.
21. M. P. Fewell, *Am. J. Phys.*, **1995**, *63*, 653.
22. M. Can, F. A. Armstrong, S. W. Ragsdale, *Chem. Rev.*, **2014**, *114*, 4149.
23. J. L. Boer, S. B. Mulrooney, R. P. Hausinger, *Arch. Biochem. Biophys.*, **2014**, *544*, 142.
24. B. Desguin, P. Goffin, E. Viaene, M. Kleerebezem, V. Martin-Diaconescu, M. J. Maroney, J.-P. Declercq, P. Soumillion, P. Hols, *Nature Commun.*, **2014**, *5*, 3615.
25. S. Guillot, K. Hattorin, *Elements*, **2014**, *9*(2), 95.
26. J. A. Brandes, N. Z. Boctor, G. D. Cody, B. A. Cooper, R. M. Hazen, H. S. Yoder Jr., *Nature*, **1998**, *395*, 365.
27. R. A. Alberty, *Thermodynamics of Biochemical Reactions*, **2003**, John Wiley & Sons, Hoboken, New Jersey.
28. R. A. Alberty, *J. Phys. Chem. A*, **1998**, *102*, 8460.
29. J. N. Israelachvili, S. Marcelja, R. G. Horn, *Quart. Revs. Biophys.*, **1980**, *13*, 121.
30. R. E. Heikkila, C. N. Kwong, D. G. Cornwell, *J. Lipids Res.*, **1970**, *11*, 190.
31. A. I. Greenwood, S. Tristram-Nagle, J. F. Nagle, *Chem. Phys. Lipids*, **2006**, *143*, 1.
32. I. Brzozowska, Z. A. Figaszewski, *Colloids Surf. B: Biointerfaces*, **2002**, *23*, 51.
33. A. Kessel, N. Ben-Tal, S. May, *Biophys. J.*, **2001**, *81*, 643.
34. R. C. Ewing, *Proc. Natl. Acad. Sci. USA*, **1999**, *96*, 3432.
35. M. J. Borda, A. R. Elsetinow, M. A. Schoonen, D. R. Strongin, *Astrobiology*, **2001**, *1*, 283.
36. G. D. Cody, N. Z. Boctor, J.A. Brandes, T. R. Filley, R. M. Hazen, H.S. Yoder Jr., *Geochim. Cosmochim. Acta*, **2004**, *68*, 2185.

37. G. D. Cody, N. Z. Boctor, T. R. Filley, R. M. Hazen, J. H. Scott, A. Sharma, H.S. Yoder Jr., *Science*, **2000**, 289, 1337.
38. Y. Novikov, S. D. Copley, *PNAS*, **2013**, 110, 13283.
39. K. Fan, W. Wang, *J. Mol. Biol.*, **2003**, 328, 921.
40. S. Akanuma, T. Kiawa, S. Yokoyama, *Proc. Natl. Acad. Sci. USA*, **2002**, 99, 13549.
41. M. Granold, P. Hajieva, M. I. Tosa, F.-D. Irimie, B. Moorsmann, *Proc. Natl. Acad. Sci. USA*, **2018**, 115, 41.
42. R. Shibue, T. Sasamoto, M. Shimada, B. Zhang, A. Yamagishi, S. Akanuma, *Sci. Reports*, **2018**, 8, 1227.
43. R. J. C. Hennet, N. G. Holm, M. H. Engel, *Naturwissenschaften*, **1992**, 79, 361.
44. R. M. Hazen, *Am. Miner.*, **2006**, 91, 1715.
45. A. Rimola, P. Ugliengo, M. Sodupe, *Int. J. Mol. Sci.*, **2009**, 10, 746.
46. R. B. Martin, *Biopolymers*, **1998**, 45, 351.
47. K. H. Lemke, R. J. Rosenbauer, D. K. Bird, *Astrobiology*, **2009**, 9, 141.
48. S. A. Benner, H.-J. Kim, M. A. Carrigan, *Accounts Chem. Res.*, **2012**, 45, 2025.
49. G. Fedoseev, H. M. Cuppen, S. Ioppolo, T. Lamberts, H. Linnartz, *Monthly Notices Royal Astronomical Soc.*, **2015**, 448, 1288.
50. D. Roy, K. Najafian, P. R. Schleyer, *Proc. Natl. Acad. Sci. USA*, **2007**, 104, 12272.
51. T. A. Glassman, C. Cooper, L. W. Harrison, T. J. Swift, *Biochemistry*, **1971**, 10, 843.
52. J. L. Bock, G. B. Crull, A. Wishnia, C. S. Springer Jr., *J. Inorg. Biochem.*, **1991**, 44, 79.
53. A. Patel, L. Malinowska, S. Saha, J. Wang, S. Alberti, Y. Krishnan, A. A. Hyman, *Science*, **2017**, 256, 753.
54. A. Stevenson, J. A. Cray, J. P. Williams, R. Santos, R. Sahay, N. Neuenkirchen, C. D. McClure, I. R. Grant, J. D. R. Houghton, J. P. Quinn, D. J. Timson, S. V. Patil, R. S. Singhal, J. Anton, J. Dijksterhuis, A. D. Hocking, B. Lievens, D. E. N. Rangel, M. A. Voytek, N. Gunde-Cimerman, A. Oren, K. N. Timmis, T. J. McGenity, J. E. Hallsworth, *The ISME Journal*, **2015**, 9, 1333.
55. A. J. Maneffa, R. Stenner, A. S. Matharu, J. H. Clark, N. Matubayashi, S. Shimizu, *Food Chem.*, **2017**, 237, 1133.
56. J. Chirife, C. Ferro-Fontan, E. A. Benmergui, *J. Food Technol.*, **1980**, 15, 59.
57. M. Falk, *Can. J. Chem.*, **1965**, 42, 314.
58. H. Sippola, P. Taskinen, *J. Chem. Eng. Data*, **2018**, 63, 2986.
59. M. T. de Gomez-Puyou, G. Perez-Hernandez, A. Gomez-Puyou, *Eur. J. Biochem.*, **1999**, 266, 691.
60. H. Suzuki, T. Kanazawa, *J. Biol. Chem.*, **1996**, 271, 5481.
61. L. de Meis, G. Inesi, *J. Biol. Chem.*, **1982**, 257, 1289.



**Citation:** J. Teixeira (2019) The puzzling problem of water properties at low temperature. An experimentalist view. *Substantia* 3(2) Suppl. 3: 57-63. doi: 10.13128/Substantia-546

**Copyright:** © 2019 J. Teixeira. This is an open access, peer-reviewed article published by Firenze University Press (<http://www.fupress.com/substantia>) and distributed under the terms of the Creative Commons Attribution License, which permits unrestricted use, distribution, and reproduction in any medium, provided the original author and source are credited.

**Data Availability Statement:** All relevant data are within the paper and its Supporting Information files.

**Competing Interests:** The Author(s) declare(s) no conflict of interest.

## The puzzling problem of water properties at low temperature. An experimentalist view

JOSÉ TEIXEIRA

*Laboratoire Léon Brillouin (CEA/CNRS) CEA Saclay 91191 - Gif-sur-Yvette Cedex France*

E-mail: jose.teixeira@cea.fr

**Abstract.** Water is at once the most familiar substance, the one for which we have the most data, and a liquid with anomalous properties that make it unique. Many theoretical models provide explanations for the abnormal behaviour of water. The most recent ones are based on numerical simulations of molecular dynamics made from effective potentials that reproduce the tetrahedral geometry of hydrogen bonds. From the experimental side, homogeneous nucleation of hexagonal ice limits the range of temperature accessible to experiments. There is therefore no experimental data at atmospheric pressure in a wide temperature range extending from the homogeneous nucleation temperature (230 K) to the glass transition (135 K). However, water anomalies are the most important in the supercooled domain. Therefore, a large number of theoretical models, often based on extrapolations of data or analogies, have been developed without being able to be compared to non-existent experimental data. In all cases, the temperature domain where homogeneous nucleation takes place plays a crucial role in the anomalies observed at low temperature. Here, we present shortly structural models that predict the existence of a low-temperature critical point and a liquid-liquid transition between two phases of different structures by comparing them with experimental data. Other models are based on dynamic transitions or the existence of two types of relaxation, at the molecular and hydrogen bonding levels, which may correspond to two glass transitions.

**Keywords.** Supercooled water, critical point, water anomalies, neutron scattering.

---

### INTRODUCTION

Water is virtually the only natural liquid on the surface of the planet Earth. The solid and vapour phases are present as well in large quantities, which is unique on Earth and rare on other planets. The importance in the biosphere, the climate and many physical and chemical processes make water the best-known substance for which the most accurate data are available. However, at the level of the fundamental physics, water is an “anomalous liquid”, i.e. whose properties are very different from those of an “ideal” liquid described by the Statistical Physics.

Among the “anomalies” of the properties of liquid water are the well-known lower density of the ice or the maximum density of the liquid at

about 4 °C even if, in reality, their banality is not currently associated with abnormal behaviour. Indeed, it is at the molecular scale that it is difficult to explain why the ordered molecules in ice occupy a larger volume than in the disordered liquid state.

Essentially all the thermodynamic and transport properties of liquid water (compressibility, specific heat, viscosity...) depend anomalously on temperature and pressure, especially at low temperature.

To find plausible models and explanations, it is therefore essential to study the properties of water at the lowest possible temperatures. Measurements of the thermodynamic properties of water can be made below  $T_m = 0$  °C, the melting point of ice, since water, like other liquids, can remain liquid below the melting point as long as there are no nuclei that initiate the heterogeneous nucleation of ice. There is however a limit to this “supercooled” state, that of the homogeneous nucleation which, at atmospheric pressure, takes place at  $T_N = 230$  K = -43 °C. Therefore, for many properties, we have measurements that extend to -25, sometimes -30 °C. In all cases, it is found that the anomalous behaviour accelerates as the temperature decreases. Thus, the density decreases by 1.6 % between 4 °C and -30 °C while the decay is only 0.7 % in the same temperature interval between 4 °C and 38 °C.

Isothermal compressibility, specific heat and other properties have similar behaviour. Figure 1 depicts the temperature dependence of isothermal compressibility at ambient pressure. There a minimum at 46 °C and an anomalous sharp increase on the low temperature side. Numerical extrapolations are consistent with a divergence although the numerical values remain far from those measured near a critical point.

To describe the properties of a liquid, semi-empirical equations of state based on numerical fits of the data are established. In the case of water, these equations of state lead to apparent divergences of several properties at temperatures a little below  $T_N$ , which raises the problem of the existence or not of a true divergence, similar to that which one would observe near a critical point or a spinodal line. Thus, for example, the remarkable equations of G.S. Kell,<sup>1</sup> which reproduces the density and the isothermal compressibility of water with an accuracy of  $10^{-5}$  between -30 and 150 °C, but extrapolates to infinite for  $T = -56$  °C and -51 °C, respectively. Equations of state describe more accurately properties of liquid water in domains of temperature and pressure covered by experiment but their extrapolations cannot be reliable, i.e. several extrapolations are numerically compatible with existing data.<sup>2</sup>

In this context, one of the first conjectures<sup>3</sup> were based on fits of thermodynamic properties by power laws

diverging at -42 °C, which postulated the existence of a re-entrant spinodal line that, passing through negative pressures would impose a stability limit in the liquid state at low temperature.<sup>4</sup> Despite the fact that formation of a glassy state by quenching does not exclude the existence of a re-entrant spinodal,<sup>5</sup> the experiments of J. Dubochet et al.<sup>6</sup> showing that the amorphous state of water can be reached by rapid quenching of the liquid, that is to say crossing the region of the postulated spinodal line, had a great impact in discussions on extrapolations.

The amorphous state obtained by quenching, glassy water, has a structure identical to that of the amorphous form obtained by deposition on a support at very low temperature. The glass transition temperature is of the order of 135 K, i.e. more than 100 °C below the supercooled domain accessible to the experiments. The temperature dependence in this vast temperature range, sometimes called “no man’s land”,<sup>7</sup> is unknown. Yet it is not trivial since the numerical divergences are only apparent. The “no man’s land” is therefore a territory of speculation! Several models have been proposed to describe the temperature dependence of the properties of water, without ever reaching discriminant tests.

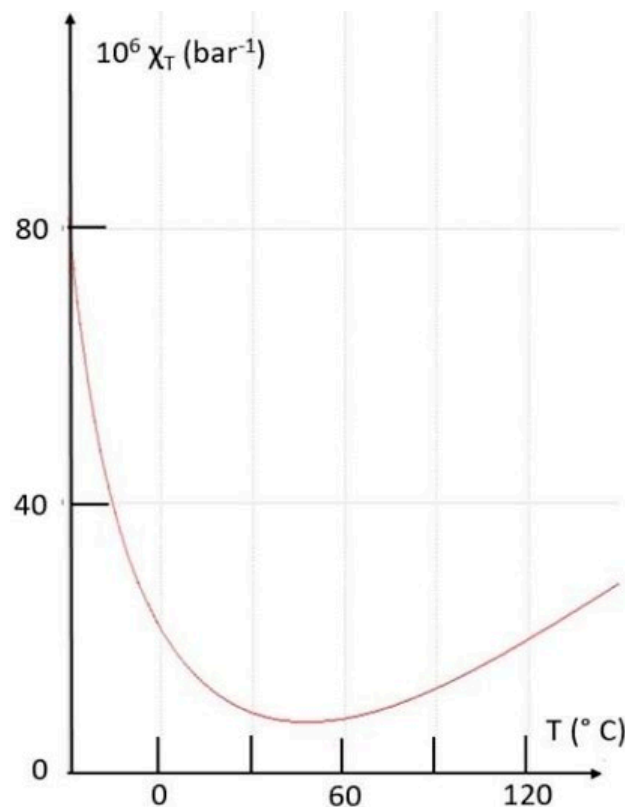


Figure 1. Isothermal compressibility of liquid water at atmospheric pressure. There is a minimum at 46 °C.

An experimental fact occupies an important place in the arguments developed on this temperature domain inaccessible to the experiment. This is the discovery in 1984 of a form of high-density amorphous (HDA) ice,<sup>8</sup> obtained by compression at very low temperature of the crystalline ice. Its density ( $1.17 \text{ g.cm}^{-3}$  at 77 K) is much higher than that of amorphous ice, which is obtained by quenching ( $0.94 \text{ g.cm}^{-3}$  at 77 K, so close to that of ice). The structural study<sup>9</sup> shows that interstitial sites between the first and second neighbours are occupied, which corresponds to strong distortions of the hydrogen bond network, probably due to the collapse of a network of very directional links as well as the weak coordination of the water molecules, barely higher than 4 in the liquid phase.

Following the discovery of HDA ice, some models of supercooled water postulate the existence of a high density liquid that would correspond to the melting of HDA ice, therefore to the existence of two forms of liquid water, having very different densities and structures, though similar to those of high and low density amorphous ice respectively.<sup>10</sup>

If, despite their metastability, the amorphous states are represented in a pseudo-phase diagram, the transition line separating the two forms of amorphous ices of different densities would be prolonged by a line separating the two liquids and a liquid-liquid transition would be the pendant of the transition between the two forms of amorphous ices. This idea consists to consider HDA as a glass, just like the amorphous form of low density, LDA is the glassy form of liquid water. The line of separation of the two liquid phases would end at a critical point where a certain number of thermodynamic properties would have a singular behaviour.

This model is supported by the fact that some numerical simulations of the molecular dynamics of water do indeed predict the existence of one critical point at low temperature and high pressure. However, such numerical simulations are based on effective potentials that try to reproduce at best the thermodynamic properties and the molecular structure in a pressure and temperature range not too far from the ambient conditions.<sup>11</sup>

Of the many potentials,<sup>12</sup> ST2 and TIP4P potentials actually predict a singular behaviour of isothermal compressibility near a critical point around 200 K and 0.1 GPa, so deep inside the no man's land.<sup>13</sup>

This critical point would be the extreme point of the transition line separating high and low density liquids, itself an extension of the line separating the two forms of amorphous ice, HDA and LDA, as mentioned above. It can therefore be seen either as a demixion point of

two liquids, or as a critical point identical to that, liquid-vapour, on the high temperature side of the phase diagram of water. Both interpretations exist in the literature. They correspond to different interpretations of certain structural measurements.

In the context of the existence of a critical point at high pressure and low temperature, anomalies observed experimentally at atmospheric pressure and at low temperature are explained by another analytical extension of the same line of separation of liquid phases beyond the critical point, line often called "Widom line".<sup>14</sup> As a result, the thermodynamic properties would only present "bumps" when crossing the Widom line. A problem remains open: how to explain that the anomalies are reduced under pressure? Concretely, starting from the ambient pressure side, a high pressure point of the phase diagram is closer to the critical point than another point at the same temperature and lower pressure. Therefore, anomalies should be larger for the second point conditions, what is not the case.

On the other hand, it is important to note that the Widom line deduced from the numerical models almost coincides with the homogenous nucleation line of ice.

Other models neglect the structural aspects and postulate rather a dynamic transition taking place also in the same field of pressure and temperature, or near the homogeneous nucleation line.

In this article, we discuss, in a non-exhaustive way, the consequences of the most popular models by comparing them with the experimental results available for supercooled water.

## MIXTURE MODELS

The idea that liquid water can be a mixture of two liquids is not new. This is even one of the first conjectures formulated to explain the maximum density at 4 °C. W. Röntgen in 1892 conjectured the existence of different types of water molecules.<sup>15</sup> Other mixing models have been proposed, including the elaborated one by G. Némethy and H.A. Scheraga,<sup>16</sup> never confirmed by experience. Mixing models envisage either different types of molecules,<sup>17</sup> or molecular arrangements such as two types of dimers or pentamers<sup>18</sup> or the coexistence of two liquids of very different structures and densities coexisting in the form of clusters, one of the two phases immersed in the second.<sup>19</sup>

All these models are hardly compatible with measurements of the structure of liquid water. Indeed, the pair correlation function,  $g(r)$ , shows the existence of a single very narrow peak at  $2.8 \text{ \AA}$ , representative of the



distance between close neighbours, perfectly defined by the intermolecular links.<sup>20</sup> The existence of aggregates of different densities is equally incompatible with X-ray scattering measurements,<sup>21-22</sup> which show that small-angle scattering is due solely to the number fluctuations at the origin of isothermal compressibility. Moreover, the isothermal compressibility, so the small angle scattering of water, are very weak compared to those of other liquids. As well, if one limits oneself to the known thermodynamic data, it is impossible to explain the maximum of density or the minimum of compressibility by the mixture of two liquids whose density would differ by about 10%.<sup>23</sup>

About these models, one can note the ambiguity of the definition of the critical point at low temperature. If it is a demixing point, nucleation of one of the two phases should be detected but there would be no anomaly in the isothermal compressibility. In contrast, density fluctuations with increasing coherence length explain the increase in compressibility observed at low temperatures.

In a recent experiment, X-ray and neutron scattering at very low temperature and high pressure<sup>24</sup> measured the water-lithium chloride eutectic mixture. No anomalies were observed what excludes enhanced density fluctuations or nucleation of a distinct phase. Therefore, solid poly- amorphism does not imply liquid poly-amorphism.

Nevertheless, it is important to note that measurements made on aqueous solutions can only provide additional information on the behaviour of bulk water. Indeed, the addition of small amounts of any solute decreases or eliminates abnormalities of pure water, as for example in the case of ethanol<sup>25</sup> even in the presence of hydrogen bonds. In fact, the breaking of the tetrahedral structure is sufficient to make the behaviour of water similar to that of other associated liquids. The same applies to samples of water confined in small pores. There is a very significant reduction in the melting temperature, or even its suppression,<sup>26</sup> but the thermodynamic anomalies are also suppressed.

#### DYNAMIC MODELS

In other approaches, the abnormal behaviour of water was attributed to purely dynamic transitions. Thus, measurements of the molecular dynamics of hydration water on lysozyme protein,<sup>27</sup> can be interpreted by a discontinuity of the temperature dependence of the relaxation time associated with diffusion. At high temperature this time varies very strongly with temperature (sometimes called “fragile” liquid behaviour) while at low temperature, the temperature dependence is of the

Arrhenius type (“strong” liquid). The fit of the experimental neutron quasi-elastic neutron scattering<sup>27</sup> data sets the transition to 220 K at atmospheric pressure, so very close to the homogeneous nucleation temperature  $T_N$  and the postulated Widom line. This may actually correspond to a dynamic transition.

In addition, the measurements made on samples of bulk water demonstrate the coexistence of two times characterizing the molecular dynamics,<sup>28,29</sup> which depends on time in a very different way. The residence time, a measure of the time during which a molecule is inside the cage formed by neighbouring molecules, follows the anomalous temperature dependence of other transport properties, such as viscosity. A much shorter time, of the order of the ps, is related to the lifetime of the intermolecular bonds and its dependence of the temperature is of the Arrhenius type even at the lowest temperatures accessible to this type of experiments, that is to say -20 °C. Spin echo relaxation time measurements, with momentum transfers selected in order to be able to discriminate these two times,<sup>30</sup> as well as measurements of the imaginary part of the susceptibility by X spectroscopy,<sup>31</sup> also show the existence of two relaxation times. Finally, it is remarkable that in the analysis of the quasi-elastic spectrum of neutrons on the melting line of the ice VII, one always finds this short time, which characterizes the dynamics of the hydrogen bonds.<sup>32</sup>

The strong directionality of the intermolecular potential due to the hydrogen bonds is at the origin of a very short life time if one takes into account the energy, which is of the order of 8 kJ / mol, thus greater than 1000 K. We speak here of the time during which a hydrogen atom remains inside the cone where the bond can be established, whose opening is of the order of 30°. This is the time of allegiance defined by F. Stillinger.<sup>33,34</sup> Otherwise, a bond can break and reform between the same neighbouring molecules. This often happens at low temperatures when the number of “intact” hydrogen bonds is very large, which generates a gel-like structure with residence times that increase very rapidly with temperature. Figure 2 shows the residence times and lifetime of the hydrogen bonds as a function of temperature in a Arrhenius plot. The apparent divergence of the first should correspond to the formation of a macroscopic gel. Yet, as we have seen, the homogenous nucleation of ice takes place around -43 °C, when the liquid is still very fluid.

In addition, the structure of the supercooled liquid changes rapidly as the temperature decreases. It is remarkable that, also towards -25 °C, the position of the first peak of the structure function,  $S(k)$ , decreases approaching that of the amorphous ice.<sup>35</sup> This means

that, between this limit temperature of possible measurements and  $T_g$ , thus in all the extension of the no man's land, there is practically no structural changes. Only hydrogen bonds maintain a fast dynamic over this wide temperature range because of the smooth Arrhenius temperature dependence of its characteristic time.

This amounts to admitting the existence of two glass transitions. The first, occurring near  $-43^\circ\text{C}$ , corresponds to the arrest of the molecular diffusion. Indeed, the structure measured at the lowest accessible temperatures ( $-30^\circ\text{C}$ ) is practically identical to that of the low-density amorphous ice, LDA, however  $100^\circ$  above  $T_g$ .<sup>35</sup> Near the homogeneous nucleation temperature, it is the hydrogen bonds, which keep a sufficiently fast dynamic to prevent the formation of the amorphous phase. Between  $T_N$  and  $T_g$ , small displacements of the hydrogen atoms are sufficient to form the crystalline phase. It is only at 135 K that the hydrogen bonds are frozen and that the LDA phase is formed with a small change of enthalpy.

This type of behaviour is the analogue of the alpha and beta dynamics that characterize the dynamics of many polymers. However, in the case of water, it is the beta dynamics, that of the hydrogen bonds, that determines the thermodynamic properties and the existence of a vast no man's land.

It remains to explain the existence of several amorphous phases, including that of high density (HDA) that can be obtained by compression of hexagonal ice or compression of low-density amorphous ice (LDA). On the one hand, there is not exactly one line of coexist-

ence of these two forms of amorphous ice. In fact, one goes from LDA to HDA only by compression, while the transition HDA towards LDA results from the heating of HDA above 120 K. Thus, HDA is stable at atmospheric pressure if the temperature is sufficiently low. More important is the question of whether there is a liquid with the HDA ice structure, i.e. if HDA is a symmetrical glass of glass having the LDA structure. Recent results of C.A. Tulk et al.<sup>36</sup> show that HDA is rather a kinetically arrested transformation between low-density ice I and high-density ice XV.

As a result, the water anomalies must actually go through bumps near the temperature  $T_N$  of nucleation of ice. For example, the compressibility must reach a maximum value towards  $T_N$  and remain practically constant between  $T_N$  and  $T_g$ . Therefore, the line that defines the homogeneous nucleation in the plane (P, T) plays a capital role, formally analogous to that of line Widom but in the absence of a critical point and liquid-liquid transition. As far as compressibility is concerned, one can try to evaluate a coherence length of density fluctuations. There is no exact method to do this because it is a very small effect but we can say that it is a very small value, certainly less than  $1\text{ nm}$ <sup>21,37</sup> which can be explained by the formation of the gel phase.

This does not exclude the fact that, in certain situations of confinement, water can have a high apparent density. This is the case of hydration water at hydrophilic sites of proteins.<sup>38</sup>

## CONCLUSION

From the large amount of data available, it can be said that liquid water is a homogeneous liquid at all temperatures and pressures. The various theories that have been proposed agree on the existence of anomalies of the temperature dependence of most thermodynamic and transport properties near the line that defines the nucleation of hexagonal ice, i.e. around  $-43^\circ\text{C}$  at atmospheric pressure.

Computer simulations of molecular dynamics predict divergences in response properties, including isothermal compressibility and specific heat. Two actual potentials even foresee the existence of a critical point situated towards 200 K and a few kbar of pressure, in spite of the fact that the anomalies of the water at ambient temperature decrease quickly under pressure.

Given the intrinsic difficulty of entering the "no man's land", it is possible that extrapolations, analogies and speculations continue to be made on the behaviour of deeply supercooled liquid water. Nevertheless, recent

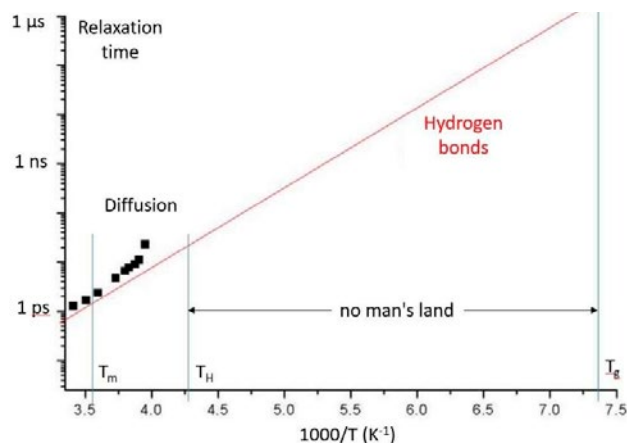


**Figure 2.** Schematic representation of the two times that characterize dynamics of liquid water. Squares represent experimental evaluations of the molecular residence time showing the anomalous super-Arrhenius temperature dependence. The red line is an extrapolation of the hydrogen bond lifetime evaluated at temperatures above  $-20^\circ\text{C}$ .<sup>28</sup>  $T_m$ ,  $T_H$  and  $T_g$  are the melting, homogeneous nucleation and glass transition temperatures, respectively.

results show that high-density amorphous ice is not a glass, what eliminates the possibility of a high density liquid. Also, the consideration of two characteristic times (that of the molecular dynamics and the one of the hydrogen bonding) makes it possible to reach relatively classical explanations of the unusual behaviour of the water.

Probably, future studies should look more in detail at the nature of the hydrogen bond, which implies approaches beyond the thermodynamic scale. In fine, a complete knowledge of hydrogen bonds in water could lead to the determination of the true molecular potential.

#### REFERENCES

1. D.S. Kell, Density, Thermal Expansivity, and Compressibility of Liquid Water from 0° to 150°C: Correlations and Tables for Atmospheric Pressure and Saturation reviewed and expressed on 1968 Temperature Scale, *Journal of Chemical and Engineering Data* 20, 97-105 (1975).
2. F. Caupin, V. Holten, C. Qiu, E. Guillerm, M. Wilke, M. Frenz, J. Teixeira and A.K. Soper, Comment on “Maxima in the thermodynamic response and correlation functions of deeply supercooled water”, *Science* 360 (6390), eaat1634 (2018).
3. R.J. Speedy and C.A. Angell, Isothermal compressibility of supercooled water and evidence for a thermodynamic singularity at -45 °C, *J. Chem. Phys.* 65, 851-858 (1976).
4. M.E.M. Azouzi, C. Ramboz, J.F. Lenain and F. Caupin, A coherent picture of water at extreme negative pressure, *Nature Physics* 9, 38-41 (2013).
5. G. Pallaresa, M. El Mekki Azouzi, M.A. González, J.L. Aragonés, J.L.F. Abascal, C. Valeriani and F. Caupin, Anomalies in bulk supercooled water at negative pressure, *Proc. Natl. Acad. Sci. U.S.A.* 111, 7936-7941 (2014).
6. J. Dubochet, R. Lepault, A. Freeman, J.A. Berri-man and J.-C. Homo, Electron microscopy of frozen water and aqueous solutions, *J. of Microscopy*, 128, 219-237 (1982).
7. H.E. Stanley, S.V. Buldyrev, M. Canpolat, O. Mishima, M. R. Sadr-Lahijany, A. Scala and F. W. Starr, The puzzling behavior of water at very low temperature, *Phys. Chem. Chem. Phys.* 2, 1551-1558 (2000).
8. O. Mishima, L.D. Calvert and E. Whalley, ‘Melting ice’ I at 77 K and 10 kbar: a new method of making amorphous solids, *Nature* 310, 393-395 (1984).
9. L. Bosio, G. P. Johari and J. Teixeira, X-Ray study of high-density amorphous water, *Phys. Rev. Lett.* 56, 460-463 (1986).
10. C. Huang, K.T. Wikfeldt, T. Tokushima, D. Nordlund, Y. Harada, U. Bergmann, M. Niebuhr, T.M. Weiss, Y. Horikawa, M. Leetmaa, M.P. Ljungberg, O. Takahashi, A. Lenz, L. Ojamäe, A.P. Lyubartsev, S. Shin, L.G.M. Pettersson and A. Nilsson, The inhomogeneous structure of water at ambient conditions, *Proc. Natl. Acad. Sci. U.S.A.* 106, 15214-15218 (2009).
11. C. Vega and J. L. F. Abascal, Relation between the melting temperature and the temperature of maximum density for the most common models of water, *J. Chem. Phys.* 123, 144504 (2005).
12. B. Guillot, A reappraisal of what we have learnt during three decades of computer simulations on water, *J. Mol. Liquids* 101, 219-260 (2002).
13. J.C. Palmer, F. Martelli, Y. Liu, R. Car, A.Z. Panagiotopoulos and P.G. Debenedetti, Metastable liquid-liquid transition in a molecular model of water, *Nature* 510, 385-388 (2014); K.T. Wikfeldt, C. Huang, A. Nilsson and L.G.M. Pettersson, Enhanced small-angle scattering connected to the Widom line in simulations of supercooled water, *J. Chem. Phys.* 134, 214506 (2011).
14. L. Xu, S.V. Buldyrev, C. A. Angell and H. E. Stanley, Thermodynamics and dynamics of the two- scale spherically symmetric Jagla ramp model of anomalous liquids, *Phys. Rev. E* 74, 031108 (2006).
15. W.C. Röntgen, Ueber die Constitution des flüssigen Wassers, *Annalen der Physik und Chemie* XLV, 91-97 (1892).
16. G. Némethy and H.A. Scheraga, Structure of Water and Hydrophobic Bonding in Proteins. I. A Model for the Thermodynamic Properties of Liquid Water, *J. Chem. Phys.* 36, 3382-3400 (1962).
17. C.A. Cerdeiriña, J. Troncoso, D. González-Salgado, P.D. Debenedetti and H.E. Stanley, Water’s two-critical-point scenario in the Ising paradigm, *J. Chem. Phys.* 150, 244509 (2019).
18. O. Mishima and H.E. Stanley, The relationship between liquid, supercooled and glassy water, *Nature* 396, 329-335 (1998).
19. L.G.M. Pettersson and A. Nilsson, The structure of water; from ambient to deeply supercooled, *J. Non-Crystalline Solids* 407, 399-417 (2015).
20. A.K. Soper and M.G. Phillips, A New determination of the structure of water at 25 °C, *Chem. Phys.* 107, 47-60 (1986).
21. L. Bosio, J. Teixeira and H.E. Stanley, Enhanced density fluctuations in supercooled H<sub>2</sub>O, D<sub>2</sub>O, and Ethanol-Water solutions: Evidence from Small-Angle X-Ray Scattering, *Phys. Rev. Lett.* 46, 597-600 (1981).

22. A. K. Soper, J. Teixeira, and T. Head-Gordon, Is ambient water inhomogeneous on the nanometer-length scale?, *Proc. Natl. Acad. Sci. U.S.A.* **107**, E44 (2010).
23. G. Johari and J. Teixeira, Thermodynamic analysis of the two-liquid model for anomalies of water, HDL-LDL fluctuations and liquid-liquid transition, *J. Phys. Chem. B* **119**, 14210-14220 (2015).
24. L.E. Bove, F. Pietrucci, A.M. Saitta, S. Klotz and J. Teixeira, On the link between polyamorphism and liquid liquid transition: the case of salty water, *J. Chem. Phys.* **151**, (2019).
25. O. Conde, J. Teixeira and P. Papon, Analysis of sound velocity in supercooled H<sub>2</sub>O, D<sub>2</sub>O and Water- Ethanol mixtures, *J. Chem. Phys.* **76**, 3747-3753 (1982).
26. J. C. Dore, B. Webber, M. Hartl, P. Behrens, T. Hansen, Neutron diffraction studies of structural phase transformations for water-ice in confined geometry, *Phys. A: Stat. Mech. Appl.* **314**, 501-507 (2002).
27. S.-H. Chen, L. Liu, E. Fratini, P. Baglioni, A. Faraone, and E. Mamontov, Observation of fragile-to-strong dynamic crossover in protein hydration water, *Proc. Natl. Acad. Sci. U.S.A.* **103**, 9012-9016 (2006).
28. J. Teixeira, M.-C. Bellissent-Funel, S.-H. Chen and A. J. Dianoux, Experimental determination of the nature of diffusive motions of water molecules at low temperatures, *Phys. Rev. A* **31**, 1913-1917 (1985).
29. J. Qvist, H. Schober and B. Halle, Structural dynamics of supercooled water from quasielastic neutron scattering and molecular simulations, *J. Chem. Phys.* **134**, 144508 (2011).
30. J. Teixeira, A. Luzar and S. Longeville, Dynamics of Hydrogen Bonds: How to Probe their Role in the Unusual Properties of Liquid Water, *J. Phys.: Cond. Matter* **18**, S2353-S2362 (2006).
31. A. Arbe, P. Malo de Molina, F. Alvarez, B. Frick, and J. Colmenero, Dielectric Susceptibility of Liquid Water: Microscopic Insights from Coherent and Incoherent Neutron Scattering, *Phys. Rev. Lett.* **117**, 185501 (2016).
32. L. E. Bove, S. Klotz, Th. Strässle, M. Koza, J. Teixeira and A.M. Saitta, Translational and rotational diffusion in water in the gigapascal range, *Phys. Rev. Lett.* **111**, 185901 (2013).
33. F.H. Stillinger, Water revisited, *Science* **209**, 451-457 (1980).
34. A. Luzar and D. Chandler, Hydrogen-bond kinetics in liquid water, *Nature* **379**, 55-57 (1996).
35. M.-C. Bellissent-Funel, L. Bosio, J. Dore, J. Teixeira and P. Chieux, Spatial correlations in deeply supercooled water, *Europhys. Lett.* **2**, 241-245 (1986).
36. C.A. Tulk, J.J. Molaison, A.R. Makhluif, C.E. Manning and D.D. Klug, Absence of amorphous forms when ice is compressed at low temperature, *Nature* **569**, 542-545 (2019).
37. G.N.I. Clark, G.L. Hura, J. Teixeira, A.K. Soper and T. Head-Gordon, Small-Angle Scattering and the Structure of Ambient Liquid Water, *Proc. Nat. Acad. Sci. (USA)* **107**, 14003-14007 (2010).
38. D. Russo and J. Teixeira, Mapping water dynamics in defined local environment: From hindered rotation to vibrational modes, *Journal of Non-Crystalline Solids* **407**, 459-464 (2015).





**Citation:** H.-M. Peter, C. Sutter, W. Schwenk (2019) Study of a Section of a Self-Purifying Stream in Specific Relation to its Water Flow Behaviour. *Substantia* 3(2) Suppl. 3: 65-70. doi: 10.13128/Substantia-371

**Copyright:** © 2019 H.-M. Peter, C. Sutter, W. Schwenk. This is an open access, peer-reviewed article published by Firenze University Press (<http://www.fupress.com/substantia>) and distributed under the terms of the Creative Commons Attribution License, which permits unrestricted use, distribution, and reproduction in any medium, provided the original author and source are credited.

**Data Availability Statement:** All relevant data are within the paper and its Supporting Information files.

**Competing Interests:** The Author(s) declare(s) no conflict of interest.

## Study of a Section of a Self-Purifying Stream in Specific Relation to its Water Flow Behaviour

HEINZ-MICHAEL PETER, CHRISTINE SUTTER\*, WOLFRAM SCHWENK

*Institut für Strömungswissenschaften, D-79737 Herrischried*  
E-mail: [c.sutter@stroemungsinstitut.de](mailto:c.sutter@stroemungsinstitut.de)

**Abstract.** The Mettma, a mountain stream in the Black Forest in Germany, had been polluted at a point source by effluent discharge from a brewery, and showed a section of self-purification along 8 km, without further interferences, following the effluent outfall. This section of stream had served as an excellent study model of the self-purification phenomenon, as much in the physico-chemistry and biology as in the hydrodynamic attributes of the water. The biological evolution along the stretch of self-purifying stream showed a succession of species typical of the food chain. To document the hydrodynamics of the stream water the Drop Picture Method, a standardized testing method developed by Theodor Schwenk, was used, based on optically revealing internal flow structures. The watersamples upstream of the pollution source showed diverse and well shaped flow structures, whereas the samples at the effluent outfall appeared with a drastic reduction and inhibition of flow shape diversity and differentiation. After that point the internal flow structures became increasingly intense and diverse the further downstream. This evolution in movement diversity proceeded in parallel to the development of the biotic community, which showed a similar increase in diversity, differentiated morphology and functional differentiation away from the pollution point to the extent that at a distance of 8 km of the point source downstream a state similar to upstream of the effluent outfall was re-established.

**Keywords.** Self-purification, water quality, flow structure, hydrodynamics, drop picture method.

---

### INTRODUCTION

The evaluation of water quality in lotic systems relies in principle on the analysis of physical, chemical and biological characteristics. Our proposition here is to study a new descriptor of water quality, not just based on its constituent elements but taking into account the general and most outstanding characteristics of water as a liquid: its ability to move and flow, an essential function in its role as a life mediator. The hydrodynamics of water can be shown by using the Drop Picture Method, developed by Theodor Schwenk and published in 1967.<sup>1</sup> We looked at this new criterion of hydrodynamic behaviour and applied this methodology along a length of stream polluted at point source by biodegradable organic effluent, and compared the results with customary testing parameters.



## I. STUDY FRAMEWORK AND SAMPLING

This study included ten measurement campaigns from 1972 to 1977 carried out on the Mettma,<sup>2</sup> a mountain stream in the Black Forest, in collaboration with the Institute of Limnology, University of Freiburg (Germany).<sup>3,4,5</sup> The Mettma is a trout-inhabited stream, oligotrophic and with a low flow rate (150 to 1500 L/s) depending on the season. The ten surveys were done in different situations, including all seasons of the year. In this article however, we used the results collected in a testing survey carried out during a period of low water (192 L/s), the 26<sup>th</sup> of July 1974. At a certain point a brewery discharged organic pollutant into the stream, in a row effluent quantity of 6000 inhabitants equivalent. Subsequently, the stream crossed a wooded mountainous zone and had no other interference apart from a dilution factor of 3 due to small tributaries. The study was terminated by the installation of a treatment plant at the brewery in 1977, and was spatially limited by the construction of a weir 9 km downstream of the effluent injection. The study included 11 sampling stations, one upstream and further stations 50, 300, 700, 1450, 1800, 3000, 3900, 5100, 7150 and 8000 m downstream of the effluent injection. Different parameters were measured: temperature, pH, surface tension, dissolved oxygen, ammonium, phosphate and nitrate concentration. In addition, the biological situation of the ecosystem at the stations and the hydrodynamical quality of the water were analysed.

## II. ANALYSIS AND SEQUENCE OF PHYSICAL-CHEMICAL PARAMETERS

### II.1 Temperature

The introduction of effluent increased the stream temperature from 10 to 13°C. The temperature was only slightly reduced over the total study section of 8000 m (Fig. 1)

### II.2 pH

The Mettma is naturally slightly acidic, with pH values of typically between 6.1 and 7.0. Immediately downstream of the effluent injection, pH values oscillated between 6.1 and 10.4 because of the neutralization of the effluent. The pH levels stabilized after 3000 m.

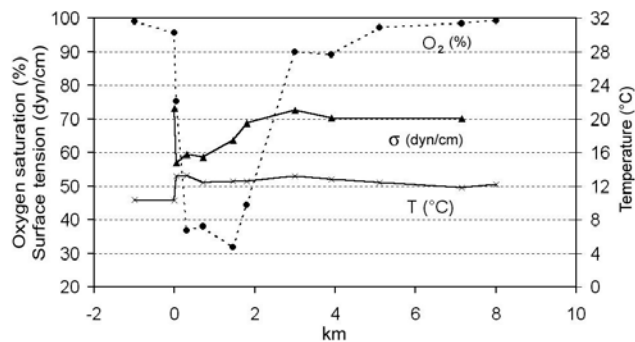


**Figure 1.** Evolution of temperature, dissolved oxygen and surface tension along the length of study section of the self-purifying stream (Peter 1994).

### II.3 Surface Tension

The initial surface tension values corresponded to water free of surface-active substances, but decreased drastically at the effluent injection from 73 to 57 dyne/cm. The brewery effluent was chiefly composed of organic matter. 3000 m downstream, surface tension values stabilized at levels somewhat lower than the initial values (Fig. 1).

### II.4 Dissolved Oxygen

Close to total saturation upstream of the outfall, the dissolved oxygen values dropped dramatically to 35% at the injection due to the high oxygen demand of bacterial activity and oxidation of organic matter. Oxygen levels progressively returned to their initial values 7150 m downstream (Fig. 1).

### II.5 Ammonium and Phosphates

Organic nitrogen and phosphorus were introduced by the effluent and microbially mineralised to ammonium and phosphates. Phosphates reached maximum concentrations 50 m and ammonium 300 m downstream as products of the breakdown of the introduced organic matter. These pollutants were totally metabolised at the downstream checkpoint of 7150 m (Fig. 2).

### II.6 Nitrate

A product of the oxidation of ammonium, nitrate was initially only present at low levels. Its concentration increased progressively along the length of the study section, levels did not totally stabilize at 8000 m downstream of the effluent injection (Fig. 2).

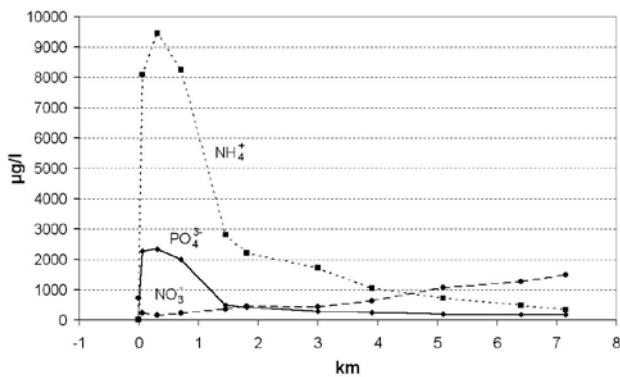


**Figure 2.** Ammonium (NH<sub>4</sub><sup>+</sup>), nitrate (NO<sub>3</sub><sup>-</sup>) and phosphate (PO<sub>4</sub><sup>3-</sup>) concentration in µg/l, as well as the oxygen saturation in % (Peter 1994).

### III. BIOLOGICAL ANALYSIS

#### III.1 Evolution of the Biotic Community

Initially, the Mettma was an oligosaprobic balanced stream ecosystem typical to the trout zone. It was inhabited by a wide variety of animal and plant species which constituted its biotic community. 40 different species of benthic fauna were indicative of this diversity (Fig. 3).

The brewery effluent added an organic load equivalent to the raw effluents of 6000 inhabitants. This profoundly modified the ecological equilibrium of the ecosystem (Fig. 4). The system became polysaprobic. Life conditions favoured the development of filamentous

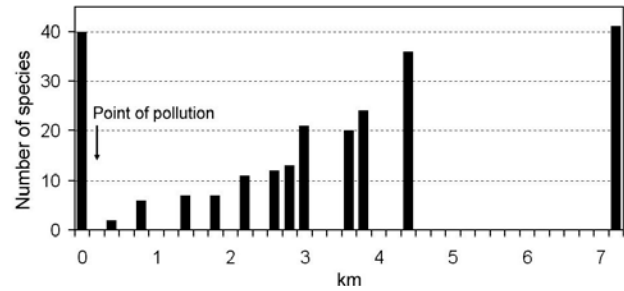


**Figure 3.** Number of species (taxa) of animals on the stone substrate during the course of the self-purifying section (after Schreiber 1975<sup>6</sup>).

bacteria (*Sphaerotilus natans*) and ciliates and excluded other species. In this first polysaprobic zone which stretched for approximately 300 m, the number of benthic species plummeted to 2. The filamentous bacteria eventually detached themselves and were transported several hundred meters further, where they were deposited and became important nutrients for colonies of sludge-worms (*Tubifex tubifex*) and chironomid larvae (*Prodiamesa olivacea*). This degradation zone where the breakdown of organic matter dominated, ended with the appearance of blackfly larvae (*Odagmia ornata*) and monocellular algae 2000 m downstream of the injection point. This marked the beginning of the primary production zone, with a succession of plant species from algae and mosses to higher vegetation. Species of herbivores, such as freshwater limpets (*Ancylus fluviatilis*) and mayfly larvae (*Baethis rhodani*) as well as carnivores, such as stream amphipods (*Gammarus fossarum*) and

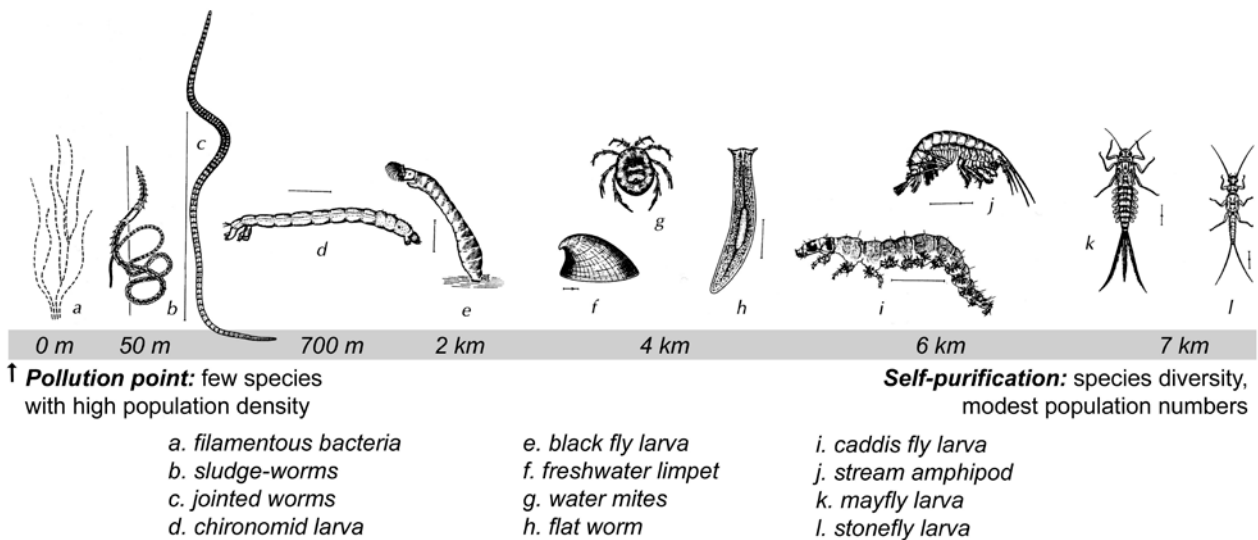


**Figure 4.** Typical representatives of the benthic fauna the length of the self-purifying stream section (according to Peter 1994).

predatory larvae of various insect species, reinhabited the biotope. The trout-zone had fully regenerated after 7000 to 8000 m, the number of fauna species in the benthic zone reattaining its initial value.

### III.2 Polarities

If we take into consideration the evolution, distribution, variety, morphology, mode of nutrition and locomotion of the benthic fauna, the following can be observed:

- At the beginning of the self-purifying study section, species diversity was very reduced while population density was high. The organisms generally had a homogeneously segmented morphology with radial symmetry. Sensorial organs were very primitive. Most organisms were sedentary and saprophage. Their rhythm of activity depended only on the supply of nutrients, their life activity being orientated towards metabolism.
- At the end of the self-purifying study section - as before the effluent outfall - there was a greater species diversity while the population numbers remained modest. The morphology of the organisms was more complex with heterogeneous segmentation, axial symmetry and a greater body surface area. Sensorial organs were located at the head, organisms were more mobile and were herbivores or carnivores. They followed day-and-night and seasonal rhythms. Their activities were orientated towards sensorial functions and locomotion.

## IV. HYDRODYNAMIC ANALYSIS

### IV.1 The Drop Picture Method

The Drop Picture Method, developed by Theodor Schwenk, allows the study of water's aptitude for movement, its hydrodynamics. The method is carried out by the systematic and controlled agitation of a water sample through the impact of drops of distilled water released at 5 second intervals. Each impact on the very shallow water sample creates internal movement and flow forms. The addition of a tiny amount of glycerine to the water samples facilitates the photographic optical visualization of the flow movements via a Schlieren optic system. Successive drops renew the created flow movements, so that a whole series of 30 drop-generated images was documented for each sample (Fig. 5).

The Drop Picture Method was examined in the 2000s to optimise and standardize the testing methodology.<sup>7,8</sup> The results are usually interpreted qualitatively, but may additionally be analysed based on quantitative analysis of for example the degree of development of vortex forms. The Drop Picture Method indicates the given movement capacity of a water sample based on the level of complexity and differentiation of its internal flow forms. It is a morphological method, complementary to physical-chemical analysis, revealing more information about the hydrodynamic qualities of a water sample than its chemical composition. It is a system to evaluate water quality based on positive, life-giving criteria, rather than on exclusion of negative criteria.

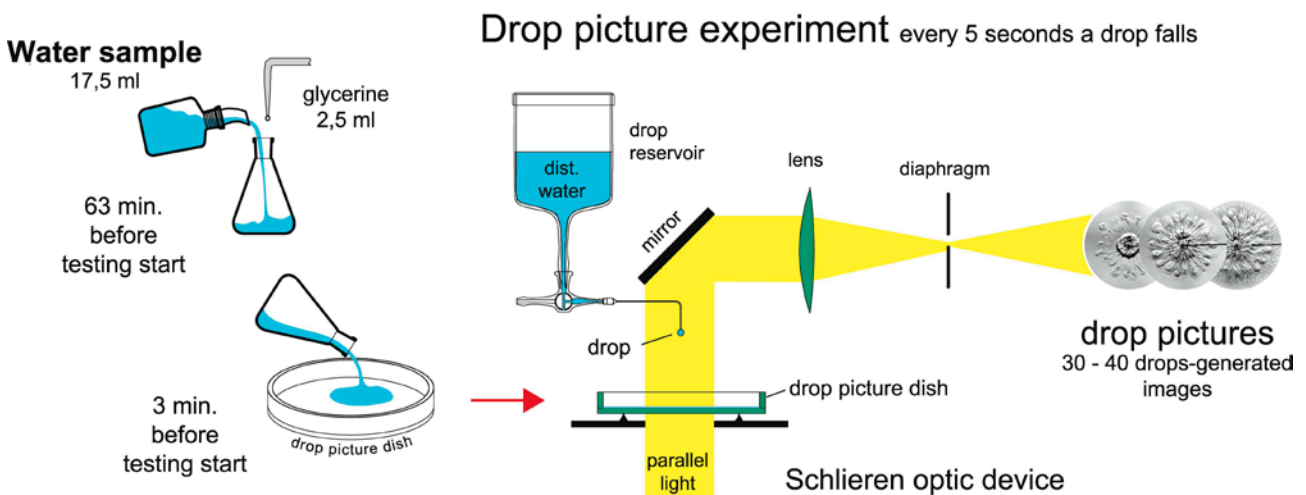
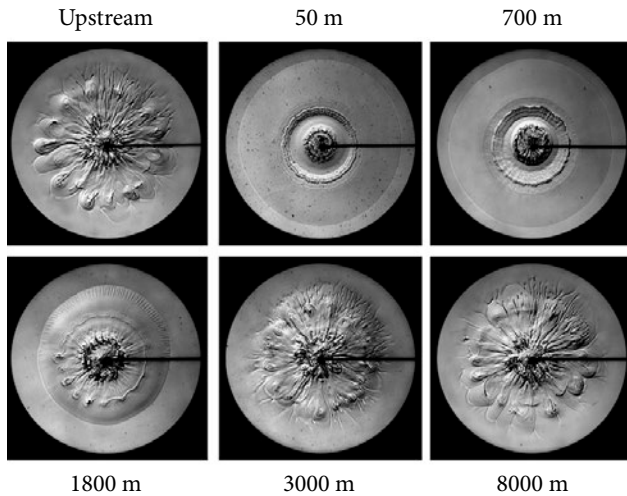


Figure 5. Drop Picture Method procedure and chlieren optic device.



**Figure 6.** Drop-generated images after the 20<sup>th</sup> drop the length of self-purification.

#### IV.2 Application to the Section of Self-Purifying Stream

The testing points were identical to those of the previous studies. The water samples were analysed on the same day as they were collected. 30 images were produced for each water sample. Here the 20<sup>th</sup> is selected to facilitate comparison between samples (Fig. 6). We will now discuss the most distinctive phases along the stream self-purifying section. Upstream of the effluent outfall, drop-generated image revealed a garlanded composition of vortices where more extended vortices alternate with more stocky ones. Leafy vortices could be observed, as well as radial dendritic structures. The successive 30 images during the analyse were relatively balanced, showing differentiated and varied structures, which were regenerated with each successive drop.

Downstream of the effluent injection the drop-generated images were significantly different. They were simply and solely composed of a disc-shape structure centred on the central point of impact. The forms were rudimentary, undifferentiated and monotonous.

- 1800 m downstream, the disc-shape structure shrunk while in the centre the beginnings of differentiation - the buds of heads of vortices - could be identified.
- About 3000 m downstream, the beginnings of leafy vortices and dendritic structures could be observed again. The closed disc-shape form had disappeared.

By the end of the studied stretch of stream, the internal flows of the drop-generated image had returned to be the varied, complex and differentiated and polymorphic as in the sample upstream of the effluent injection.

## V. COMPARISON OF THE DIFFERENT DESCRIPTORS

### V.1 Physical-Chemical Parameters and Hydrodynamic Evaluation

#### V.1.1 Point of Inflexion

The evaluation of the hydrodynamics of a given water sample is not based on any one drop-generated image but rather on the evolution of the ensemble of images. At some point each of the samples reaches a state where after a certain number of drops the garlanded structure shrinks, disappears and is replaced by a more rigid disc-shaped structure. This is what we call the “point of inflexion”, which occurs sooner or later in the tests, depending on the hydrodynamic qualities of the sample in question. This is a useful parameter. The drop number at which it occurs can be used to compare water samples taken along the length of study stream in question. When a disc-shaped structure appears in the first drop-generated image, the point of inflexion has already taken place before the start of the testing.

#### V.1.2 Comparison of Results

The graphical comparison of the levels of oxygen saturation, the point of inflexion and surface tension demonstrated a relationship between levels of oxygen and the point of inflexion. This relationship was however not causal but demonstrated that there is a correlation between these two factors and water quality. In most of the measurement surveys, the evolution of physical and chemical parameters stabilised well upstream compared to where the point of inflexion had stabilised (Fig. 7). This in contrast only returned to its pre-effluent levels at the very end of the length of studied stream, parallel to the reestablishment of the biotic community to its initial

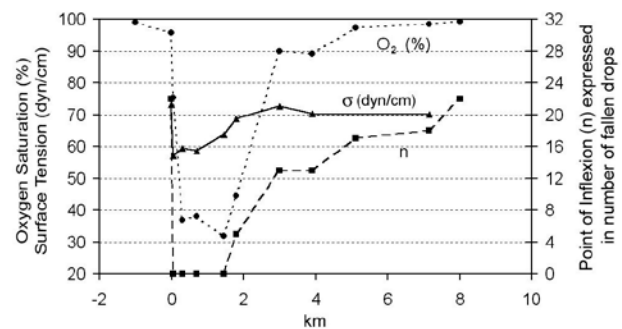


**Figure 7.** Evolution of oxygen saturation, surface tension and point of inflexion (Peter 1994).

levels. This point of inflexion thus appeared to be a more sensitive descriptor, indicative of the overall state of the stream ecosystem.

### V.2 The Biotic Gradient and Stream Hydrodynamics

It appeared that along the stream in question:

- Where the drop-generated image, in reference to previous images, had a closed, disc- and monotonous shape
- Where the drop-generated image showed a lack of mobility and a predetermined evolution,
- There was the least species diversity, with the presence of sedentary, simple-structured organisms, whose activities were confined to their metabolic activity, that is to say after the effluent outfall.

In addition:

- Where the drop-generated images revealed a maximum of polymorphic, diverse flow shapes, with the greatest complexity of movement in the water, where the images had a differentiated structure without being predetermined in their evolution
- This is where biotic populations were varied and balanced, individual organisms having a more differentiated anatomy, complex nutrition and locomotion as well as being more sensitive to their environment due to more advanced sensorial organs, that is to say upstream of the effluent outfall and at the end of the stretch of self-purification.

### CONCLUSIONS

This comparative study of the physical-chemical, biological, and hydrodynamic characteristics of a self-purifying section of the Mettma proved that there are parallels between the degree of diversity in the biotic community and the degree of movement diversity in water samples from the same testing stations. In the degradation zone, where metabolism processes determined the physiology and activity of the animal population, water samples showed monotonous and weakly defined flow shapes. In contrast, in the primary production zone where, thanks to primary production by vegetation, anabolic processes dominated, the water samples showed diverse and differentiated water flow shapes. Thus, very different phenomena could carry the same signature of a shared intrinsic quality. Physical-chemical parameters are descriptors of a specific moment of the stream. The biological indicators reveal a more integrated long-term picture of the water, whereas the hydrody-

namic analysis revealed the momentary but holistic state of the water.

### REFERENCES:

1. Schwenk, T. (1967). *Bewegungsformen des Wassers*. Stuttgart.
2. Peter, H. M. (1994). Das Strömungsverhalten des Wassers in der biologischen Selbstreinigungsstrecke des Schwarzwaldbaches Mettma. *Sensibles Wasser* 4, 1-160, Herrischried.
3. Franke, U. & Schwoerbel, J. (1972). Hydrographie, Chemie und Nährstoffracht eines mit organischen Abwässern verunreinigten Gebirgsbaches. *Arch. Hydrobiol. Suppl.* 42, 95-124.
4. Reichardt W. & Simon, M. (1972). Die Mettma - ein Gebirgsbach als Brauereivorfluter. Mikrobiologische Untersuchungen entlang eines Abwasser-Substratgradienten. *Arch Hydrobiol. Suppl.* 42, 125-138.
5. Schwoerbel, J. (1972). Falkauer Fließwasser-Untersuchungen an der Mettma. *Arch Hydrobiol. Suppl.* 42, 91-94.
6. Schreiber, I. (1975). Biologische Gewässerbeurteilung der Mettma anhand des Makrozoobenthos: Methodenvergleich. *Arch. Hydrobiol. Suppl.* 47, 432-457.
7. Wilkens, A., M. Jacobi & W. Schwenk (2000). Die Versuchstechnik der Tropfbildmethode. Dokumentation und Anleitung. *Sensibles Wasser* 5, Herrischried.
8. Wilkens, A., M. Jacobi & W. Schwenk (2005). *Understanding Water*. Edinburgh.

---

Original title: Suivi du parcours d'autoépuration d'un ruisseau par la dynamique de ses eaux (2004). Société Hydrotechnique de France. *SHF-publications 28<sup>èmes</sup> Journées de l'Hydraulique*, 31-38. Paris



**Citation:** E. Zürcher (2019) Water in Trees - An essay on astonishing processes, structures and periodicities. *Substantia* 3(2) Suppl. 3: 71-83. doi: 10.13128/Substantia-507

**Copyright:** © 2019 E. Zürcher. This is an open access, peer-reviewed article published by Firenze University Press (<http://www.fupress.com/substantia>) and distributed under the terms of the Creative Commons Attribution License, which permits unrestricted use, distribution, and reproduction in any medium, provided the original author and source are credited.

**Data Availability Statement:** All relevant data are within the paper and its Supporting Information files.

**Competing Interests:** The Author(s) declare(s) no conflict of interest.

## Water in Trees

### An essay on astonishing processes, structures and periodicities

ERNST ZÜRCHER

*Dr. sc. nat., Forestry engineer ETHZ, Professor em. for Wood Science Bachelor & Master Wood, Bern University of Applied Sciences, Architecture, Wood and Civil Engineering Solothurnstrasse 102, P.O. Box, CH-2500 Biel-Bienne 6*  
E-mail: ernst.zuercher@bfh.ch

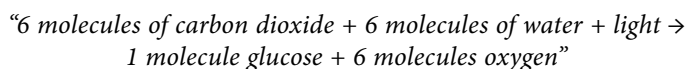
**Abstract.** This essay shows that the relations between water and trees have far-reaching, unexpected aspects and consequences. The local and the global terrestrial water cycles are directly or indirectly linked to the presence of trees and forests. A more precise consideration of photosynthesis reveals that this process is not only producing biomass and oxygen, but is also the place of water synthesis. This newly formed water probably shows properties according to the new water-paradigma proposed by G. Pollack (2013). This must also be the case for the water absorbed in the soil and flowing upwards through capillar wood structures, forming vortices at the microscopic cellular and at the macroscopic tree level. Another lesser-known phenomenon is linked to periodical changes in the wood-water relation, according not only to the solar influence (photoperiodism, seasonality), but also to more subtle lunar rhythmicities having an effect on wood properties. This last aspect represents a kind of rehabilitation of traditional practices often considered as mere superstitions.

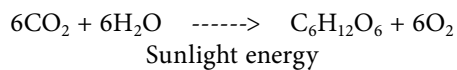
**Keywords.** Water cycle, photosynthesis, water synthesis, wood structure, vortices, lunar rhythmicities.

---

#### WATER AT THE CENTER OF THE FUNDAMENTAL PROCESS OF LIFE

Photosynthesis is the common process to all plants, but trees, due to their outreaching dimensions and to the formation of forests in specific multispecies associations, perform 2/3 of the global photosynthesis on earth. A closer study of this process reveals that there is a hidden face of photosynthesis. In many textbooks or even dictionaries, an uncomplete equation of photosynthesis is still usual, which is misleading for a correct understanding of the most important physiological process making life possible on earth. Effectively, following equation is often figuring:



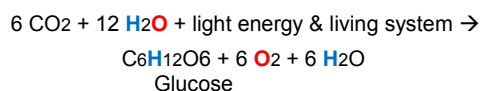


Where:  $\text{CO}_2$  = carbon dioxide  
 $\text{H}_2\text{O}$  = water  
 Light energy is required  
 $\text{C}_6\text{H}_{12}\text{O}_6$  = glucose  
 $\text{O}_2$  = oxygen

The researcher who finally refutes this incomplete and tenacious portrayal is the microbiologist Cornelis Van Niel (1897–1985) of Stanford University, following work as a young student on the photosynthetic activities of various types of bacteria. One particular group of these – the purple sulphurous bacteria (*Thiorhodobacteria*) – is capable of reducing the  $\text{CO}_2$  into carbohydrates, in an atmosphere devoid of oxygen (anaerobic conditions) and without emission of oxygen. The substrate necessary here is not water  $\text{H}_2\text{O}$ , but hydrogen sulphide  $\text{H}_2\text{S}$ . What is released by the process, on the other hand, in addition to the carbohydrates, is water  $\text{H}_2\text{O}$  and elemental sulphur  $\text{S}_2$  accumulated in the globules within the bacteria and identifiable under a microscope. Van Niel did not stop here and he extrapolated his discovery by proposing a generalised equation for photosynthesis. This came down to affirming that the source of the oxygen produced by chlorophyllian photosynthesis was in fact the water and not the carbon dioxide.

This brilliant speculation put forward in the 1930's received its proof in the following decade when researchers from Berkeley used a heavy isotope of oxygen ( $^{18}\text{O}$ ) to mark the water molecule entering the reaction. Result: the oxygen released comes exclusively from the  $\text{H}_2\text{O}$  molecule. In terms of process, this comes down to understanding that the primary action of the sun's rays in photosynthesis consists of the splitting or photolysis of water. The newly produced water takes its oxygen from the carbon dioxide absorbed (Ray 1972; Lance 2013).

The complete and balanced equation for the production of glucose by photosynthesis, within a living system without which nothing can happen, thus includes an extra constituent. The destination of the atoms of the water molecules taking part in the reaction can be shown by using colours and bold type:



By converting into moles (molecule-grammes, according to chemists' terminology), it is possible to

illustrate the flows of matter by weight (in grammes), with indication of the energy required (in kilo-Joules):

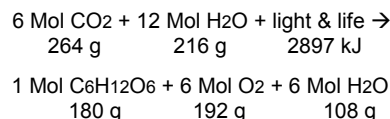
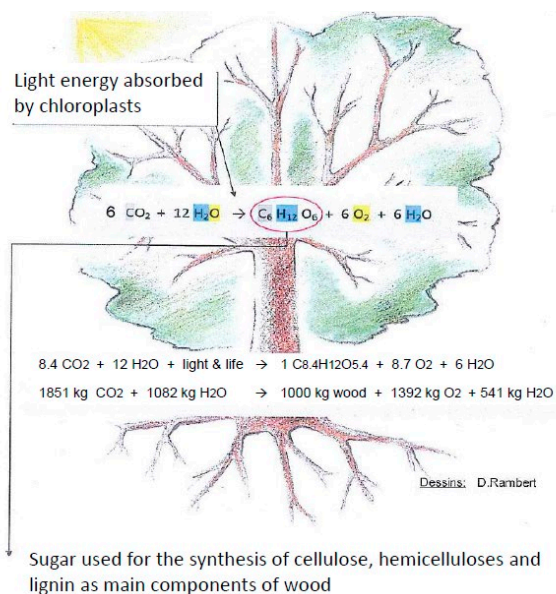


Figure 1 also presents the values corresponding to the synthesis of wood, originally based on glucose, but characterised by a slightly different formula used by physiologists (Zimmer and Wegener, 1996). Some remarkable facts emerge from this new vision of the process:

- For each dry tonne of wood made by the tree, a mass of 1.851 tonnes of gaseous  $\text{CO}_2$  is removed from the atmosphere, reducing by that amount the greenhouse effect and global warming which preoccupy humanity at present. We have here a 'carbon sink', persisting as long as the wood is not burned or decomposed releasing an analogous quantity of  $\text{CO}_2$  into the atmosphere. It will therefore be important in the future to incorporate wood on a long-term basis either into buildings as a material or into soils in order to increase the content of stable organic matter.
- Each anhydrous tonne of wood made by the tree is accompanied by a mass of 1.392 tonnes of newly-formed oxygen, coming from the photolysis of water. This represents a considerable volume: 973  $\text{m}^3$  of pure oxygen, or 4,636  $\text{m}^3$  mixed at a proportion of 21% into the air we breathe to stay alive. A rather unorthodox question, coming from a quality point of view: Does newly-formed oxygen of this kind, entering the biosphere for the first time in this form, have different properties from "old" oxygen? Could this possibly be one of the reasons why forest air has always been felt to be particularly beneficial to health?
- Each anhydrous tonne of wood made by the tree is accompanied by a mass of 541 kilos of newly-formed water. As for the preceding component, we have here perfectly pure water, which has never before entered into the great cycle "evapotranspiration – cloud formation – condensation / precipitation – running-off / percolating – accumulation – resurgence". It is likely that this new water soaks the green parts of the plants and circulates with the elaborated (phloem) sap down to their lower organs, contributing to their growth. Here too arises the question of qualities, properties or specific virtues of such water, especially given the many forms of pollution to which the external water cycle is subjected. Such a question can be placed in a modern scientific debate, very con-





**Figure 1.** Complete general equation of photosynthesis, with an indication of the destination of components (above) and average proportions accepted for wood, with indication of weight ratios compared to the dry matter of wood, according to Zimmer and Wegener (1996) (below) [drawing D. Rambert].

traversal at the outset, but finding more and more renowned defenders: that of the ‘memory of water’, as developed by pioneers such as Jacques Benveniste, Xy Vinh Luu, Marc Henry, Luc Montagnier or Gerald Pollack. We should mention here, to underline the credibility of the protagonists and the importance of the subject, that Professor Luc Montagnier received the Nobel Prize for Medicine in 2008.

## TREES AND THE LATEST FINDINGS ABOUT WATER

The emergence of a new understanding of water allows us to adjust our view of the structures and functioning of trees. A chance observation made in a Japanese laboratory followed by a series of experiments starting at the beginning of this century has led to a progressive confirmation of a hitherto-unknown property of water. In the presence of hydrophilic membranes (natural or synthetic) and over a distance reaching sometimes several tenths of a millimetre, water acquires a state which seems both liquid and solid at once, a fact which suggested to the discoverer, a researcher and professor of bioengineering already well-known for his book ‘Cells, Gels and the Engines of Life (Pollack 2001), the expressions of ‘exclusion zones, EZ’ (EZ water / linked to its particularly pure state) and ‘fourth phase of water’.

in addition to the solid, liquid and vapour phases. The research on the subject which continues to this day has recently received a coherent overall structure in the form of a publication which did not go unnoticed by the scientific community: ‘The Fourth Phase of Water – Beyond solid, liquid and vapor’ (Pollack 2013).

The anatomical structures of plants and trees in particular, composed of a complex system of membranes and cells with hydrophilic walls showing dielectric properties (as postulated by Pollack) and the mechanisms of transport of water towards the crown and the metabolism linked to photosynthesis can, through this new concept, be interpreted more precisely. It should be mentioned that this water close to hydrophilic membranes can be distinguished from ‘normal’ water by many criteria such as level of purity, pH, viscosity, refraction index, the absorption of light energy, electrical charge, oxygen content or again the formation of a supramolecular network.

The formation of ‘new’ water resulting from photosynthesis, in addition to the carbohydrates and oxygen, thus gains additional significance, since it occurs within complex membrane systems, corresponding to the criteria of formation of water of the ‘EZ’ type. The fact that this new water takes 89% of its mass from part of the oxygen of the atmospheric  $\text{CO}_2$  is already remarkable in itself, making the plant – and in a particular way the tree – both a consumer and a producer of water. It is recognised that carbohydrates and oxygen are necessary for life. We may now ask whether new water with its special properties (which still need analysing) might not also be of fundamental importance.

## STRUCTURES

### *A functional approach / Xylem as water conducting system*

The function of conducting water requires bringing water from the root system to the crown, where the assimilation takes place. This occurs through a conducting system made of cells called tracheids in conifers and connecting alignments of cells called vessels in broad-leaved species. The first engineering problem is: How to bring cold water (heavy) up to the high parts exposed to heat, sometimes more than 100 metres for the largest trees? How can the physical law of gravity be overcome?

The solution is proposed by the physiologists with the ‘theory of cohesion – tension’: Water is sucked up, with its diluted mineral salts, along the cellular channels by the ‘negative pressure’ resulting from the foliar transpiration of the tree (Zimmermann 1989; Koch et al. 2004; Johnson 2013). To go beyond the critical height

of 10 metres (linked to the atmospheric pressure), the water must contain absolutely no gas bubbles and thus have access to the totality of its internal cohesive forces (which allow, for example, two glass plates to stick together). This state of liquid purity is made possible in conifers by bordered pits. These are mobile contact structures between a tracheid and its neighbour with an effect simultaneously of valve and sieve in order to avoid any embolism due to air bubbles which could accumulate. This system of water transport with special specifications functions at the periphery of the bole's section, in the xylem, the living part of the wood characterised

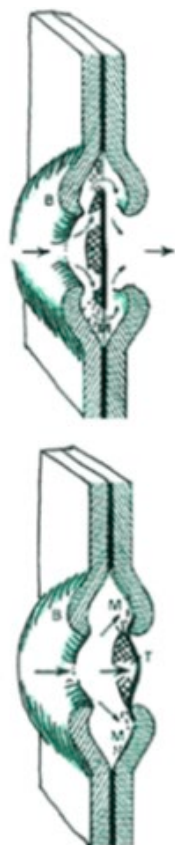


**Figure 2.** Diagramme of the workings of a bordered pit: when functioning normally (top), the water skirts the central impermeable zone of the shared membrane and enters the neighbouring tracheid; in the case of a wound with air bubbles (accidental entry of air), the relative increase in pressure causes the membrane to be flattened, by suction, against the inside of the opposite pit (bottom), blocking the flow of water in the damaged part [modifies after Zimmermann 1983]. The recent discoveries about water encourage the supposition that this forced passage through the fibrillar weave of the peripheral membrane confer on the water an additional proportion in the 'crystalline-liquid' phase with high viscosity and lowered freezing point, an essential characteristic for species growing in cold regions.

by bio-electric fields. Gerald Pollack's recent discovery (mentioned above) reveals that water running through tracheids or vessels the most directly in contact with the hydrophilic cell wall acquires a particular structure ('liquid crystals') and unexpected physical, chemical and electrical properties, probably essential to the physiological exploits of trees. Running through capillary systems allows the water to stay liquid down to low temperatures, around  $-15^{\circ}\text{C}$  for certain species, instead of damaging the structures by the formation of ice crystals in winter. As for the electrophysiologists, they observe that the differences in electrical potential generated by the living tissues stimulate the flow of raw sap. These observations follow on logically from old experiments testing the effect of glass capillaries on the fluidity and sensibility of water (Maag 1928).

This function of conducting water in an upward direction is fulfilled in conifers by tracheids of early-wood (formed in the spring and the beginning of summer) containing many bordered pits. The latter represent the points where water passes from one cell to its neighbour during its flow towards the crown, site of photosynthesis. Comparatively, the tracheids of late wood (formed towards the end of the vegetative period) possess a much thicker cell wall endowed with fewer pits; their function is no longer conducting raw sap, but primarily the support of the whole structure. The functioning of a bordered pit, a local cell wall modification essential to the security of the conduction system, is presented in Figure 2: we have here an efficient and 'ingenious' system, a characteristic component of the functional anatomy of conifers.

Compared to conifers, the anatomy of broad-leaved trees is much more complex, with its forms of functional specialisation. Depending on the tree species, we find generally two types of arrangement of vessels: in porous zones in the case of a marked contrast between early and late wood, or in diffuse pores, when the vessels are of practically constant diameter, spread regularly over the whole of the annual ring.

### *Spirality and the Golden Ratio*

The helical arrangement observed in the needles of a young Scots Pine shoot follows a general principle of pronounced geometrical nature, which Goethe (1749–1832) considered as fundamental and called "spiral tendency, which reigns in Nature", and which is always found in combination with the "vertical tendency". It was shown by a philosopher and naturalist from Geneva, Charles Bonnet (1720–1793), that the position of leaves or needles along a stem (subject of phyllotaxy) or the

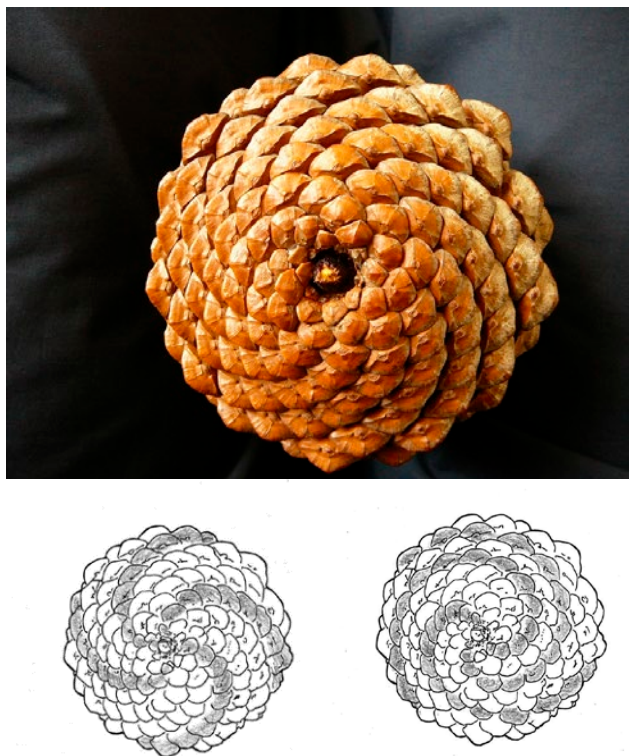


**Figure 3.** Cone of a Maritime pine (*Pinus pinaster*) growing in the western Mediterranean (above), showing an arrangement of the scales according to two series of spirals with a ratio 13 / 8 (below).

structure of a fir-cone or pine-cone, or indeed that of a thistle flower head, follow a series of crossed spirals. These are subject to a particular relationship: the Golden Ratio. This ratio, originally defined by Euclid (325–265 BC), is found among others in the famous number sequence developed by Leonardo of Pisa, also called Fibonacci (approx. 1170 – 1250) :

1 – 1 – 2 – 3 – 5 – 8 – 13 – 21 – 34 – 55 – 89 – 144 – ... , where each element is the sum of the two preceding ones. This series allows the constitution of a set of rational ratios  $2/1, 3/2, 5/3, 8/5, 13/8, \dots, 144/89, \dots$ , which tend towards the number Phi ( $\phi$ ) = 1.61803 ... . Similarly, the series  $1/2, 2/3, 3/5, 5/8, \dots$  etc. converges towards the number phi ( $\phi$ ) = 0.61803 ... ( $\phi = \phi - 1$ ). A cone of the Scots Pine (*Pinus sylvestris*) observed from its base shows an arrangement of scales (also called bracts) according to two spiral systems: a group of 13 rightward (clockwise) spirals and a group of 8 leftward (anti-clockwise) spirals. An Eastern White (*Weymouth*) Pine (*Pinus strobus*) is also formed according to the Golden Ratio, but with a ratio of 8/5. These arrangements are illustrated by the example of a Maritime Pine in Fig. 3. Analysis of a specimen of Spear thistle (*Cirsium vulgare*), an annual plant, shows the seeds on a dried

head to be arranged according to a double spiral system with a ratio of 26/16, which can also be written  $13 \cdot 2 / 8 \cdot 2$ , thus is part of the Fibonacci series. Interestingly - and to make a link with the 2019 International Year of the Periodic Table of Chemical Elements – the elements of the Mendeleev's table can be geometrically arranged according to a spiral following the Fibonacci pattern (Morton 1977).

#### Where Life surges up

Usually (as was the case in Figure 3), the right-handed and left-handed spiral patterns (also called parastiches) are counted from the base either clockwise or anti-clockwise, which corresponds to an upwards direction for the axis of the cone or for the stem carrying leaves or buds.

But we could also consider, like the famous Austrian forester-hydrologist Viktor Schauberger (1885-1958), that in the genesis of plant organs, series of upward spirals cross downward spirals. In his vision of the living world, he talks of female upward energies which are fertilised by male downward energies moving in the opposite direction. In practice, the axillary buds arranged along the shoot and the seeds developing at the receptacle or along the axis of the cone (at the base of the scales) could be understood as germs of life appearing within a “flow – counterflow” system according to the precise mathematical-geometrical ratios of the Golden Ratio. In a conception of the plant as interacting with the astronomical rhythms modulating among others gravitational forces, these germs of life would thus appear at the points where terrestrial and cosmic ‘force lines’ meet and cross-fertilise (Fig. 4).

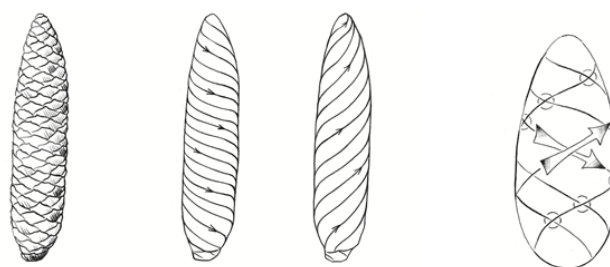


**Figure 4.** Left: diagrammatic representation of two “energy flows (male downwards / female upwards)” intersecting in a helical fashion (in Coats 1996). Right: Spatial arrangement of the seed location at the intersections of the spiral patterns characteristic of the species; the seed represent dormant meristematic points, destined to develop as new specimen. Drawing D. Rambert.

### Viktor Schaubberger (1885–1958)

Austrian forester remaining voluntarily outside university circles, Viktor Schaubberger was a hydrologist and inventor who stupefied the technical and academic circles of his time. His first achievement was making channels for floating wood of a revolutionary type, seeming to defy the laws of physics of the time. A great observer of natural phenomena, he explored the diverse properties of water and drew from them technical applications including regeneration systems. He saw water as the basis not only of all life, but also of the whole of the ‘terrestrial consciousness’. His thoughts and discoveries led him to direct applications in forestry, agriculture and hydrology (waterways, dams, vitalising water, organisation of forest areas). He designed an ecology in symbiosis with nature well before the contemporary approach (Alexandersson 2002; Bartholomew 2014).

This concept of special places for life to surge up where two flows meet can also be applied to the first cambial cells separating the conducting bundles of young stems, and to the widened ‘secondary’ cambium forming a closed cylindrical meristematic layer, in charge of the growth in thickness of the trunk: both are placed exactly between the upward xylem flow (in the wood) of raw sap and the downward phloem flow of phloem sap.

### Vortex flows revealed

By means of injections of liquid colourings into the sapwood at the base of the trunk, some physiologists (see Bosshard 1974; Harris 1989 on this subject) found that the upward flow of raw sap does not occur in a straight line, but in a manner which is generally helical, in a progression around the axis of the tree. According to the species, but also according to their growth conditions, five ways of transporting water up to the branches were described, of which four were clearly not straight, in the form of upward spirals turning towards the right, or towards the left, or even swinging from one direction to the other (Fig. 5). These flows are linked to the anatomical structure of the wood, presenting a ‘spiral grain’, with conducting cells deviating from the axis to a greater or lesser extent, including radical changes in direction during the change from juvenile to adult status in many conifers. These phenomena serve to guarantee that each root can provide water to each branch or nearly, with priority given to the apex, the most essential part of the crown.

An analogous experiment remains to be carried out with the downward flow in the phloem: will we find downward spirals in the opposite direction?

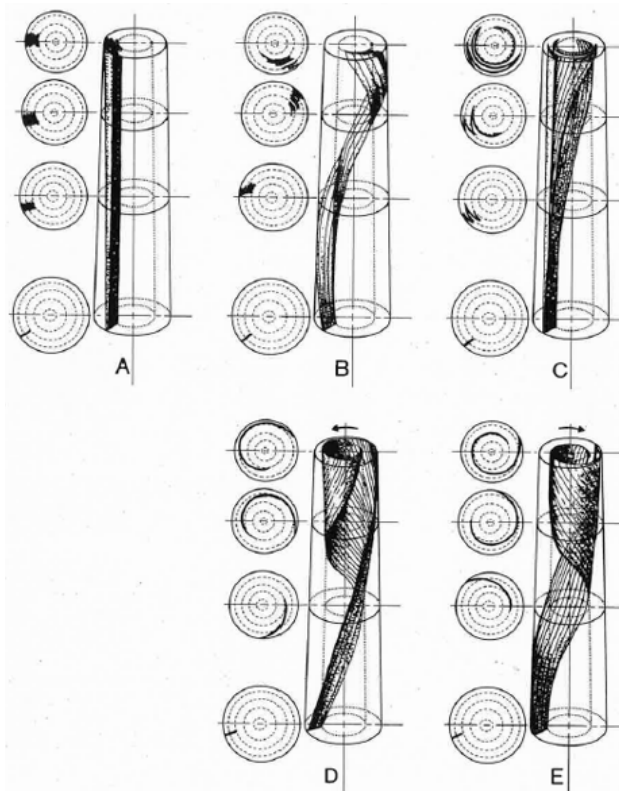


**Figure 5.** Ascent of dye solutions in stems of standing trees, after injections radially at the base of the stem. A: sectorial straight; B: sectorial winding; C: interlocked; D: spiral turning left; E: spiral turning right (In Harris 1989, after Vité 1967).

This elucidation of the upward flow of raw sap using dye solutions injected at the base of the stem showed the paths to the crown were not direct but helical (in a vortex) compared to the axis of the trunk. An interesting similarity underlining the coherence of biological systems: the flow of blood in the large vessels and in the human heart, studied using Doppler echocardiography and cardiac magnetic resonance, also form vortices (Day 1998; Sengupta et al. 2012; Caro et al. 2013). In the more recent development of research on water, based on the discovery of a ‘fourth phase of water’, particularly in contact with organic hydrophilic membranes, the part played by vortex flows appears in a new light. One of the particularities is that the vortices increase the oxygenation of the water and its amount of energy-rich hydrogen bonds (Ignatov et al. 2015). Simultaneously, the emission of energy by radiation is reduced, while significantly decreasing the temperature when before and after vortexing is compared (Pollack 2013). This last feature had been discovered by Viktor Schaubberger mentioned above, who considered it very important for the health



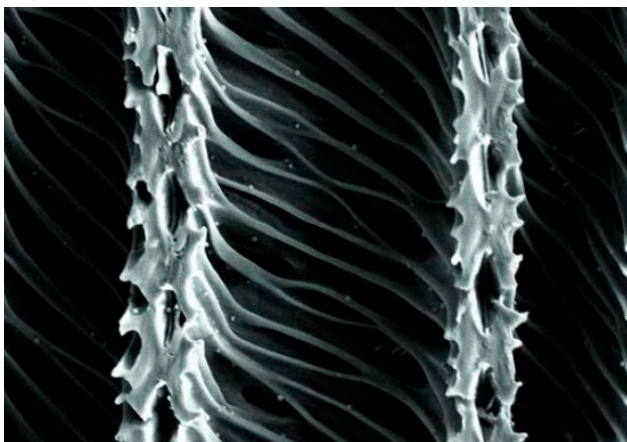


**Figure 6.** The clematis (*Clematis vitalba*) is a woody plant which is not self-supporting, belonging to the group of lianas, which have the highest-known speeds of transport of the raw sap. A maximum of 222 metres per hour was measured by Kucera and Bossard (1981). The strongly helical structure of the vessel walls probably plays here an essential role (Photo T. Volkmer).

of ‘biological systems’ such as trees or even waterways. Figure 6 may illustrate the phenomenon at the anatomical level.

## PERIODICITIES

### *Chronobiological studies on felling dates of trees and properties of wood related to water*

The exact moment when a tree is felled to harvest the wood, or simply the moment when samples are taken, has an importance which is generally ignored or underestimated. Indeed, we should think of this material as a dense tissue of organic matter saturated with water by forces and to an extent which fluctuate in a cyclic manner. The behaviour when drying (loss of water, shrinkage) and the resulting final density, as well as mechanical resistance (to compression for example) and even resistance to decomposing agents such as fungi or insects, will all be influenced one way or the other by the date of harvesting.

### *Traditional practices which are still very much alive*

Still today, maxims about felling linked to the moon are applied by certain workers of wood. An interesting fact: these rules come from traditions which persist in many regions of the world where links remain with ancestral culture. Here we will not deal with the multiple “lunar calendars”, very trendy nowa-

days, covering numerous areas fairly comprehensively, without any experimental basis. The examples which follow concern cases known directly to the author, or taken from scientifically documented sources; their aim is to illustrate the great variety of uses of wood for which the moon factor is considered important for obtaining certain exceptional properties. It should be pointed out that in most cases this factor comes only in second or third position, the most important being in general the time of year, with a high value placed on “winter wood”, and the situation in terms of the growing conditions, mountain wood from slow-growing natural forest stands being particularly appreciated. Sometimes winds are mentioned, such as the Foehn in the Alps, which could negatively impact certain properties of the wood.

### *Large-scale research*

In order to tackle the question more fundamentally and with a large data base, a new trial was carried out simultaneously on 4 sites in Switzerland, with 48 successive fellings (each Monday and each Thursday) – not linked to any experimental hypothesis – of 3 trees per site over 5 ½ months, representing a total of more than 600 trees felled over the winter of 2003-2004 (Zürcher et al. 2010). The species were Spruce (*Picea abies*) and Sweet Chestnut (*Castanea sativa*). Before the beginning of the experiment, a reference sample was taken the same day from each of the trees which were later felled (a prismatic sample at chest level). Each tree provided at different levels of the trunk a series of samples of sapwood and a series of samples of heartwood. The drying behaviour of this material was followed under standardised laboratory conditions.

Among the different rhythmicities first observed and then confirmed statistically for three principal criteria, let us mention here the water loss, which varied systematically in Spruce, particularly between the fellings immediately preceding the full Moon and those following it. The type of variation is probably due not to differences in initial water content, but to the fact that the forces binding the water to the cell wall of the ligneous tissues could be subject to fluctuations. The ratio between the water easily extractable from the wood, designated ‘free’, and the water extracted below the saturation point of the fibres, or ‘bound’ water, fluctuates according to lunar cycles, and probably also according to the seasons, the ‘lunar’ variations being more marked during the period from October to February (Zürcher et al. 2012). Moreover, the rhythmicities are manifested differently according to the species: the Chestnut also

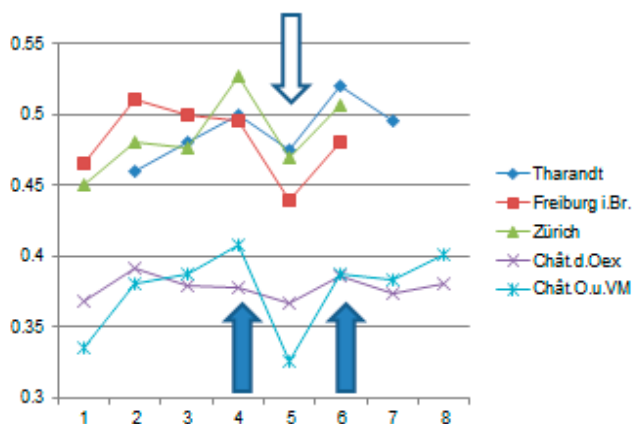


**Figure 7.** Variation of dry (anhydrous) densities of wood (sapwood) of Spruce (*Picea abies*) with felling period and moon phases, according to research done in different places and years. Upper: Tharandt 1996-97 (Triebel 1998); Freiburg i.Br., 1997-98 (Seeling and Herz 1998, 2000); Zürich, 1998-99 (Bariska and Rösch 2000) / lower: Château-d'Oex 2003-04 (Zürcher et al. 2012) Means waxing Moon – waning, resp. Château-d'Oex 2003-04 around the Full Moon – before / after). Waxing Moon dates 1, 3, 5, 7; waning Moon dates 2, 4, 6, 8. Similar variations can be observed especially in the second half of the trial period, from December onwards (4). Reminder: most of the technological properties of wood are closely linked to its density.

shows statistically significant lunar variations, but distinct from those of the Spruce.

These systematic variations in water loss cause a variation in the density of the wood after drying: - For the case of Spruce, it confirms what the previous studies mentioned had already observed (Fig. 7 – lower).

#### *Drying wood felled around the Full Moon*

In the Spruce samples (*Picea abies*; sapwood and heartwood together), a systematic and statistically significant variation of water loss is detectable. This fluctuation occurs according to the synodic lunar cycle on felling, subdivided into 8 periods of 3.7 days, beginning with the moment of the New Moon. The most marked variations occur during the passage from the period preceding the Full moon (high water loss) to the one beginning with the Full moon (minimal water loss) then the one preceding the Last quarter (high water loss). [Zürcher et al. 2010]

The statistical analysis indicates unexpectedly not only rhythms of a synodic type, but also a marked sidereal rhythmicity. Scientific research is thus able to affirm that behind the 'lunar' phytopractices of foresters resides a kernel of objective observations. This the case both for

synodic lunar phases (the cycle New Moon – Full Moon linked to the position of our satellite relative to the Sun) and for the sidereal cycle (position of the Moon compared to fixed constellations), also mentioned in a roundabout and somewhat curious way in certain felling rules. Note that these results, while confirming the existence of the 'Moon' factor as mentioned in country lore, appear in a much more complex form than imagined at the start of this research, Theophrastus's rule seeming to be very close to the synodic phenomena observed in Spruce (see below).

#### *Focus on a representative site*

The systematic variations over the course of the synodic lunar month can be illustrated in another fashion with the graph of variation around the general mean of this same criterion 'water loss' for the 48 successive felling dates, using a representative series: the sapwood samples of the site of Château-d'Oex (Zürcher et al. 2012). This material is relatively homogeneous because all the trees are of the same age, belonging to an even-age-managed mountain forest deriving from a plantation. Figure 8 A shows the visible change which occurred around the Full Moons of November, December and January. Even if the February Full Moon is included, where there was almost no difference between the values before and after the Full Moon, the respective variations around the Full Moon for this winter period of four months are not insignificant, the general mean indicating a reduction in water loss of 4.5%.

#### *Tests of water absorption (after drying)*

One of wood's most important physical properties, decisive for its bad-weather behaviour and its resistance to rot, is its hygroscopic nature – a very hygroscopic wood is more prone to rot than one which is less hygroscopic. This property is generally expressed by the equilibrium state in a given atmosphere, with a given temperature and relative humidity. When they are completely waterlogged, the cell walls are in a state designated 'fibre saturation point', below which the loss of bound water following the drying process causes deformations (shrinkage). The test method chosen for estimating the hygroscopic variations due to felling date was to expose the samples to a direct contact with water (Zürcher et al. 2012). A series of measurements was made using small rods from felled trees, previously air-dried under controlled conditions. They were all fixed (12 x 48 = 576 samples per site) by one end to a slab, the other end being immersed over a length of 5mm for 9 minutes in

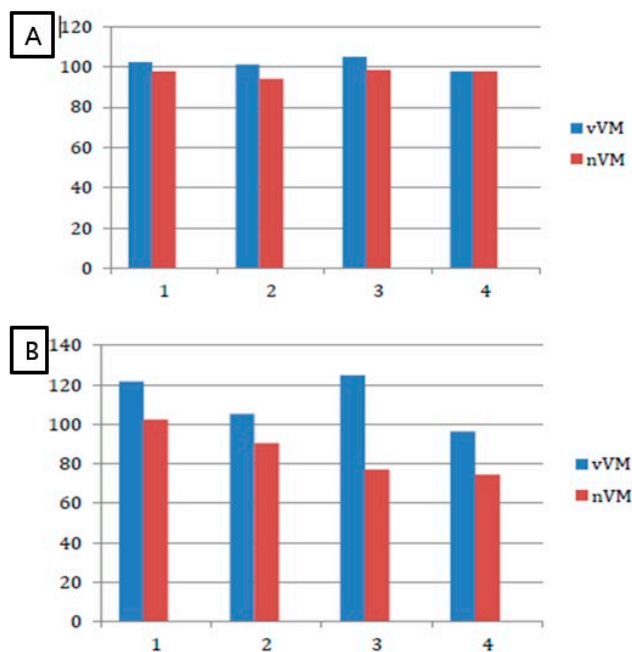


**Figure 8A.** Variation of water loss during drying of Spruce (*Picea abies*) samples, comparing the felling dates occurring in the 3.5 days running up to the Full Moon (vVM), with those of felling occurring during the 3.5 days after the Full Moon (nVM), for the months of November 2003 (1), December (2), January 2004 (3) and February (4). The samples from before the Full Moon of November, December and January lost slightly more water than those from fellings performed after the Full Moon. Values calculated from the general mean.

**Figure 8B.** Variation of capillary water absorption by the dried Spruce (*Picea abies*) samples, comparing the felling dates occurring in the 3.5 days running up to the Full Moon (vVM), with those of felling occurring during the 3.5 days after the Full Moon (nVM), for the months of November 2003 (1), December (2), January 2004 (3) and February (4). The samples from before the Full Moon of November, December, January and February absorbed considerably more water than those coming from fellings performed after the Full Moon. Values calculated from the general mean.

a bowl of water with ink as a dye. Figure 8B shows the variations in absorption of water by capillarity in the samples taken during this experimental period. Both the limitation of the lunar effect to the 4 winter months and the systematic and marked decrease in water absorption directly after the Full Moon are very similar to what was observed concerning initial water loss described above at Figure 8A. It is noteworthy that for the reabsorption of water by capillarity, the mean amplitude of the decrease (25.9%) for the samples taken just after the Full Moon is comparatively much more pronounced than for water loss and is evident even for February.

The second test method for quantifying the degree of hygroscopicity was applied by immersion of samples pre-

viously used for the determination of the density. In the same way, 576 cubic samples for each site (4 per tree, 12 for the felling date) were immersed in water at 20°C for 7 days. The absorption is expressed in this case as the percentage increase in mass. There too, systematic lunar variations in hygroscopicity occur, in obvious coherence with the loss of water. For the four months from November to February, the mean reduction between the days before the Full Moon and the days immediately after is 12.6%, half the value obtained for absorption of water by capillarity.

These results show us that the reversible variations linked to the Moon are not limited to the loss of water and the relative density (and shrinkage) in the course of drying: the phenomenon is even more marked for the absorption of water (by capillarity and by immersion) of previously dried wood samples. It should however be pointed out that these hygroscopic variations linked to the lunar cycles are much weaker than the differences due to the site and the type of forestry, since Spruce samples from a naturally-regenerating mountain forest show much lower water absorption than those from a plantation.

These encouraging results have to be confirmed by tests of durability before definitive conclusions can be made about Spruce wood for outdoor use. It could nevertheless be expected that differences in the resistance to decay of Spruce wood might follow the following rule: “low durability of wood cut not long before the full moon, because very hygroscopic; higher durability of less hygroscopic wood cut immediately after the full moon between November and February” – which would correspond to the oldest documented rule, written by the Greek naturalist Theophrastus (371–287 b.C), stipulating that the best construction timber is obtained when trees are felled in winter, in the first days after full moon. Indeed, it is well known that woods whose fibres can be highly saturated by water are more easily attacked by fungi and xylophagous insects than woods with a comparatively low saturation level of their cell walls.

#### *Implications and perspectives concerning periodicities*

This insight into lunar cycles detected in the plant world, and in particular in trees and their wood, shows a real phenomenon, which is additional to the exogenous rhythms of mostly solar origin whose action is well known, both on a daily and a seasonal level, and linked over the longer term to the cycle of sunspot activity, varying over an 11 year period. The Moon modulates this principal exogenous rhythm on an hourly basis, through the gravimetric tides occurring with two high and two low tides per day, as well as over the week and the lunar



month, according to the synodic, tropical, sidereal or anomalistic (perigee and apogee) cycle. It seems that the lunar rhythms become apparent when the influence of the sun is reduced, either naturally or due to an experimental set-up.

What kind of forces are involved here? Where the synodic and anomalistic rhythms are concerned, the gravitational force causing tides is too weak to explain even a tiny part of the lunar phenomena observed in plants: it is not more than 0.08 millionths of the force exerted by gravity on a mass situated at the surface of the Earth.

For the largest tree measured in Europe, described by Klein in 1908, a Silver Fir *Abies alba* in the Black Forest (height 68m, diameter 380cm, bole volume 140 m<sup>3</sup>, weight estimated at 100 t), the tidal (gravitational) lunar force represents a light daily pull then relaxation of 8 grammes only – the weight of two sugar lumps!

The variations of the geomagnetic field, weak but distinct, with a period of half a lunar day (12 hours 25 minutes), due to the gravimetric tides, present a similar situation.

The French chronobiologist Lucien Baillaud (2004) points out quite rightly: “Where the moon is concerned, the supporter [...] wants to be shown the basis of the link between the Moon and the living being, with a breakdown of how the phenomena fit together – or at least wishes us to suggest a hypothesis”.

It seems to us more and more obvious, as has been mentioned several times, that this basis is none other than the essential element for every organic process: water. This was the direction of the conclusions of researchers working on the cyclic variations of certain chemical reactions in aqueous medium in controlled laboratory conditions, such as Giorgio Piccardi, Joseph Eichmeier or Soco Tromp. We should mention also the work of Vladimir Voeikov and Emilio Del Giudice (2009) on the fluctuations of water in its electronic charge and its capacity to react with oxygen, bringing them to the concept of “water respiration”.

Already in the 1920s, experiments had been performed on the variations in surface tension of water using extremely fine glass capillary tubes, where the frequency of drop formation was observed (Maag 1928). They demonstrated lunar rhythmicities (monthly, but also daily) appearing as soon as the capillaries became fine enough, showing then the effect of certain planetary conjunctions. Meanwhile, it was observed that when it is in capillary systems, either of glass or organic like plant cells (with their vacuole and their partially porous membrane), water undergoes an important change in its properties, like for example the ability to remain liquid

at temperatures as low as – 15°C. It would be interesting to analyse again the effect of the ‘time’ factor on these essential properties of water using modern technologies.

A relatively recent double publication in theoretical physics by Gerhard Dorda (2004), co-author with von Klitzing of the discovery of the “Quantum Hall Effect”, winner of the Nobel Prize for Physics 1985, puts forward a new astro-geophysical model of the role of gravitation in living processes. This model integrates static and dynamic aspects of gravitation according to the orbital movement of celestial bodies, leads to a ‘quantisation’ of gravitation and of time, and demonstrates a reversible effect linked to the Sun on one hand and to the Moon on the other, on the supra-molecular structure of water. This model leads to the determination of reversible states of aggregation or coherence (‘clusters’) of water, in a quantitative ratio of a considerable size, from 1 to 2200, according to whether the interaction involved is Sun-Earth or Moon-Earth, the latter being modulated by the lunar day, but also according to the waxing/waning phase. Dorda considers that this rhythmic fluctuation of water in a system with 3 celestial bodies, constitutes the biological clock sought up to now in organic structures. This model was validated independently thanks to experimental measurements already published by Mario Cantiani et al. (1994) and interpreted in keeping with lunar chronobiology by E. Zürcher, M.-G. Cantiani, F. Sorbetti-Guerri and D. Michel in 1998.

Martial Rossignol and his colleagues, some years before (1990), highlighted the role of electromagnetic phenomena linked to lunar cycles (polarisation of light, modulation of wavelength, ionisation of the atmosphere, atmospheric pressure) and considered a possible link with the induction of bio-electric potentials at the cell level.

Not long after, in 2004, Philippe Vallée devised a new experimental method for proving in a reproducible manner that weak, low-frequency electromagnetic fields have a durable effect on water. This researcher stresses the importance of interfaces between water and its solid or gaseous inclusions: an essential aspect, since interfacial water plays a fundamental role in the organic world.

And now, a new scientific sensation has just come out, and brings an essential component to reinforce the hypotheses formulated here: ‘The Fourth phase of Water’ (Pollack 2013). The discovery and the demonstration of a “liquid crystal” phase of water in contact with hydrophilic membranes with dielectrical properties (wood corresponds to these criteria) allows Pollack to explain a whole series of ‘anomalies’ of water which were until now unexplained, and to open horizons beyond expectation.

All these discoveries and interpretations on a purely physical level do not however provide a reply to the question of why differences are observed between certain living plant species, both annual and woody, in their physiological reactions to lunar cycles and the behaviour of their wood. Indeed, trials on germination and initial growth have shown that simultaneously growing plants of different species are actually impacted by the factor “Moon”, but in counterphase, some species being positively stimulated of days before the New Moon, while others start their growth better in days before Full Moon (Zürcher 1992).

#### ENDANGERED GLOBAL CONTEXT

The described processes, structures and periodicities probably play a major role in the water cycles activated by forests, especially in equatorial zones. The last ones are probably of much higher existential importance for the life on earth than commonly admitted.

Trees produce clouds, but forests make also their own rain. Be it above the Amazonian tropical forest or boreal coniferous forests, the formation of clouds and the rainfall that follows happen thanks to a form of ‘seeding’ by micro-particles of organic origin. The gaseous substances given off by the trees, volatile organic compounds, undergo a photochemical condensation caused by light and behave as ‘cloud condensation nuclei’. Mushroom spores, pollen grains and microscopic vegetable debris which are also given off into the atmosphere have the same effect (Pöschl et al. 2010; Ehn et al. 2014). It is then easy to imagine that the rain regime could dramatically change if the forest cover should be reduced, not only because of then lacking “cloud producers”, but also because of the absence of “rain provokers”.

In his description of the geoclimatic role of the Amazonian forest, Peter Bunyard (editor of the British journal *The Ecologist*, 2015) draws attention to the new geoclimatic model developed by Victor Gorshkov and Anastassia Makarieva, of the Department of Theoretical Physics of the Institute of Nuclear Physics of Saint-Petersburg (2007, 2014). The analysis of the climatological and hydrological data leads them to the conclusion that it is not the movement of air masses which set off the hydrological cycle (the generally accepted model up to now), but on the contrary the changes in phase of the water in the atmosphere above forests which bring about the movement of air masses. Indeed, water needs considerable energy to evaporate from forests (around 600 calories per gramme, depending on temperature and

atmospheric pressure), and it returns this energy as heat in the high atmosphere when it condenses to form rain. Thus, the extreme impact of solar radiation around the equator is absorbed, thanks to the ecosystems rich in water and biomass found in these zones of the globe. In parallel, the rapidity of the condensation process compared to the slowness of the evapo-transpiration creates a pressure difference with a suction effect. The Amazonian forest thus acts like a gigantic hydrological heart (‘biotic pump’), attracting air masses from the Atlantic and enriching them in water, performing half a dozen cycles of evapo-transpiration – precipitation, moving from East to West, and finally rising in the Andes and moving north (Central and North America) and south (Argentina) giving rise to warm rains in latitudes far from the equator. The tropical forests can therefore be seen as components of the biosphere ensuring both the functioning and the stability of the great geoclimatic water cycle. In this context, the researchers bring to light another essential phenomenon: if a coastal zone is deforested over a width of 600 km or more, the masses of humid ocean air can no longer move inland, thus condemning their forests to perish.

#### REFERENCES

- Alexandersson, O. (2002). *Living Water: Viktor Schauberger and the Secrets of Natural Energy*. Gill Books, Dublin, Ireland.
- Baillaud, L. (2004): *Chronobiologie lunaire controversée: de la nécessité de bonnes méthodologies*. Bulletin du Groupe d’Etude des Rythmes Biologiques (35) 3 : 3-16.
- Bariska, M., Rösch, P. (2000): *Fällzeit und Schwindverhalten von Fichtenholz*. Schweizerische Zeitschrift für Forstwesen 151 (2000) 11: 439-443.
- Bartholomew, A. (2014) : *Le génie de Viktor Schauberger*. Le Courrier du Livre, Paris
- Bosshard, H. H. (1974): *Holzkunde, Band 2, Zur Biologie, Physik und Chemie des Holzes*. Birkhäuser Verlag, Basel und Stuttgart
- Bosshard, H.H. (1974): *Holzkunde Bd. 2 - Zur Biologie, Physik und Chemie des Holzes*. Birkhäuser-Verlag, Basel
- Bunyard, P. (2015): *Without its rainforest, the Amazon will turn to desert*. *The Ecologist*, 2nd March 2015.
- Cantiani, M. (†), Cantiani, M.-G., Sorbetti Guerri, F. 1994: Rythmes d’accroissement en diamètre des arbres forestiers. *Revue Forestière Française* 46: 349-358.
- Caro, C.G., A. Seneviratne, K.B. Heraty, C. Monaco, M.G. Burke, R. Krams, C.C. Chang, G. Coppola, and P.

- Gilson (2013). Intimal hyperplasia following implantation of helical-centreline and straight-centreline stents in common carotid arteries in healthy pigs: influence of intraluminal flow. *J R Soc Interface*. 2013 Oct 16; 10 (89):20130578.
- Coats, C. (1996): *Living Energies. An Exposition of Concepts Related to the Theories of Viktor Schauberger*. Gateway Books, Bath, U.K.
- Day, M. Let the blood run free. *New Scientist* 158 (2134):19, May 16, 1998
- Dorda, G. (2004): *Sun, Earth, Moon - the Influence of Gravity on the Development of Organic Structures*. Part II: The Influence of the Moon. Sudetendeutsche Akademie der Wissenschaften und Künste, München. Bd 25: 29-44.
- Ehn M, Thornton JA, Kleist E, Sipilä M, Junninen H, Pullinen I, Springer M, Rubach F, Tillmann R, Lee B, Lopez-Hilfiker F, Andres S, Acir IH, Rissanen M, Jokinen T, Schobesberger S, Kangasluoma J, Kontkanen J, Nieminen T, Kurtén T, Nielsen LB, Jørgensen S, Kjaergaard HG, Canagaratna M, Maso MD, Berndt T, Petäjä T, Wahner A, Kerminen VM, Kulmala M, Worsnop DR, Wildt J, Mentel TF. (2014): A large source of low-volatility secondary organic aerosol. *Nature*, 2014 Feb 27; 506 (7489): 476-9.
- Harris, J.M. (1989): *Spiral Grain and Wave Phenomena in Wood Formation*. Springer, New York.
- Ignatov, I., Mosin, O. and Bauer, E. (2015): Vortex Power Spring Water: Physical-Chemical Qualities of this Water compared to Mountain and Melt Water from Bulgaria, Russia and Glacier Rosenlauri from Swiss Alps. *Advances in Physics Theories and Applications*, Vol.45, 2015
- Johnson, B. (2013): The Ascent of Sap in Tall Trees: a Possible Role for Electrical Forces. *Water* 5, 86 – 104, Nov. 2013.
- Koch, G.W., Sillett, S.C., Jennings, G.M., Davis, S.D. (2004): “The limits to tree height”, *Nature* 428, 22 April 2004, pp. 851 - 854
- Kucera, L.J., Bosshard, H.H. (1981) : Die Waldrebe - Clematis vitalba L. *Vierteljahrsschrift der Naturforschenden Gesellschaft in Zürich* (1981) 126/l: 51-71
- Lance, C. (2013) : Respiration et photosynthèse - Histoire et secrets d'une équation. Edp sciences, Grenoble
- Maag, G. (1928): Planeteneinflüsse, West-Ost-Verlag, Konstanz
- Makarieva A.M., Gorshkov V.G., Sheil D., Nobre A.D., Bunyard P, Li B.-L. (2014) Why does air passage over forest yield more rain? Examining the coupling between rainfall, pressure, and atmospheric moisture content. *Journal of Hydrometeorology*, 15, 411-426.
- Makarieva, A.M., Gorshkov, V.G. (2007): Biotic pump of atmospheric moisture as driver of the hydrological cycle on land. *Hydrol. Earth Syst. Sci.*, 11, 1013 – 1033, 2007.
- Morton, A.A. (1977): The Fibonacci Series and the Periodic Table of Elements. *The Fibonacci Quarterly* Vol.15, Number 2, April 1977
- Pollack, G. H. (2013) : The Fourth Phase of Water - Beyond solid, liquid and vapor. Ebner and Sons, Seattle, USA
- Pollack, G. H. (2001) : Cells, Gels and the Engines of Life. Ebner and Sons, Seattle, USA.
- Pöschl U, Martin ST, Sinha B, Chen Q, Gunthe SS, Huffman JA, Borrmann S, Farmer DK, Garland RM, Helas G, Jimenez JL, King SM, Manzi A, Mikhailov E, Pauliquevis T, Petters MD, Prenni AJ, Roldin P, Rose D, Schneider J, Su H, Zorn SR, Artaxo P, Andreae MO. (2010): Rainforest aerosols as biogenic nuclei of clouds and precipitation in the Amazon. *Science* 2010, Sep 17; 329 (5998):1513-6.
- Ray, P. M. (1972): *The Living Plant*. (2nd Ed.) Holt, Rinehart, and Winston, New York
- Rosignol, M., S. Benzine-Tizroutine and L. Rosignol. (1990). Lunar cycle and nuclear DNA variations in potato callus or root meristem. In Tomassen, G.J.M., de Graaff, W., Knoop, A. A. and Hengeveld, R. (eds), *Geo-cosmic relations; the earth and its macro-environment. Proceedings of the First International Congress on Geo-cosmic Relations*, April 19-22, 1989, Amsterdam. Pudoc, Wageningen, The Netherlands.
- Seeling, U. (2000): Ausgewählte Eigenschaften des Holzes der Fichte (*Picea abies* (L.) Karst.) in Abhängigkeit vom Zeitpunkt der Fällung. *Schweizerische Zeitschrift für Forstwesen / Journal Forestier Suisse* 151 (2000) 11: 451-458.
- Seeling, U., Herz, A. (1998): Einfluss des Fällzeitpunktes auf das Schwindungsverhalten und die Feuchte des Holzes von Fichte (*Picea abies*) - Literaturübersicht und Pilotstudie. Albert-Ludwigs-Universität Freiburg i.Br., Institut Forstbenutzung und Forstliche Arbeitswissenschaft. Arbeitspapier 2-98 (66p).
- Sengupta, P. et al. (2012) : Emerging Trends in CV Flow Visualization. *JACC - Cardiovascular Imaging*, Vol.5, No.3 : 305 – 16
- Triebel, J. (1998): Mondphasenabhängiger Holzeinschlag - Literaturbetrachtung und Untersuchung ausgewählter Eigenschaften des Holzes von Fichten (*Picea abies* Karst.). Diplomarbeit, Institut für Forstbenutzung und Forsttechnik, TU Dresden (108 p).
- Vallée, Ph. (2004): Etude de l'effet de champs électromagnétiques basse fréquence sur les propriétés physico-

- chimiques de l'eau. Thèse de Doctorat, Université Pierre et Marie Curie (Paris VI).
- Voeikov, V. L., Del Giudice, E. (2009): Water Respiration - The Basis of the Living State. *WATER* 1, 52 - 75, 1 July **2009**
- Zimmer, B. & Wegener (1996): Stoff- und Energieflüsse vom Forst zum Sägewerk. Holz als Roh- und Werkstoff 54 (**1996**): 217-223.
- Zimmermann, M. H. (**1983**): *Xylem Structure and the Ascent of Sap*. Springer-Verlag, Berlin – Heidelberg - New York – Tokyo
- Zürcher, E. (**1992**): *Rythmicites dans la germination et la croissance initiale d'une essence forestiere tropicale*. (Rhythmizitäten in der Keimung und im Initialwachstum einer tropischen Baumart) Schweizerische Zeitschrift fuer Forstwesen (Switzerland) v. 143(12) p. 951-966
- Zürcher, E. (**2016**) : *Die Bäume und das Unsichtbare*. AT-Verlag, Aarau (CH) und München (D)
- Zürcher, E. (**2016**): *Les Arbres, entre Visible et Invisible*. Actes Sud, Arles (F)
- Zürcher, E., Cantiani, M.-G., Sorbetti-Guerri, F., Michel, D. (**1998**): Tree stem diameters fluctuate with tide. *Nature* 392: 665-666.
- Zürcher, E., Rogenmoser C, Soleimany Kartalaei A, Ramber D. (2012): Reversible Variations in Some Wood Properties of Norway Spruce (*Picea abies* Karst.), Depending on the Tree Felling Date. In: *Spruce: Ecology, Management and Conservation*. Eds. Nowak KI and Strybel HF. Nova Science Publishers, Hauppauge, New York 2012; 75-94.
- Zürcher, E., Schlaepfer, R., Conedera, M., Giudici, F. (**2010**): Looking for differences in wood properties as a function of the felling date: lunar phase-correlated variations in the drying behavior of Norway Spruce (*Picea abies* Karst.) and Sweet Chestnut (*Castanea sativa* Mill.). *TREES* (2010) 24: 31-41.









September 2019

No walls. Just bridges



Vol. 3 – n. 2  
Suppl. 3

# Substantia

An International Journal of the History of Chemistry

## Table of contents

|  |    |
|--|----|
| <b>Luigi Dei</b><br>Preface  | 7  |
| <b>Marc Henry</b><br>Editorial<br>Water and the periodic table   | 9  |
| <b>Everine B. van de Kraats, Jelena S. Muncan, Roumiana N. Tsenkova</b><br>Aquaphotomics - Origin, concept, applications and future perspectives                   | 13 |
| <b>Marc Henry, Laurent Schwartz</b><br>Entropy export as the driving force of evolution  | 29 |
| <b>Josè Teixeira</b><br>The puzzling problem of water properties at low temperature.<br>An experimentalist view  | 57 |
| <b>Heinz-Michael Peter, Christine Sutter, Wolfram Schwenk</b><br>Study of a Section of a Self-Purifying Stream in Specific Relation to its Water<br>Flow Behaviour | 65 |
| <b>Ernst Zürcher</b><br>Water in Trees. An essay on astonishing processes, structures and periodicities  | 71 |

